# GLYOXALASE 1 AS A NOVEL MOLECULAR MARKER OF HIGH-GRADE PROSTATIC INTRAEPITHELIAL NEOPLASIA AND CAUSATIVE EFFECTOR IN THE PROGRESSION OF PROSTATE CANCER

by

Liliana Rounds

---



A Dissertation Submitted to the Faculty of the

GRADUATE INTERDISCIPLINARY PROGRAM IN CANCER BIOLOGY

In Partial Fulfillment of the Requirements

For the Degree of

DOCTOR OF PHILOSOPHY

In the Graduate College

THE UNIVERSITY OF ARIZONA

2022

THE UNIVERSITY OF ARIZONA
GRADUATE COLLEGE

As members of the Dissertation Committee, we certify that we have read the dissertation prepared by: **Liliana Rounds**, titled:

**Glyoxalase 1 as a Novel Molecular Marker of High-Grade Prostatic Intraepithelial Neoplasia and Causative Effector in the Progression of Prostate Cancer**

and recommend that it be accepted as fulfilling the dissertation requirement for the Degree of Doctor of Philosophy.

Georg T Wondrak, PhD — Date: 12-17-2021

Raymond B. Nagle, MD PhD — Date: 12-17-2021

Donato Romagnolo, PhD — Date: 12-17-2021

Pavani Chalasani, MD PhD — Date: 12-17-2021

Michael Riggs, DVM PhD — Date: 12-17-2021

Esteban Roberts, PhD — Date: 12-17-2021

Final approval and acceptance of this dissertation is contingent upon the candidate's submission of the final copies of the dissertation to the Graduate College.

I hereby certify that I have read this dissertation prepared under my direction and recommend that it be accepted as fulfilling the dissertation requirement.

Georg T. Wondrak, PhD — Date: 12-17-2021
Dissertation Committee Chair
Department of Pharmacology and Toxicology
Cancer Biology Department

# ACKNOWLEDGEMENTS AND DEDICATIONS

The work presented here signifies the consummation of a lifelong dream, the one dream that would take me from my home country to a new country that I now call ‘home’.

First, I would like to thank God for persevering with me for the past five and a half years. His faithful love carried me through very difficult times when I thought I could not walk one more step in this journey. He reassured me time after time that His timing was perfect and that I had to fear nothing for He was with me. He provided the peace and calm through all the stormy days when anxiety sought to take hold of me.

I would like to dedicate this work to the following individuals whose support never wavered;

To my husband Matthew and son Christopher whom I love more than words can express. The ones who in many ways helped me to endure difficult days, the ones who patiently waited day after day and never doubted I would accomplish my lifelong dream.

To my mother Felicitas, sisters Gaby and Carmen, aunts, uncles whose enthusiasm and words of encouragement were so important to keep me going. To my uncles Jesus and Sergio who have been a fatherly figure to me and who taught me work ethic and many life skills as well as to never give up when facing difficulties. To my mother who always devoted much of her time to help me grow and whom now watches me soar high, Thank you!

To my colleagues at Roche Tissue Diagnostics/Ventana Medical Systems Inc. who always encouraged and motivated me to pursuit my dreams. To my manager Liz Vela and to Andrea Muranyi, two women whom from the moment I decided to pursuit this degree, advocated for me and supported me every step of the way, Thank you!

To Dr. Georg Wondrak who was willing to give me the opportunity to fulfill my dream without hesitation and from whom I have learned a great deal of knowledge in many areas of science, Thank you! He allowed me to pursuit an area of research completely new to him; such patience and trust helped me to mature as a young scientist. To Dr. Jana Jandova for her willingness to take me under her wing and helping me with the completion of this work, Thank you!

To Dr. Raymond B. Nagle, one of the greatest Pathologists and scientists in the field of prostate cancer and the one who devoted much time to guide me and teach me the beauty that exists in the complexity of tissue, Thank you! It is only fair to say that without his help and contribution, this research project had not come to fruition.

Finally, I would like to acknowledge my Dissertation Committee: Drs. Raymond B. Nagle, Donato Romagnolo, Pavani Chalasani, Michael Riggs and Esteban Roberts. Thank you for embarking with me on this adventure and for devoting time out of your busy schedules to reviewing my work throughout the past five years. I am forever thankful for your kindness, patience and understanding as I navigated a busy work and graduate school life.

# TABLE OF CONTENTS

# LIST OF TABLES

# LIST OF FIGURES

# LIST OF ABBREVIATIONS

| | |
|---|---|
| 34βE12 | Anti-keratin (34βE12) |
| ACO2 | Aconitase 2 |
| ADT | Androgen depravation therapy |
| AGE | Advanced glycation end-products |
| AKT | Protein kinase B |
| AMACR | α-methylacyl-CoA racemase |
| AMPK | AMP-activated protein kinase |
| AR | Androgen receptor |
| ARE | Antioxidant response element |
| ARG1 | Arginase 1 |
| Arv7 | Androgen receptor splice variant 7 |
| AS | Active surveillance |
| ATM | Ataxia-telangiectasia mutated protein |
| ATP | Adenosine triphosphate |
| BCa | Breast cancer |
| Bcl2 | B-cell lymphoma-2 protein |
| BCR | Biochemical recurrence |
| BPH | Benign prostate hyperplasia |
| BRCA1 | Breast cancer type 1 protein |
| BRCA2 | Breast cancer type 2 protein |
| CAF | Cancer associated fibroblast |
| CAIX | Carbonic Anhydrase IX |
| CC1 | Cell conditioning I |
| CCP | Cell cycle progression |
| ccRCC | Clear cell renal cell carcinoma |
| cDNA | Complimentary Deoxyribonucleic acid |
| CEL | Nepsilon-(1-carboxyethyl)lysine |
| cfDNA | cell-free Deoxyribonucleic acid |
| CHC | α-cyano-4-hydroxycinnamic acid |
| Cip/Kip | CDK interacting protein/Kinase inhibitory protein |
| CK | Cytokeratin |
| c-MYC | MYC Proto-oncogene |
| CNV | Copy number variation |
| CP | Capsular penetration |
| CRISPR/Cas9 | Clustered Regularly Interspaced Short Palindromic Repeats. Genome editing tool. |
| CS | Citrate synthase |
| CTC | Circulating tumor cells |
| Cz | Central zone |
| DAB | Diaminobenzidine |
| DCIS | Ductal carcinoma *in situ* |
| DHAP | Dihydroxyacetone phosphate |
| DHH | Desert hedgehog |

| | |
|---|---|
| DHT | Dihydrotestosterone |
| DNA | Deoxyribonucleic acid |
| DRE | Digital rectal examination |
| DWI | Diffusion-weighed imaging |
| ECM | Extracellular matrix |
| EGF | Epidermal growth factor |
| EGFR | Epidermal growth factor Receptor |
| EMT | Epithelial to Mesenchymal Transition |
| ENO1 | Enolase 1 |
| ERG | ETS Transcription Factor ERG |
| ERK | Extracellular signal-regulated kinase |
| ESR | Estrogen Receptor |
| ESR1 | Estrogen receptor 1 |
| ESR2 | Estrogen receptor 2 |
| ETS | ETS family of transcription factors |
| FANCA | FA Complementation Group A protein |
| FASN | Fatty Acid Synthase protein |
| FDG | $^{18}$F-fluorodeoxyglucose |
| FFPE | Formalin fixed paraffin embedded |
| FGF-2 | Fibroblast growth factor 2 |
| FGFR1 | Fibroblast growth factor receptor 1 |
| FH | Fumarate hydratase |
| FISH | Fluorescence in situ hybridization |
| FOXA | Forkhead box A1 |
| fPSA | Free prostate-specific antigen |
| Fru-2,6-$P_2$ | Fructose 2,6-bisphosphate |
| FTIR | Fourier-transform infrared spectroscopy |
| Fz | Fibronuclear zone |
| G3P/GA3P | Glyceraldehyde 3-phosphate |
| GABA A | Gamma-aminobutyric acid neurotransmitter |
| GAPDH | Glyceraldehyde 3-phosphate dehydrogenase |
| G-CIMP | Glioma CpG island methylator phenotype |
| GEMM | Genetically engineered mouse model |
| GEP-NET | Gastroenteropancreatic neuroendocrine tumor |
| GLO1 | Glyoxalase 1 |
| GLUT1 (*SLC2A1*) | Glucose transporter protein type 1 |
| GLUT10 (*SLC2A10*) | Glucose transporter protein type 10 |
| GLUT12 (*SLC2A12*) | Glucose transporter protein type 12 |
| GLUT3 (*SLC2A3*) | Glucose transporter protein type 3 |
| GOLM1/GOLPH2/GP73 | Golgi membrane protein 1 |
| GPS | Genomic prostate score |
| GR | Glucocorticoid receptor |
| GSH | Glutathione |
| GSTP1 | Glutathione S-transferase pi gene |
| GSTpi | Glutathione S-transferase pi enzyme |
| H&E | Hematoxylin and Eosin |

| | |
|---|---|
| HGPIN | High-grade prostatic intraepithelial neoplasia |
| HIF-1α | Hypoxia inducible factor 1α |
| HK1 | Hexokinase 1 |
| HK2/HKII | Hexokinase 2 |
| HLA | Human leukocyte antigen |
| HP | Hyperpolarized |
| HR | Hazard ratio |
| HRD | Homologous recombinant defect |
| Hsp27 | Heat shock protein 27 |
| HSP90 | Heat shock protein 90 |
| HWMCK | High molecular weight cytokeratins |
| IFNγ | Interferon gamma |
| IHC | Immunohistochemistry |
| IL-12 | Interleukin 12 |
| IL-2 | Interleukin 2 |
| IL-6 | Interleukin 6 |
| IL-7 | Interleukin 7 |
| IL-8 | Interleukin 8 |
| IR | Infrared |
| IRE | Insulin response element |
| ISUP | International society of urological pathology |
| *KDM4A*/JMJD2A | Lysine demethylase 4A/Jumonji domain 2 |
| Keap1 | Kelch-like ECH-associated protein 1 |
| KGF | Keratinocyte growth factor |
| Ki | Inhibitory constant |
| Ki-67 | Nuclear marker of proliferation |
| KLK | Kallikreins |
| KO | Knock-out |
| KRT14 | Keratin 14 |
| KRT18 | Keratin 18 |
| KRT19 | Keratin 19 |
| KRT5/6 | Keratin 5/6 |
| KRT8 | Keratin 8 |
| Lac/Pyr | Lactate/Pyruvate |
| *Lbr* | Lamin B receptor gene |
| *Ldha* | Lactate dehydrogenase-A gene |
| LDHB (*Ldhb*) | Lactate dehydrogenase-B |
| LDHV | Lactic dehydrogenase virus |
| LGPIN | Low-grade prostatic intraepithelial neoplasia |
| LI | Labeling index |
| LPS | Lipopolysaccharide |
| MACC1 | Metastasis–associated in colon cancer protein 1 |
| mACON | Mitochondrial aconitase |
| MCM | Mini-chromosome maintenance |
| MCT | Monocarboxylate transporter |
| MCT1/4 | Monocarboxylate transporters 1 and 4 |

| | |
|---|---|
| MDH2 | Malate dehydrogenase |
| MDR | Multidrug resistance |
| MG | Methylglyoxal |
| MG-H1-3 | MG-derived hydroimidazolones |
| MLH1 | MutL homolog 1 |
| mM | Millimolar |
| MMR | Mismatch repair |
| MODIC | 2-ammonio-6-([2-[(4-ammonio-5-oxido-5-oxopentyl) amino]-4-methyl-4,5-dihydro-1*H*-imidazol-5-ylidene]amino)hexanoate) |
| MOLD | Methylglyoxal-derived lysine dimer |
| MPC2 | Mitochondrial pyruvate carrier 2 |
| mpMRI | Multiparametric MRI |
| MRE | Metal response element |
| mRNA | messenger Ribonucleic acid |
| MRSI | Magnetic resonance spectroscopic imaging |
| MSH2 | MutS Homolog 2 |
| MSH6 | MutS Homolog 6 |
| mTOR | Mammalian target of rapamycin |
| c-MYC | Cellular myelocytomatosis; proto-oncogene |
| NAD+ | Nicotinamide adenine dinucleotide |
| NADH | Nicotinamide adenine dinucleotide (NAD) + hydrogen (H) |
| NADPH | Nicotinamide adenine dinucleotide phosphate |
| NCCN | National comprehensive cancer network |
| NE | Neuroendocrine |
| NEPC | Neuroendocrine prostate cancer |
| NFAT | Nuclear factor of activated T-cells |
| NF-KB | Nuclear factor kappa B |
| nmol/g | nanomol/gram |
| NRF2 | Nuclear factor-erythroid factor 2-related factor 2 |
| NSAID | Non-steroidal anti-inflammatory drugs |
| NSCLC | Non-small cell lung cancer |
| OC | Organ confined |
| OGDH | Oxoglutarate dehydrogenase |
| OR51E2 | Olfactory receptor family 51 subfamily E member 2 |
| ORG2058 | 16α-ethyl-21-hydroxy-19-norprogesterone |
| OS | Overall survival |
| OXPHOS | Oxidative phosphorylation |
| p27 | Protein regulator of cell proliferation |
| p504s | a.k.a. Racemase (AMACR) |
| p63 | Tumor protein 63 |
| PARP | Poly (ADP-ribose) polymerase |
| PCa | Prostate carcinoma/cancer |
| PDGFR | Platelet-derived growth factor receptor |
| PDX | Patient-derived xenograft |
| PFK | Phosphofructokinase |

| | |
|---|---|
| PFK1 | 6-phosphofructo-1-kinase |
| PFK-2 | 6-phosphofructo-2-kinase |
| PFKFB | 6-phosphofructo-2-kinase/fructose-2,6-bisphosphatase |
| PFKFB2 | 6-Phosphofructo-2-Kinase/Fructose-2,6-biphosphatase 2 |
| PFKFB3 | 6-Phosphofructo-2-Kinase/Fructose-2,6-biphosphatase 3 |
| PFKFB4 | 6-Phosphofructo-2-Kinase/Fructose-2,6-biphosphatase 4 |
| PFKP | Phosphofructokinase, Platelet |
| PFS | Progression free survival |
| Pgr | Periurethral gland region |
| PHD | Prolyl hydroxylase |
| PI3K | Phosphoinositide 3-kinases |
| PIN | Prostatic intraepithelial neoplasia |
| pKa | -log of the acid dissociation constant |
| PMS2 | PMS1 homolog 2, mismatch repair system component |
| PPP | Pentose phosphate pathway |
| PR | Progesterone receptor |
| PRE | Progesterone response element |
| PSA | Prostate specific antigen |
| PTC1 & PTC2 | Protein phosphatase 2C homolog 1 & 2 |
| PTEN | Phosphatase and tensin homolog |
| PTM | Post-translational modifications |
| Pz | Peripheral zone |
| RAGE | Receptor of advanced glycation end products |
| RCS | Reactive carbonyl species |
| RNA | Ribonucleic acid |
| RNAseq | RNA sequencing |
| ROS | Reactive oxygen species |
| RSK | Ribosomal S6 kinase |
| RT-PCR | Reverse transcription polymerase chain reaction |
| SCC | Squamous cell carcinoma |
| SERPINB1 | Serpin family B member 1 |
| SERPING1 | Serpin family G member 1 |
| SHH | Sonic hedgehog |
| siRNA | small interference ribonucleic acid |
| SLC26A3 | Solute carrier family 26 member 3 |
| SLC2A3 | Solute Carrier Family 2 Member 3 |
| SLIT2/ROBO1 | Slit guidance ligand 2 |
| Slnl | Sarcolipin |
| Smad | Signal transducer for receptor TGF-β |
| SMC | Smooth muscle cells |
| SMS | Spermine synthase |
| TACMASR | Tissue acquisition and cellular/molecular analysis shared resource |
| TAM | Tissue associated macrophage |
| TCA | Tricarboxylic cycle |

| | |
|---|---|
| TET/TET2 | Ten-eleven translocation (TET) methylcytosine dioxygenases. |
| TGF-β | Transforming growth factor-β |
| THP | Tetrahydropyrimidine |
| TIGAR | TP53-induced glycolysis and apoptosis regulator |
| TIL | Tumor infiltrating lymphocyte |
| TMA | Tissue microarray |
| TMC | Tucson medical center |
| TME | Tumor microenvironment |
| TMPRSS2 | Transmembrane protease serine 2 gene |
| TP53 | Tumor protein 53; tumor suppressor |
| TP63 | Tumor protein 63 |
| TRAMP | Transgenic adenocarcinoma of the mouse prostate |
| Tz | Transitional zone |
| UGE | Urogenital sinus epithelium |
| UGS | Urogenital sinus |
| USPTF | United States preventive services task force |
| VEGF (*VEGF*) | Vascular endothelial growth factor |
| ZEB1 | Zinc finger E-box binding homeobox 1 |
| ZIP1-4 | Zinc transporters |
| $Zn^{2+}$ | Zinc |
| ZnT1-10 | Zinc transporters |

# ABSTRACT

The prostate is a male accessory sex gland that functions to produce many components of the seminal fluid including zinc and citrate, both of which are crucial to men fertility. The prostate gland has two main compartments: the stroma and the epithelium. Three cell types comprise the prostatic epithelium: secretory epithelial cells, basal/stem cells, and neuroendocrine cells. The prostatic epithelium is unique in that they are the only healthy human cells that produce energy by glycolysis rather than the Krebs cycle. Changes in the prostatic epithelium leading to malignant proliferation increase in incidence with age.

Prostate carcinoma (PCa) is the leading malignancy and the second leading cause of cancer-associated deaths in the USA male population. PCa is a disease of the elderly and risk prediction becomes crucial. Most patients present low-risk, relatively indolent tumors; however, 20-30% of these men present tumor characteristics associated with high-risk PCa. High Grade Prostatic intraepithelial neoplasia (HGPIN) is the only widely accepted histological condition and precursor of invasive PCa.

High glycolytic activity is an oncometabolic hallmark of cancer. Cancer cells turn to aerobic glycolysis for energy production in a process referred to as ‘the Warburg effect’ leading to accumulation of methylglyoxal (MG), a cytotoxic glycolytic byproduct responsible for the adduction of macromolecules, a process called advanced glycation end-products (AGEs) formation. Glyoxalase 1 (GLO1), also known as lactoylglutathione lyase (EC: 4.4.1.5), is part of the glyoxalase system, playing a crucial role in cellular detoxification of spontaneously formed MG. In a two-step reaction, GLO1 first catalyzes the conversion of highly reactive MG to S-D-lactoylgluthatione. The resulting thioester, in

the case of MG, is then hydrolyzed by GLO2 to produce D-lactate and reformed glutathione (GSH). The cytoprotective glyoxalase system prevents formation of AGEs and promotes cell survival. GLO1 upregulation has been described in the context of metabolic and inflammatory stress *in vitro* and *in vivo*, serving as a cellular mechanism to detoxify high levels of MG, particularly in cancer, where high glycolytic rates as a result of the 'Warburg effect' are observed.

Our laboratory has demonstrated GLO1 upregulation during tumor progression, observable in HGPIN and PCa versus normal prostatic tissue by immunohistochemistry in archival tumor samples. GLO1 upregulation was identified as a novel hallmark of HGPIN lesions. In PCa specimens, GLO1 expression correlated with intermediate–high risk Gleason grade but not with patient age, biochemical recurrence, or pathological stage. Using CRISPR/Cas9 we genetically engineered *GLO1* knock-out isogenic clones from DU-145 prostate carcinoma cells to further examine the role of GLO1 in PCa. Interestingly, we showed upregulation of *TXNIP* (encoding the thioredoxin-interacting protein) in the DU-145-*GLO1*_KO as a function of *GLO1* status. TXNIP is a master regulator of cellular energy metabolism and redox homeostasis, also considered a tumor suppressor. Furthermore, *GLO1* elimination had a profound detrimental effect in the clonogenicity and invasiveness capacity. We also identified *MMP-3* (encoding matrix metalloproteinase-3) and *SPP1* (encoding secreted phosphoprotein 1) as the two genes displaying the most profound downregulation in response to *GLO1* elimination. MMP-3 and SPP1 are two effectors implicated in the development of prostate cancer in the bone, tumor-associated inflammation, facilitating metastasis, and promoting drug resistance. Additionally, based on The Human Protein Atlas data, decreased survival probability

correlated with high MMP-3 mRNA expression levels in tissue from prostate cancer patients suggesting that GLO1 expression status is a novel and underappreciated determinant of PCa invasiveness and patient survival. Our published GLO1 data generated some excitement in the private sector with a potential translational application for GLO1 in the clinical setting. Current studies performed at Roche Diagnostics seek to develop a methodology for the detection of malignant biochemical signatures in tissue by spectroscopic imaging. These signatures can be used as biomarkers of early prostate cancer associated with aggressive disease. GLO1 promises to be one of the targets of study.

Our future goals seek to (a) have a better understanding of the molecular mechanisms underlining oncometabolic dysregulation in PCa, (b) an improved understanding of the molecular basis underlying early PCa with a focus on HGPIN lesions pursued in relevant murine models, (c) identify improved molecular therapeutics that allow early interventions targeting HGPIN and mPCa. Translationally, we seek to aid in the development of powerful prognostic and diagnostic biomarkers identifying HGPIN and PCa and the discovery and development of novel optics-based technologies for the antibody independent diagnosis and prediction of PCa grade and progression.

# CHAPTER I

## The Normal Prostate and Early Changes Leading to the Development of Prostate Adenocarcinoma

## 1.1. Normal Prostate Physiology

The prostate is a male accessory sex gland found exclusively in mammals. It functions to produce many components of the seminal fluid [1-4]. The prostatic fluid is rich in zinc, citrate and kallikreins (KLKs) all of which are pivotal components of the seminal plasma. Zinc (trace element actively stored within the cytoplasm of the prostatic epithelial cells) and citrate (intermediate metabolite of the Krebs cycle) play a central role in the regulation of the prostate epithelium homeostasis and in ejaculation [5]. Therefore, the prostate gland plays a crucial role in men fertility. The glandular epithelium of the peripheral zone is responsible for accumulating and secreting extraordinarily high levels of citrate (40-150 mM) and zinc [6].

The prostate organ was first described by Lowsley as having 5 lobes and unlike the rat prostate, the human prostate organ has distinct zones within a uniform gland. It is organized in alveoli-like structures (grape bunch) in fibrous gelatin [7]. There are two main compartments, the stroma and the epithelium [5]. Three cell types comprise the prostatic epithelium: secretory epithelial cells (tall columnar), basal/stem cells (cuboidal epithelial) and neuroendocrine cells. The prostatic stroma consist of smooth muscle cells (SMCs), fibroblasts and endothelial cells [7].

The prostatic epithelium is unique in that they are the only healthy human cells that produce energy by glycolysis rather than the Krebs cycle. Glycolysis is a means of energy production by cancer cells and a hallmark of proliferating cancer cells [5, 8, 9]. Another unique property of the normal human prostate is that it accumulates the highest levels of zinc of any soft tissue in the human body (~4% of the total $Zn^{2+}$ in the human body). The

zinc accumulation, uptake and release cycle is accomplished in an androgen-dependent manner via the ZIP1-4 (uptake) and the ZnT1-10 (release) transporters [10, 11]. Zinc has a dual inhibitory function: a) inhibition of the mitochondrial aconitase enzyme (mACON) and, b) temporary inactivation of the KLKs. mACON oxidizes citrate to isocitrate, thus its inhibition leads to accumulation of citrate in prostatic epithelial cells. Temporary inactivation of the KLKs occurs at the Zymogen level (pre-pro KLKs) where zinc binds allosterically inhibiting the KLK proteolytic cascade until the proper cues are triggered by the ejaculatory stimuli. Zinc and citrate accumulation, Krebs cycle inhibition and prostatic fluid release are regulated by testosterone and DHT (dihydrotestosterone) Il via the androgen receptor (AR) [5].

Luminal and basal epithelial cells express unique keratins and other differentiation markers [12] and represent most of the prostatic epithelium. Neuroendocrine (NE) cells, derived from the neural crest [13], represent only a small percent and express serotonin and chromogranin A. Anatomically, the human prostate gland is divided into three zones: a) central zone, b) transition zone, and c) peripheral zone. Clinically, it is divided into lateral lobes separated by a central sulcus and a middle lobe. Structurally, the prostate gland is made of ducts with an inner layer of epithelium surrounded by stroma [5] (**Figure 1**).

| | |
|---|---|
| **Transition zone** | Surrounds the urethra proximal to the ejaculatory ducts. |
| **Central zone** | Surrounds the ejaculatory ducts & projects under the bladder base. |
| **Peripheral zone** | Most of the apical, posterior and lateral aspects of the prostate. |

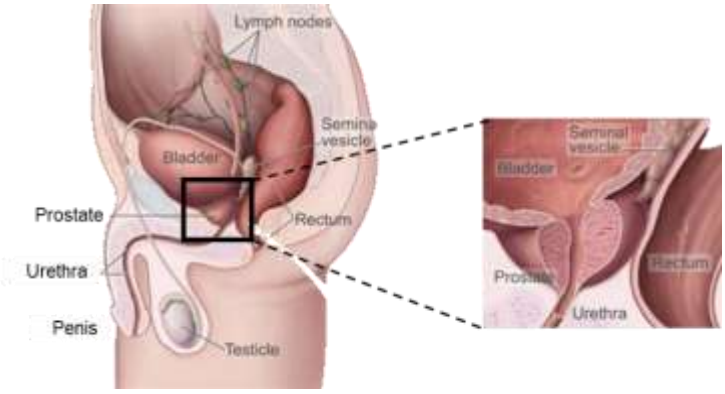


**Figure 1. Anatomical characteristics of the prostate gland**. The prostate gland is located below the bladder and it is traversed by the urethra as shown on the schematic (right; adapted from a Wikimedia Commons). The prostate can be divided into three anatomical zones: transition, central and peripheral zones. The transition zone surrounds the urethra; central zone surrounds the ejaculatory ducts. The peripheral zone is the region containing the majority of prostatic glandular tissue with the largest area at the back of the gland, closest to the rectal wall.

Epithelial buds from the embryonic urogenital sinus (UGS) give rise to the prostate organ. There are six stages during prostatic development: a) pre-bud UGS, b) emergence of solid prostatic epithelial buds from urogenital sinus epithelium (UGE), c) bud elongation and branching, d) canalization of the solid epithelial cords, e) differentiation of luminal and basal epithelial cells, and f) secretory cytodifferentiation. This latter stage occurs late in the second as well as in the third trimester of gestation (**Table 1**) [12].

During prostatic development, final differentiation into luminal and basal epithelial cells, and final anatomical placement follows canalization of the solid prostatic epithelial cords, basal epithelial cells lose luminal cell markers and vice versa [7, 12].

**Table 1.** Epithelial differentiation markers in the pre-bud stage. Adapted from Cunha, et al. [2].

| Developmental event | Human age | Markers | Pre-bud UGE | Solid buds | Canalized ducts | | |
|---|---|---|---|---|---|---|---|
| | | | | | Basal cells | Luminal cells | NE cells |
| Pre-bud stage | 8-9 wks | KRT5/6 | | + | + | - | |
| | | KRT19 | + | + | + | + | |
| | | KRT18 | + | + | - | + | |
| | | KRT14 | + | + | + | | |
| | | KRT8 | + | + | | + | |
| | | TP63 | + | + | + | - | |
| | | AR | | | | + | |
| | | ESR | | | - | -/+ | |
| | | ESR2 | | + | + | + | |
| | | PSA | | - | - | - | |
| | | EGFR | | + | + | + | |
| | | Bcl2 | | + | + | + | |
| | | p27 | | - | - | - | |
| | | 5α-reductase | | stroma (+) | | | |
| | | SHH | | + | | + | |
| | | DHH | | + | | + | |
| | | PTC1 & PTC2 | | + | | + | |
| | | Glil | | + | | + | |
| | | GSTpi | + | + | | + | |
| | | Chromogranin A | | | | | + |
| | | Serotonin | | | | | + |

wks = weeks; NE= neuroendocrine

Development of the human prostate is dependent on androgens; moreover, prostatic epithelial identity, ductal morphogenesis and glandular differentiation all require signaling through stromal AR [14]. Expression of AR in the prostatic stroma has been reported as early as 11.5 weeks and it is consistently expressed through term. Androgens regulate epithelial proliferation via paracrine signaling which requires expression of AR in the stroma [2]. Consequently, androgens are essential for the development, differentiation, growth, and function of the prostate through interactions between epithelial and stromal

cells [15]. Both, testosterone and DHT can directly bind and activate the AR; however, DHT is more potent (10-fold higher affinity) and critical in prostatic development. DHT is synthesized by the enzyme 5α-reductase within the developing UGS [16]. Other ARs such as ESR1 and ESR2 have been detected in the human fetal prostate [17, 18] and although prostatic development is not dependent on estrogen receptors, it is susceptible to the effects of estrogens [19].

## 1.2. Early Prostate Events Leading to Prostate Cancer

As stated before, androgens control prostate homeostasis via AR, the main intracellular effector. AR has a dual function, it serves as an intracellular receptor and as a transcriptional factor once bound to its ligand, 5α-dihydrotestosterone [20]. AR acts as transcriptional activator of the *AR* gene which represents a positive feedback loop through activation of its own transcription upon binding to DHT. AR activation also leads to transcription of genes essential to prostatic epithelial homeostasis and decrease risk of malignant progression during prostate carcinoma (PCa). Circulating levels of testosterone and intraprostatic DHT decrease with age compromising the proper function of the prostate gland and the ability to maintain adequate levels of zinc, citrate and KLKs. Impairment in the ability of the prostate to maintain high levels of zinc and citrate causes a metabolic switch favoring mitochondrial respiration, a metabolic state that promotes prostatic epithelial cell carcinogenesis [5].

The human prostate is an immunocompetent organ with resident cells that consist of scattered stromal and intraepithelial T and B lymphocytes, macrophages, and mast cells [21]. The prostate is the target site of various types of inflammatory and infectious

conditions and can also undergo benign and malignant proliferative changes with increased incidence in the aging male [5].

### 1.2.1. Benign Prostatic Hyperplasia

Inflammation in the prostate is likely to promote structural changes commonly associated with benign and malignant processes [21]. In addition, inflammation is reportedly associated with the onset and progression of benign prostatic hyperplasia (BPH). Androgens and growth factors (such as KGF and EGF), have been extensively studied and are known to play a critical role in the onset and progression of BPH. Androgens and the aforementioned growth factors promote proliferation of the prostatic tissue. These critical players, in concert with infiltrating inflammatory cells and pro-apoptotic growth factors such as TGF-1, promote the chronic wound healing process leading to prostatic enlargement [22, 23]. T and B lymphocytes and macrophages in the adult male prostate can stimulate cytokine release (IL-6, IL-8 and IL-7) and increase growth factor concentration by promoting their release (IL-2, IFN-γ, FGF-2 and TGF-β) thus damaging epithelial and stromal cells. These events promote an abnormal remodeling process followed by fibromuscular growth [21]. Additionally, chronic inflammation due to infections, dietary factors, hormonal changes, corpora amylacea and urine reflux can contribute to prostate cancer etiology [24].

Benign prostatic hyperplasia (BPH) is a condition characterized by growth of the prostatic tissue late in life. BPH is the most common non-malignant proliferative abnormality found in any internal organ [25, 26] and one of the most common diseases of older men [26]. Prostate adenocarcinoma is a malignant condition characterized by abnormal

enlargement of the gland with subsequent loss of function due to formation of new ductal-acinar architecture [25]. Hormone-dependent growth and anti-androgen therapy are common traits shared by BPH and PCa. While both, BPH and PCa are characterized by abnormal enlargement of the prostate, they differ in the histological features and localization [27]. Histologically, BPH is defined as microscopic or macroscopic nodules with hyperplasia of stromal cells and epithelial cells, to a lesser extent, often times located in the transition zone of the prostate gland [28]. Prostate adenocarcinoma arises primarily from epithelial cells in the peripheral zone and only a small proportion from epithelial cells in the transition zone [28, 29]. Unlike PCa, BPH is not a lethal disease; however, it can cause morbidity and reduce quality of life [27].

Although BPH and PCa frequently coexist, it is not all clear if BPH is a precursor of PCa [27]. Some reports suggest that BPH is not a known risk factor for PCa [26] while others suggest that larger and more thorough epidemiological studies are needed to understand the intricate pathways connecting BPH and PCa [27]. Certainly, the strongest predictor of PCa risk is age along with family history [26]. The etiology of both BPH and PCa is not well understood, although they have shared risk factors including inflammation, metabolic factors, hormonal influences and genetic variation [27]. BPH is reported to affect 70% of men over the age of 70 years [30].

### 1.2.2. High Grade Intraepithelial Neoplasia (HGPIN)

High Grade Prostatic intraepithelial neoplasia (HGPIN) is the only widely accepted histological condition and precursor of invasive PCa [31-33], although it is unclear if HGPIN arises from normal prostatic tissue or dysplastic epithelial cells [34-37].

Morphologically, prostatic epithelial neoplasia (PIN) is presented as an atypical epithelial proliferation within the pre-existing prostatic acini and ducts. A PIN gland has a benign architecture yet lined with atypical cells [33]. On the basis of the degree of cytological atypia, PIN is divided into low-grade (LGPIN) and high-grade (HGPIN) [38]. Although HGPIN can be referred to as PIN, it is important to make the distinction between low and high-grade given the strong association of HGPIN with invasive PCa [39-42].

The evidence suggests that HGPIN shares many histopathological, morphometric and genetic features with PCa [43, 44]. Associations between PIN and PCa have been made since the first autopsy studies of prostate glands in the 1950's [29]. Many reports examining the histology, biochemistry, epidemiology and genetics of the two diseases have confirmed the initial findings [27]. Davidson et al. reported a 15-fold increase in relative risk of PCa on repeat biopsy if HGPIN was present in the initial biopsy [45].

Ashida et al. provided further evidence demonstrating that the genetic expression profile in HGPIN is very similar to that of PCa. In this study, the molecular features of HGPIN were compared to early stage PCa and normal prostatic epithelium [46]. Using hierarchical clustering of the gene transcripts the study showed that HGPIN morphological features clustered with that of the low grade PCa cases. Moreover, the screen identified 21 upregulated and 63 downregulated genes common to HGPIN and PCa compared to normal prostatic epithelium. Interestingly, genes upregulated in both, HGPIN and PCa included *AMACR* (α-methyl acyl-CoA racemase), *OR51E2* (olfactory receptor, family 51, subfamily E, member 2), *RODH* (3-hydroxysteroid epimerase) and *SMS* (spermine synthase), all of which are presumably involved in early stages of PCa [47-51]. Two genes that were downregulated during progression from normal prostatic

epithelium to HGPIN and PCa were *SERPINB1* and *SERPING1*. SERPING1 decreased expression is observed in PCa and it has been correlated to higher Gleason score and lower overall survival [52]. SERPINB1 decreased expression has also been associated with metastatic and locally advanced PCa and it is a predictor of poor outcome. Therefore, SERPINB1 and SERPING1 are considered key regulators of prostate growth. Considering that almost all the genes that were up- or downregulated in HGPIN were also up- or downregulated in PCa strongly suggests HGPIN as a precursor to PCa [46].

Detection of HGPIN is important because it has a high predictive value as a marker of adenocarcinoma with cancer developing in most patients within 10 years. Therefore, detecting these lesions is important in devising a clinical plan of action. Biopsy, the only means of detection, needs to be performed repeatedly to monitor the presence of invasive carcinoma [33]. Current standard of care upon an initial HGPIN finding in a biopsy includes a secondary biopsy between the time of the finding and 6 months [38] (**Table 2**).

HGPIN often shows a moderate increase in total prostate specific antigen (PSA) levels and a low percentage of free PSA (fPSA) [53]. Although percentage of fPSA in serum is low in patients with prostate cancer is still significantly lower compared to the percentage of fPSA in men with HGPIN alone, BPH and a normal prostate [54] [55]. A study evaluating levels of fPSA in normal, BPH, HGPIN and PCa patients showed that those in the normal prostate group had higher percentage of fPSA (27.7) when compared to those in the HGPIN (20.8%), BPH (20.1%) or PCa (14.9%). While there was no significant difference in the percentage of free PSA in men with HGPIN compared to those with PCa, there was significant difference between those in the HGPIN compared to the normal

group [54]. Importantly, HGPIN did show significantly lower percentage of fPSA indicating a tendency towards malignancy.

**Table 2**. High grade intraepithelial neoplasia (HGPIN) clinical, molecular, and demographical characteristics. Adapted from Zhou et al. [38].

| | |
|---|---|
| **Definition** | • Secretory epithelial proliferation with severe cytological atypia within the pre-existing prostatic acini and ducts |
| **Prevalence, Race and Age Distribution** | • Increased prevalence with age<br>• Higher prevalence and more extensive HGPIN in African Americans (7-91%) compared with Caucasian Americans (8-53%) between third and eight decades[1] |
| **Clinical Features** | • Does not result in abnormal digital rectal examination (DRE) or elevated PSA<br>• Diagnosis is only by histological examination |
| **Radiological Features** | • May appear as a hypoechoic lesion, indistinguishable from PCa |
| **Molecular and Genetic Features** | • Incidence of aneuploidy of 50-70%<br>• Chromosome 8 changes: loss of 8p and gain of 8q<br>• Gains of chromosome 10, 7, 12, and Y<br>• Loss of 10q, 16q and 18q<br>• Decreased expression of NKX3.1 (prostate specific homeodomain transcription factor) and p27 (cell cycle regulatory protein)<br>• *TP53* gene mutation and protein accumulation and *c-myc* (*MYC*) gene amplification in some lesions<br>• 70% of the lesions present *GSTP1* (detoxification) inactivation by promoter hypermethylation<br>• Overexpression of α-methylacyl-coA racemase (AMACR) |
| **Prognosis and Treatment** | • Presumptive premalignant lesion<br>• 20-25% risk of finding PCa on subsequent biopsy if found at initial biopsy<br>• Re-biopsy (0 to 6 months)<br>• No treatment for HGPIN as an isolated finding in needle biopsy |

[1]Biopsy study

Cancer prediction following a diagnosis of HGPIN on needle biopsy remains a controversial topic. In a recent publication, Tosoian et al. provides a general overview of recent published studies examining the risk of PCa following isolated HGPIN diagnosis

on prostate biopsy [56]. In view of the dramatic shift on prostate cancer screening and diagnosis in the past 10 years, they make the following assertions regarding approach to management of patients with HGPIN findings:

- The risk of PCa detection following a positive HGPIN biopsy is only ~20-30%, which is not significantly higher than that following a benign biopsy
- PCa diagnosis following HGPIN primarily fall under Gleason grade group 1 (Gleason 6).
- Repeat biopsy is not required for men with a single core positive to HGPIN.
- Multifocal diagnosis of HGPIN on initial biopsy may have an increased risk of PCa on repeat biopsy. Monitoring could include serum and urine tests or imaging.

The standard of care approach that dictates a need for repeat prostate biopsy following an initial diagnosis of HGPIN was also examined in an earlier study. In this retrospective study including 245 men, Kronz et al. investigated how various HGPIN-related factors, other than clinical and pathological variables, could predict cancer following an initial HGPIN finding on a needle biopsy [4]. The variables included: number of HGPIN glands, maximum percentage of gland involved by HGPIN, nucleolar prominence, percentage of cells with prominent nucleoli, HGPIN pattern (flat, tufting, micropapillary, cribriform), marked pleomorphism, digital rectal examination (DRE), transrectal ultrasound findings, family history of prostate cancer, serum PSA at time of HGPIN diagnosis, and rate of change of serum PSA. Interestingly, the only independent histologic predictor of cancer diagnosis they report, was the number of cores with HGPIN. As shown in **Figure 2**, men

with 1 or 2 HGPIN positive cores had 30% chance of receiving a cancer diagnosis upon follow up biopsy. Strikingly, men with 3 or more HGPIN positive cores had an increased chance (40% and 75%, respectively), of having cancer upon follow up biopsies [3, 4].

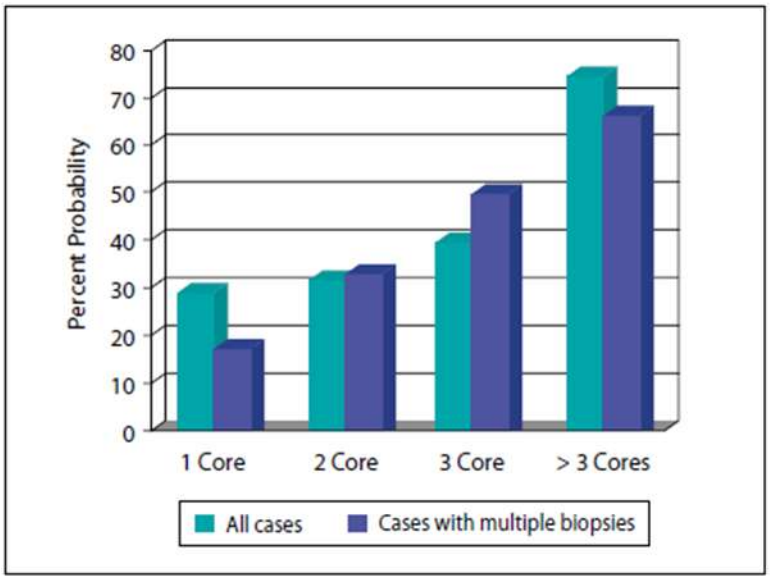


**Figure 2. Risk of PCa diagnosis upon subsequent biopsies following an initial HGPIN diagnosis.** Men with 1 or 2 HGPIN positive cores have 30% chance of receiving a cancer diagnosis upon follow up biopsy. Men with 3 or more HGPIN positive cores have an increased chance (40% and 75%, respectively) of having cancer upon follow up biopsies; as published by Partin et al. [3].

Taken together, these data provide evidence in support of the clinical utility of HGPIN diagnosis on biopsy with high cancer predictive risk in men with multifocal lesions. In these specific cases, additional follow up monitoring is necessary, and it could include multiparametric MRI (mpMRI) or assessment of serum biomarkers. It is noteworthy to mention that HGPIN is not always a feature that accompanies early PCa and some genetic features in HGPIN are not always present in PCa [32, 57, 58]. Unfortunately, significantly high levels of prostate specific antigen (PSA) are not associated with HGPIN, and these lesions cannot be detected by ultrasonography [33]. Recently, using

immunohistochemical analysis our group identified Glyoxalase 1 (GLO1), a glycolytic enzyme, to be highly upregulated in HGPIN and identified GLO1 expression as being positively correlated with early PCa progression [59]. Therefore, GLO1 could serve as an additional biomarker of clinical utility in the diagnosis of early PCa.

## 1.3. Prostate Adenocarcinoma

Epidemiologically, PCa is the leading malignancy and the second leading cause of cancer-associated deaths in the USA male population [60]. PCa is a disease of the elderly and risk prediction becomes crucial. Most patients present low-risk, relatively indolent tumors; however, 20-30% of these men present tumor characteristics associated with high-risk PCa. Such cases are more likely to progress and relapse [61].

Androgens promote cellular differentiation and proper tissue development in the prostate; however, they also promote abnormal proliferation and cell survival in prostate cancer [62]. Transcriptomic and genomic data have demonstrated the important role of androgen receptor signaling as a master regulator of cellular energy metabolism in prostate cancer. During tumor growth and progression, the androgen receptor plays a role in the reprogramming of specific metabolic pathways such as aerobic glycolysis, mitochondrial respiration, fatty acid β oxidation, and *de novo* lipid synthesis [62]. Studies have shown that ectopic expression of AR in PC3 cells (AR independent) induces a metabolic transcriptional program [63]. Testosterone and DHT are the two androgens that bind the androgen receptor (AR). DHT, however, is the most potent of them all [64, 65]. Testosterone is one of the precursors of DHT which can be inactivated by several enzymes, something that is crucial given its role in health and disease. AR expression is

found in multiple tissues with the urogenital system having the highest expression [66, 67]. Androgens are essential for the development and maintenance of the prostate gland. AR is primarily expressed in the luminal epithelial cells where it functions to promote the secretory phenotype of the prostate. In these cells, AR modulates specific genes in pathways associated to cell division, mitosis, cell cycle progression, and homeostasis of the steroid biosynthesis process [68]. PCa is therefore a hormone-dependent disease which relies in the androgen signaling pathway in order to promote cell proliferation and survival [69, 70]. The role of AR in PCa is such that androgen depravation therapy using anti-androgens (AR antagonists; enzalutamide) is the therapy of choice following PCa recurrence in men with clinical history of prostatectomy or radiotherapy. Unfortunately, most cases eventually become castration-resistant with 80% of the cases linked to AR reactivation via various mechanisms including, genomic amplification, mutation, and duplication of an upstream enhancer of AR leading to its increased expression [71-74]. In addition, tumor cells can also turn to *de novo* synthesis of steroids also known as intracrinology [69].

Citrate concentration in normal human prostate is between 8,000-15,000 nmol/g tissue compared to the lower concentrations found in other tissues (150-450 nmol/g). BPH epithelial cells are also considered citrate-producing cells since they produce similar levels of citrate as those produced by the cells in the peripheral zone. PCa citrate levels range from 1,000-2,000 nmol/g tissue and are thus considered citrate-oxidizing cells. Malignant cells also have reduced levels of zinc. This is of particular importance because normal epithelial cells of the peripheral zone are the ones associated with high levels of citrate and zinc and it is in this zone where most prostate malignancies arise [6].

Consequently, low citrate levels represent a molecular hallmark of PCa distinguishable from normal prostatic tissue and BPH. It was proposed that this biochemical alteration well precedes any obvious histological changes [75]. Indeed, the pathogenesis of PCa involves early metabolic transformation—from citrate-accumulating to citrate-oxidizing states—evident during the premalignant stage and maintained post the initial neoplastic steps during malignant transformation. These changes represent a critical step and a requirement in the progression towards malignancy: cells incapable of undergoing such metabolic transformation will stall and arrest.

## 1.4. Prognostic, Predictive and Diagnostic Biomarkers in Prostate Cancer

The clinical and molecular heterogeneity of PCa demands the use of prognostic, predictive and diagnostic biomarkers to guide treatment selection. The first step in a patient journey involves accurate diagnosis, grading and staging of PCa to further guide tissue-based molecular biomarker testing and disease management. To date, Gleason grade, developed in 1960s by Dr. Donald Gleason, remains the most prognostic indicator in prostate cancer. Briefly, Gleason grade is assigned based on the histological pattern of the prostate tissues and it ranges from 1 (normal) to 5 (most abnormal). Gleason score, which is used to determine Gleason group, ranges from 2 to 10 and it is the sum of the two most predominant patterns [76]. Importantly, Gleason grading does not inform the molecular status of tissue biomarkers. Prognostic biomarkers are of clinical utility as they inform whether definitive therapy is required in patients with localized or metastatic disease. In the case of localized disease, treatment options range from active surveillance

(AS) to a more invasive approach involving radical prostatectomy and radiation therapy. Therefore, diagnostic and prognostic biomarkers play a crucial role in a clinician's therapeutic approach.

### 1.4.1. Prognostic Biomarkers

A prognostic biomarker is defined as that which estimates the overall likelihood of an adverse clinical outcome, regardless of the specific therapeutic setting. Current prognostic biomarkers for clinically localized PCa include the proliferation marker Ki-67, PTEN (tumor-suppressor) loss and mRNA-based signatures. Importantly, Ki-67 and PTEN represent the most promising single IHC markers to date [77].

**Ki-67:** Protein encoded by the *MK167* gene, first described in Hodgkin lymphoma as highly expressed in cycling or actively proliferating cells but not in resting cells [78]. Ki-67, a regulator of cell cycle progression, has become the gold standard IHC cell proliferation marker [79-82]. In the pathology lab setting, Ki-67 labeling index (LI) or Ki-67 score is the fraction of positive tumor cell nuclei [83]. Several studies have consistently shown the prognostic value of Ki-67 in localized PCa. Specifically, the prognostic effect was observed on endpoints including biochemical recurrence (BCR)-free survival, disease-specific survival, metastasis-free survival, and overall survival [84]. Other studies have shown the independent prognostic value of Ki-67 in core needle biopsies [85-87]. Ki-67 LI was shown to be an independent prognostic factor of postoperative biochemical-free recurrence in preoperative biopsies with low volume or low Gleason grade (<7) prostate cancer [88]. In addition, Ki-LI emerged as an independent prognostic marker of tumor-specific survival in biopsies diagnosed with low Gleason grade (group 1 and 2)

[87]. Current efforts are geared towards standardization of the Ki-67 scoring as this has represented a major hurdle in validating its prognostic value and implementation in the clinical setting. Nevertheless, Ki-67 LI is a promising biomarker for AS patient selection.

**PTEN**: The Phosphatase and tensin homolog is a lipid phosphatase and a tumor suppressor in humans encoded by the *PTEN* gene. The specific role of the PTEN protein is to halt the oncogenic PI3K/AKT signaling cascade [83]. Loss of PTEN in primary PCa often results from genomic deletion, genomic rearrangement and less frequently, truncating mutations, all of which lead to its inactivation [89]. PTEN loss is among one of the most common molecular alterations in PCa, hence emerging as a robust prognostic biomarker. Fluorescence in situ hybridization (FISH) and IHC are the most common assays, and with high level of concordance, used in the clinical setting to detect *PTEN* deletions or rearrangements and protein loss, respectively [89-92]. PTEN loss is positively correlated with Grade Group and pathological stage [93]. PTEN loss in surgically treated patients is commonly observed in 20% of the patients with the prevalence increasing to 40% in metastatic tumors [94]. The prognostic value of PTEN loss comes from studies reporting a statistically significant increase in the hazard ratio (HR; 1.2 to 1.5) of BCR compared to tumors with intact PTEN [95-98]. *PTEN* zygosity dictates patient outcome: hemizygous genomic deletions generally present better outcomes than those with homozygous deletions but worse than those with the intact gene [95]. Similar to gene status, heterogeneous or subclonal protein loss results in better outcomes than those patients with clonal or homogeneous PTEN loss but worse than those with the intact protein [90-92]. Importantly, the prognostic utility of PTEN status in association with metastatic or lethal PCa has remained highly significant in nonsurgical cohorts including

transurethral resection of the prostate or needle biopsy samples managed conservatively [99, 100]. Moreover, two large studies in surgical cohorts with metastasis or death as an outcome demonstrated that PTEN loss was significantly associated with the risk of lethal PCa (HR between 2 and 5) [101, 102]. Regarding PTEN association with *ERG* gene rearrangement, loss of PTEN in the context of *ERG* rearrangement has better outcomes than in the absence of *ERG* rearrangement [100, 101, 103]. In other words, PTEN loss is strongly associated with increased risk of lethal PCa in ERG-negative tumors but not with ERG-positive tumors. In ‘Grade 1’ group tumors PTEN loss, as detected at the time of biopsy, increases the likelihood of upgrading to ‘Grade 2’ group or higher at radical prostatectomy [104]. Finally, a small case-control study showed a very interesting trend. The study found that PTEN loss was less common in patients who remained AS after 8 years of follow up compared to those with rapid upgrading [105].

Based on the previously discussed findings, the International Society of Urological Pathology (ISUP) on its 2020 report [83] made the following remarks regarding the use of PTEN and Ki-67 LI:

- Ki-67 LI and PTEN are potential useful prognostic biomarkers for Grade Group 1 (and/or Grade Group 2) PCa biopsies for determination of AS eligibility.
- High Ki-67 LI or PTEN loss would be one, among other indicators, suggesting definitive patient treatment. Intact PTEN would only be an informative result.
- The single highest grade/highest tumor volume core could be subject to testing, by IHC or FISH, with the option to testing additional cores to better capture tumor heterogeneity and cases with subclonal PTEN loss.

**mRNA-based Genomic Signatures:** These new methods are gaining popularity particularly in cases with localized PCa due to their ability to aid in prognostication, risk stratification and potential therapy response [106-108]. These tests have also been useful for AS cases [109, 110]. Table 3 highlights the most common mRNA tests available in the clinical setting, description of the assay as well as a brief description of the resuls.

**Table 3**. Commercially available RNA-based tests for analysis of PCa- associated mutational status and diagnosis. Adapted from Lotan et al. [83].

| Test | Sample type | Assay Description | Results |
|---|---|---|---|
| Oncotype Dx Genomic Health™ | Biopsy-based | RT-PCR expression analysis of 17 genes (pathways: androgen signaling, stromal response, cellular organization and proliferation). | GPS (0-100); likelihood of freedom from 4 or high Gleason score and/or non-organ confined disease. |
| Polaris (CCP) Myriad Genetics™ | Biopsy tissue-based test for patients who are AS candidates Prostatectomy tissue-based test to determine the relative risk of BCR. | Analysis of 46-gene expression signature by RT-PCR. Explores cell cycle progression genes. | Biopsy: estimates 10-year mortality risk. Post-surgery: estimates 10-year risk for BCR. |
| Decipher GenomeDx Biosciences™ | Prostatectomy tissue-based. Also used in needle biopsy to predict adverse pathology and oncology outcomes following radical prostatectomy. | Analysis of 22 gene expression using Affymetrix microarrays. Explores multiple pathways. Measures the tumor's metastatic potential. | Probability of metastasis 5 years post-surgery and 3 years post-PSA recurrence. |

GPS= Genomic Prostate Score

There is considerable progress made in the field of RNA-based assays and their utility in PCa prognosis; however, prospective studies evaluating their utility in AS cohorts are still

needed. Furthermore, additional validation studies evaluating the reliability of these tests to provide information on adjacent higher grade tumor areas are also needed. PCa is a heterogeneous disease characterized by multifocal regions hence potential for undersampling remains a concern. [83]. Regarding mRNA-based genomic signature assays, the ISUP states that these assays are of potential benefit in the AS and post-radical prostatectomy setting if the tumor area was adequately sampled. However, it is important to remember the need for further studies assessing the performance of these assays in relation to tumor heterogeneity. These studies will provide further understanding on the proper way to perform such tests (i.e., how many biopsies to test, which biopsies to test, etc).

### 1.4.2. Predictive Biomarkers

By definition, predictive biomarkers estimate the chances of response to a specific therapy, in other words, they are used to stratify patients based on likelihood to experience a favorable or unfavorable effect [77]. In the context of PCa, predictive biomarkers have been primarily studied in metastatic disease with only a few validated tissue-based predictive biomarkers available. Predictive biomarkers for advanced disease state such as *BRCA2* loss or mismatch repair gene defects can guide treatment options of poly-ADP ribose polymerase (PARP) inhibition or immune check blockade. Androgen receptor signaling inhibitors and chemotherapy are therapies guided by the presence of androgen receptor-related biomarkers or those detecting the presence of neuroendocrine PCa [83].

**DNA Repair Deficiency:** This represents an area of great diagnostic and therapeutic opportunity [111]. Surprisingly, recent sequencing data in metastatic PCa showed high rate of genomic alterations in genes involved in homologous recombination DNA repair pathways. About 20% of advanced castration resistant prostate cancer (CRPC) most commonly bear alterations in the *BRCA2*, *BRCA1*, and *ATM* genes [73]. From this data we learned that close to 10% of CRPCR cases bearing homologous recombination defects (HRD) present germline mutations in the aforementioned genes [73, 112]. The *BRCA2* and *ATM* germline mutations are seeing more frequently in lethal compared to indolent primary PCa [113]. Importantly, HRD mutations are far more prevalent in the aggressive primary PCa (Gleason pattern 5, ductal and intraductal PCa) than metastatic cases [114-118]. Mutations in the mismatch repair pathway are also more enriched in metastatic (10%) compared to the primary prostate cancer setting [119-121] yet they are more prevalent in primary tumors with aggressive histology [114, 122, 123]. However, compared to HRD, mismatch repair mutations (MMR) germline mutations are not as frequent unless they are associated with Lynch Syndrome [124, 125]. The National Comprehensive Cancer Network (NCCN) currently recommends germline testing of patients with clinically localized PCa in the high-risk subset (Grade Group 4 or higher or PSA $\geq$20 ng/mL) [126]. In addition, HRD and MMR testing should be offer to metastatic patients. HRD assessment can be performed via sequencing while MMR is performed by IHC via labeling of the MSH2, MSH6, MLH1 and PMS2 proteins [83].

One of the most frequently altered genes in CRPC is *AR* [127, 128]. The *AR* gene is often the target of point mutations and amplifications, amplification of *AR* signaling enhancers as well as expression of AR splice variants lacking the ligand binding domain resulting in

its constitutive activation [72, 73, 129-132]. Indeed, large scale genomic studies demonstrated that at least 50% of CRPC cases harbor these mutations [72, 73, 129, 130, 132]. One of the most common splice variants in CRPC is the *Arv7* gene; however, its detection in tissue has not proven strongly prognostic or predictive in these cases. On the contrary, *Arv7* detection in circulating tumor cells (CTC) using RT-PCR or IHC has shown prognostic value in the context of AR signaling inhibitors in CRPC [133-136]. The predictive value of Arv7-positive CTCs by IHC has been previously demonstrated in retrospective studies [137]. In addition, *AR* amplifications by cfDNA have also proven highly prognostic in retrospective clinical trials as well as prospective/retrospective nontribal cohorts [136, 138-144]. Although all these studies show promising results, further clinical validation of these methodologies is still required. In fact, the ISUP states that, at present, assessment of *AR* alteration in tissue has no clear clinical utility and that although Arv7 and AR amplification may be predictive, the evidence is not sufficient to justify testing. Nevertheless, *AR* amplification and *Arv7* expression are good prognostic biomarkers in CRPC [83].

### 1.4.3. Diagnostic Biomarkers

A diagnostic biomarker is used for identification of individuals positive to a disease or to define a subset of the disease [77]. These are the type of biomarkers Pathologists commonly deploy to assist in the initial diagnosis on core biopsies [83]. Our primary focus on this section will be IHC tissue-based diagnostic biomarkers.

**PSA:** The prostate-specific antigen (PSA), a blood-based biomarker discovered in 1970 by Richard Ablin [145], has been the measurement to indicate possible prostate cancer and biochemical recurrence post-treatment [146]. PSA exists as an inactive precursor enzyme which is activated via posttranslational cleavage of the amino acid pro leader sequence by human kallikreins 2 and 4 to form the mature PSA molecule [147]. PSA is produced by prostatic epithelial cells and secreted into the lumen to help in the liquefaction process of the semen ejaculate. Elevated PSA levels have been used as a biomarker of prostate cancer; however, pathological conditions including BPH, and prostatitis can elevate PSA levels thus yielding a 'false positive' result. Despite being prostate specific yet not specific to cancer, PSA measurement has led to decrease prostate cancer mortality. However, the poor specificity of PSA for prostate cancer, has led clinicians to over-diagnose and over-treat men with clinically insignificant disease [146]. Perspective studies have shown that 10% of patients subjected to radical prostatectomy or radiation therapy were overt-treated [148]. Not only that, but PSA also has low sensitivity. Current recommendation by the United States Preventive Services Task Force (USPTF) suggests the use of PSA testing for men ages 55-69 on a case-by-case basis and with informed patient consent [149].

**PSMA:** Prostate-specific membrane antigen (PSMA) is a transmembrane glutamate carboxypeptidase present on the surface of prostate cancer cells. PSMA is detectable in prostate tissue, PCa cells, and serum [150, 151]; however, it is not prostate-specific and can be detected in other tissues including central nervous system, small intestine, and salivary gland [152]. PSMA is expressed in benign and malignant prostatic cells yet levels of PSMA found in PCa patients are significantly higher [151]. Studies have shown an

increase in PSMA levels following hormone depravation therapy detectable in most metastatic CRPC. Higher levels of PSMA are associated with poor clinical outcomes and reduced cell survival [151]; therefore, PSMA is regarded as an independent marker of poor prognosis. It was recently demonstrated that PSMA has an internalization signal allowing internalization of the cell surface protein into an endosomal compartment. This distinctive feature makes PSMA not only a diagnostic marker but a promising therapeutic target [153]. Recently, the Food and Drug Administration approved the use of a $^{6}$8Ga-PSMA-11, a radioactive imaging agent that binds to PSMA, to help localize prostate cancer cells. PSMA-PET/CT is a useful imaging used not only to detect PCa in a more efficient manner but to also assess response to chemotherapy. In a recent retrospective study, PSMA expression changes as assessed by PSMA-PET/CT were associated with response to therapy and could independently predict OS [154].

**HMWCK and p63**: IHC is most commonly used for identification of basal cells during the evaluation of the prostate tissue. Basal cells are absent in PCa; however, in conditions such as adenosis, partial atrophy and HGPIN these can be very patchy and even absent. High molecular weight cytokeratin (HMWCK; 34βE12, cytokeratin [CK] 5/6) [155-160] and p63 [161-163] are the most commonly used basal cell antibodies. The HMWCK antibody cocktail is cytoplasmic while p63 is a nuclear antibody. A common practice is the use of a double cocktail combining HMWCK and p63 to increase sensitivity of basal cell detection, decreasing staining variability [47, 164, 165]. In spite of their specificity, there are some aberrant cases of acinar adenocarcinoma positive to HMWCK and p63 (to a lesser extent). This phenomenon, if present, is commonly seeing in acinar adenocarcinoma with Gleason score 8 to 10; however it can also be encountered in small

foci of Gleason pattern 3 [166]. In addition, some aberrant cases with diffuse expression of p63 have been described; however, these cases can be identified as follows: a) strong and diffuse p63 staining within the malignant glands; b) most cases with aberrant p63 show very distinct infiltrating gland morphology, nests and cords with atrophic cytoplasm, hyperchromatic nuclei, and visible nucleoli; and c) they are negative to basal cell markers such as 34βE12 and CK 5/6 [167].

**α-Methylacyl-CoA-racemase (AMACR):** Also known as p504S or racemase, this enzyme plays a role in the β oxidation of branched-chained fatty acids and their derivatives [168]. Racemase was first identified by cDNA library subtraction in conjunction with high throughput microarray screening from prostate carcinoma [169]. It is selectively overexpressed in PCa and absent in benign prostatic tissue [169]. Racemase can easily be detected by IHC and, given that the vast majority of prostate cancers are positive for it, the sensitivity can be from 82% to 100% [170-176]. Per ISUP recommendations, racemase can be used in combination with HMWCK and/or p63 in a double or triple cocktail assay [167]. Here, HWCK and p63 are labeled with a brown chromogen while a red chromogen labels AMACR. The triple stain methodology has proven superior to the single use of basal cell markers [169].

**ERG**: Perhaps one of the latest biomarkers proposed in the field of PCa diagnostics. The ETS-related gene (ERG) is a member of the e-26 transformation-specific (ETS) family of transcription factors. The primary role of ERG is critical during the developmental phase where it participates in the process of vasculogenesis, angiogenesis, hematopoiesis, and bone development [177]. Although ERG alone has oncogenic potential and it is

associated with Ewing's sarcoma and leukemia, its association with PCa is the result of a gene fusion. *ERG* is overexpressed in approximately 40% to 50% of PCa as a result of a gene fusion with the androgen-driven promoter of the transmembrane protease serine 2 gene (*TMPRSS2*) [167, 177]. These gene fusion is highly specific to prostate cancer; however, it can also be found in 16% to 20% of HGPIN [167]. Anti-ERG antibodies targeting the *TMPRSS2-ERG* gene fusion have been developed and correlate well with fusion-positive cancer.

Unlike any other cancer types, PCa is a very unique type of cancer from the metabolic standpoint. Although we discuss normal and PCa metabolism in Chapter II, it is important to highlight some advances related to biomarker development specifically targeting PCa metabolism. As mentioned before, PCa is a disease of the elderly and risk prediction becomes crucial. Earlier stage intervention may limit the development of Prostate cancer. High-grade prostatic intraepithelial neoplasia (HGPIN) is the only widely accepted histological condition preceding PCa, although it is unclear if HGPIN arises from normal prostatic tissue or dysplastic epithelial cells [34-37]. Furthermore, high-grade intraepithelial neoplasia (HGPIN) is a frequent precursor to invasive cancer and represents a premalignant state. Indeed, promising novel biomarkers and approaches are emerging in the field of prostate cancer diagnostics seeking to identify early PCa precursors. One such study used pre-biopsy diffusion-weighed imaging (DWI) and magnetic resonance spectroscopic imaging (MRSI) to detect HGPIN lesions to correlate with PCa diagnosis on clinical follow up. They observed decreased metabolite ratio [citrate/(choline+creatine)] for voxels of HGPIN regions at initial biopsy compared to normal peripheral zone. Interestingly, HGPIN metabolite ratio values were very similar to

patients diagnosed with PCa on follow up biopsy [178] highlighting the clinical utility of metabolic-based tests. Another promising biomarker is GLO1, a glycolytic enzyme recently identified as being highly upregulated in HGPIN and differentially expressed in normal prostatic tissue [59]. In Chapter II we further discuss the role of GLO1, and, in Chapter IV, we present evidence to support the novel role of GLO1 as a novel biomarker of early PCa development.

Other approaches in the field of PCa diagnostic take advantage of the known metabolic switches occurring during PCa development. For example, taking advantage of the known citrate depletion, combination of MRI and spectroscopy has proved useful in the detection of citrate depletion [179]. In addition, citrate and α-ketoglutarate depletion as measured via spectroscopy, have been investigated for their clinical utility [180]. The metabolic switch that occurs as a result of malignant transformation from normal to cancerous prostatic cells is in line with previous observations of a highly efficient TCA cycle. This is presumably as a result of AR signaling aiding to the maximum delivery of substrates to the mitochondria. Other studies report increased levels of ACO2, citrate synthase (CS), fumarate hydratase (FH), malate dehydrogenase (MDH2) and oxoglutarate dehydrogenase (OGDH) as well as some of their substrates (malate, succinate and fumarate) [181, 182]. Measurement of these metabolites for early PCa detection may prove useful in the clinical setting, especially if they can predict aggressive disease. Srihari et al., given the unique role of metabolism in prostate cancer, sought to understand the metabolic profile of PCa tumors that show aggressive relapse outcomes [183]. Resourcing to the TCGA (The Cancer Genome Atlas) mRNA expression (RNAseq) dataset, they clustered the most altered genes in the major metabolic pathways including

carbohydrate, lipid, amino acid, TCA cycle, vitamin, and cofactor metabolism. Based on this clustering, they identified six metabolic subtypes defined by C1-C6. Metabolic subtypes C5 and C3 are the ones that showed the fastest relapse in addition to having the most deregulated in pathways including synthesis and catabolism of sphingolipids and glycosphingolipids, glycosaminoglycans, glucose and galactose metabolism. Not only that but these metabolic groups, were enriched for genetic alterations in the ATM, *BRCA1*, *TP53*, *STK11*, *FANCA*, *MSH2* and *FOXA* genes. These suggests a link between these genetic alterations and the metabolic profile of these groups. Importantly, biochemical relapse for the C5 and C3 subtypes was not associated with the early relapse seeing for these two groups; these two groups showed considerable late BCR. This study further demonstrates the complexity of PCa metabolism and supports the idea that there needs to be better indicators of early aggressive PCa diagnosis other than PSA [183].

# CHAPTER II

## The Emerging Role of Energy Oncometabolites in the Origin and Progression of Prostate Cancer

## 2.1. Prostate Tumor Metabolism

Prostate tumor metabolism is as unique as the citrate-focused metabolism in the normal prostate gland. Citrate concentration in normal human prostate is between 8,000-15,000 nmol/g tissue compared to the concentration found on other tissues of 150-450 nmol/g tissue. BPH epithelial cells are also considered citrate-producing cells since they produce similar levels of citrate as those produced by the cells in the peripheral zone. PCa citrate levels range from 1,000-2,000 nmol/g tissue and are thus considered citrate-oxidizing cells. Malignant cells also have reduced levels of zinc. This is of particular importance because normal epithelial cells of the peripheral zone are the ones associated with high levels of citrate and zinc and most of the prostate malignancies arise in the peripheral zone [6]. Therefore, low citrate levels are a hallmark of PCa and a distinguishable characteristic from normal and BPH. It was proposed that this biochemical alteration well precede any obvious histological changes [75]. Indeed, the pathogenesis of PCa involves early metabolic transformation—from citrate accumulating to citrate-oxidizing— are evident during a premalignant stage, post the initial neoplastic steps in the continuum of malignant transformation. Thus, this represents a critical step and a requirement in the progression towards malignancy: cells incapable of undergoing such metabolic transformation will stall and arrest.

Prostate Intermediary energy metabolism in normal and malignant prostate involves zinc and altered citrate-related intermediate metabolism. Secretory epithelial cells (peripheral zone) are uniquely and highly specialized in zinc accumulation and citrate production. On the other hand, glandular cells of the central zone oxidize citrate and do not accumulate zinc [6]. Therefore, in normal epithelial secretory cells, citrate becomes the end product

of intermediary metabolism, [6] and it is bioenergetically costly. Studies in the early 40's and 70's reported that human prostatic adenoma tissue exhibited low respiratory rate and high aerobic glycolysis [6]; however, this studies were executed using a mixture of prostatic tissues containing various stromal components which may have confounded the results. Studies assessing prostatic epithelial cells only are needed to confirm such findings. Interestingly, Phosphofructokinase (PFK), a key regulator in the glycolytic pathway, is negatively modulated by citrate—and ATP—in mammalian cells, that is, when citrate levels rise, a feedback control occurs to decrease glycolysis. This occurs in mammalian cells when citrate levels reach concentrations of up to 0.5 mM; paradoxically, in normal prostate cells where citrate concentrations reach the 40-150 mM, PFK should be expected to be completely inhibited leading to low glycolytic rates, yet these cells exhibit high glycolytic flux, representing a molecular phenomenon that warrants further investigation.

As described in Chapter I, zinc accumulation in the normal prostatic epithelium leads to inhibition of mitochondrial aconitase and truncation of the TCA cycle and preservation of citrate, a physiologically relevant molecule secreted as part of the seminal fluid. During oncogenic transformation, there is a loss of zinc transporters leading to zinc depletion and reactivation of the TCA cycle. Citrate is then oxidize or secreted to the cytoplasm when it serves as a substrate in lipogenesis [184]. Although AR is not responsible for the downregulation of zinc transporters, it promotes deregulated cellular proliferation by directly regulating various metabolic pathways, specifically glycolysis.

Unlike other tissues, the prostate gland has a unique metabolic program, which is highly specialized to enable production of prostatic fluid. Glandular secretory epithelial cells

have an impaired TCA cycle. High levels of citrate in prostatic epithelial cells impair the activity of mitochondrial aconitase preventing the conversion of citrate to isocitrate. This results in accumulation of citrate and it secretion as part of the seminal fluid [185]. Therefore, this unique metabolic program in the normal prostatic epithelium dictates the metabolic reprogramming occurring in prostate tumorigenesis and progression. Primary prostate tumors differ than the rest of the solid tumors in that they primarily rely in oxidative phosphorylation and lipogenesis rather than glycolysis ('Warburg effect') [9, 184, 186] all of which is orchestrated by AR [187, 188]. This is evidenced by the dramatic regression of PCa upon withdrawal of androgens, similar to normal prostatic tissue [187, 188]. Unfortunately, due to various mechanisms such as intracrine steroidogenesis and maintenance of intratumoral androgens [189], AR eventually reactivates leading to PCa progression, metastasis and lethality- phenomenon called castration-resistant PCa [189-195]. AR regulates expression of glycolytic players such as GLUT1, HK1, HK2, PFK2/PFKFB2 [196, 197]. It also regulates the pentose phosphate pathway (PPP) via G6PD [198], oxidative phosphorylation (MPC2 and PHD) [199, 200] among other pathways involved in cellular metabolism [196].

Consistent with these observations, clinical application of the radiolabeled glucose analogue $^{18}$F-fluorodeoxyglucose (FDG) has proven ineffective in the detection of organ-confined PCa [201]. In contrast, AR independent neuroendocrine prostate cancer (NEPC)— a progression of a final dedifferentiation of prostate adenocarcinoma enriched in the tumor during long term androgen depravation therapy (ADT)— avidity for FDG suggests a switch to a glycolytic metabolisms that occurs during the transition from an $AR^+$ to an $AR^-$ malignancy [185, 202, 203].

Studies have shown that AR can induce expression of GLUT1 (*SLC2A1*), GLUT3 (*SLC2A3*), GLUT10 (*SLC2A10*), and GLUT12 (*SLC2A12*) [204, 205]. Other glycolytic genes including *HK1*, *HK2*, *PFK*, *PFKP*, *ENO1* and *PFKFB2* (60, 62, 63). Importantly, positive regulation of LDHA by AR has been published [65, 206, 207]. Patient derived xenograft (PDX) PCa models from AR-dependent castration resistant PCa shows higher aerobic glycolysis signature compared to AR-independent PDXs [208]. Thus, AR promotes expression of the metabolic gene signature associated with the 'Warburg effect'. mTOR is also a target of AR; it becomes rapidly activated upon androgen stimulation in PCa cells, particularly after *PTEN* loss [209]. AR activation of mTOR promotes its nuclear localization where they form a complex. These factors are then co-recruited in close vicinity to genes involved in glycolysis and oxidative phosphorylation (OXSPHOS) including *SLC26A3*, *FASN*, *HK2* and *mTOR* itself. The mTOR-AR axis is involved in the metabolic reprogramming of PCa cells where AR activation of mTOR leads to induction of glucose consumption, lactate production, mitochondria biogenesis and activity, and lipid synthesis [207].

The unique features of the metabolic reprogramming in PCa have led scientist to study the metabolic profile of the disease with the sole purpose of identifying metabolic alterations. One such study [210] identified sarcosine, uracil, kynurenine, glycerol-3-phosphate, leucine, and proline increased in PCa progression. Fatty acid synthase (FASN) and 5' adenosine monophosphate –activated protein kinase (AMPK) key lipogenic enzymes are among those receiving particular attention for their potential as therapeutic targets [211]. Another important player in prostate carcinogenesis with and critical impact on metabolic reprogramming is the tumor suppressor PTEN, the primary

gene deleted in PCa. Studies have shown that genetic depletion of PTEN by siRNA in the DU-145 cell line results in an increase in most intracellular metabolites involved in glycolysis and glutaminolysis—the two main energy production pathways and carbon sources—, as well as those involved in fatty acid *de novo* synthesis, fatty acid beta oxidation and branched chain amino acid catabolism [212].

Ectopic expression of fibroblast growth factor receptor 1 (FGFR1) also contributes to PCa progression. It was reported that it exerts its effect vial the tyrosine kinase domain which regulates the expression of the various LDH isozymes thus contributing to reprogramming of energy metabolism. Specifically, FGFR1 phosphorylation of LDHA increases its stability while on the other hand it reduces expression of LDHB by inducing promoter methylation thus supporting aerobic glycolysis and the shift from oxidative phosphorylation [213]. This was evidenced in an *in vivo* study using DU-145 xenograft with CRISPR/Cas9 genetic deletion of the *Ldha* and *Ldhb* alleles. Although $DU145^{\Delta Ldha}$ and $DU145^{\Delta Ldhb}$ induced expression of compensatory glycolytic-associated proteins; ablation of LDHA resulted in smaller tumors and LDHB larger tumors compared to the parental DU-145 cell line derived xenografts [213].

Critical to this field is the identification of metabolic dependencies in PCa and NEPC, metabolic pathways and specific metabolites that can serve as therapeutic targets. One such oncometabolite still being studies in prostate cancer is methylgloxal (MG). Our group has reported upregulation of GLO1, a key MG-detoxifying enzyme, at early stages of PCa, but most importantly in HGPIN, a known precursor to aggressive PCa [59]. Given the peculiar nature of PCa metabolism, the current focus has turned to metabolites with the potential of serving as prognostic markers. Herein, we describe some of the most

prominent oncometabolites part of the glycolytic pathway, their role in energy metabolism and prostate cancer, and clinical relevance with the main focus on MG and GLO1, two effectors largely studied in our laboratory.

## 2.2. Prominent Oncometabolites in Cancer

### 2.2.1. Fructose 2,6 bisphosphate (Fru-2,6-$P_2$)

*Role in energy metabolism:* Fructose-2,6-bisphosphate results from enzymatic activity of the dual kinase/phosphatase family of enzymes 6-phosphofructo-2-kinase/fructose-2,6-bisphosphatase (PFKFB) and the TP53-induced glycolysis and apoptosis regulator (TIGAR) [214]. However, the primary enzymes involved in Fru-2,6-$P_2$ are the PFKFB family of isoenzymes. TIGAR hydrolyzes Fru-2,6-$P_2$ into Fru-6-P which can enter the Pentose Phosphate Pathway (PPP) to synthesize NADPH and ribose-5-phosphate which help reducing ROS, producing nucleotide precursors essential for DNA repair, biosynthesis and cellular proliferation [215]. Notably, Fru-2,6-$P_2$ is not considered TIGAR's primary physiological substrate [216]. Fru-2,6-$P_2$ is an allosteric activator of PFKFB, a key modulator of glycolysis and glycolytic flux, and gluconeogenesis.

The concertation of Fru-2,6-$P_2$ is determined by the activity of PFK-2 which synthesizes Fru-2,6-$P_2$ from Fru-6-P and ATP, and from fructose 2,6-bisphosphatase (FBPase-2) which hydrolyzes Fru-2,6-$P_2$ into Fru-6-P and inorganic phosphate [214]. Fru-2,6-$P_2$ has a dual function, increases the affinity of PFK1 for Fru-6-P and releases the enzyme from ATP-mediated inhibition. Fru-2,6-$P_2$ increases affinity of PFK1 for AMP (positive allosteric effector of the enzyme). In contrast, Fru-2,6-$P_2$ and AMP inhibit FBPase1 [217-221]. Fru-

2,6-$P_2$ stabilizes PFK1 and promotes tetramer association and higher oligomers with enhanced activity [218, 222]. In summary, the regulatory activity of PFK1 and FBPase1 is dependent on Fru-2,6-$P_2$ concentration [214] thus playing a key role in the Fru-6-P/Fru-1,6-$P_2$ substrate cycle and the intensity and direction of glycolysis.

Given the critical role of Fru-2,6-$P_2$ in carbohydrate metabolism, its synthesis and degradation must be regulated to allow the right concentration needed for the cell. The complexity involved in regulating Fru-2,6-$P_2$ in different tissues is dependent on the different PFK-2/FBPase-2 isoenzymes which can adapt to the different conditions [223-225]. The *PFKFB2* gene encodes for the isoenzyme present in cancer cells among other tissues. However, the *PFKFB3* gene encodes for the isoenzyme most expressed in proliferating and cancer cells and several tumor types [214]. PFKFB3 is an isozyme with high kinase and low bisphosphatase activity thus favoring synthesis of Fru-2,6-$P_2$ resulting in high concentrations of the metabolite in proliferating and tumor cells [226].

*Role in oncogenic metabolic reprogramming:* Fructose-2,6-bisphosphate concentration is significantly higher in tumor cells than normal cells [227-229]. Fru-2,6-$P_2$ promotes proliferation by indirectly promoting ubiquitination and proteosomal degradation of the Cip/Kip protein p27 [230] and it can readily activate 6-phosphofructo-1-kinase (PFK1) in human lymphomas and gliomas (PFK1 is more sensitive to Fru-2,6-$P_2$ activation) [227, 231]. PFKFB4 primary role in transformed cells and tumors is to synthesize Fru-2,6-$P_2$ via its kinase activity and it is required for the glycolytic reprogramming of cancer cells [232]. Ischemia and hypoxia induce phosphorylation of PFKFB2 (S466) which in turn increases Fru-2,6-$P_2$ and stimulates glycolysis [223, 233]. TIGAR, a regulator of Fru-2,6-$P_2$, shows an increased expression in multiple cancers. The function of TIGAR in a

specific cell type depends on the metabolic state of the cell and PFKFBs activities that determine Fru-2,6-$P_2$ [214] concentration and glycolytic flux.

In malignant human gastric tumors, PFKFB2 upregulation is associated with HIF-1α dependent genes, VEGF and Glut1 thus suggesting HIF-1α as a regulator of *PFKFB2* [234]. Hepatocellular carcinoma, metastasis–associated in colon cancer protein 1 (MACC1) correlates with high expression of PFKFB1, both of which are associated with malignant phenotype [235]. In BRAF-mutated melanoma cells, maintaining a glycolytic metabolism requires MAPK-activated RSK which directly phosphorylates PFKFB2 [236]. The SLIT2/ROBO1 axis promotes proliferation, inhibits apoptosis, and contributes to the 'Warburg effect' in osteosarcoma cells via activation of the SRC/ERK/c-MYC/PFKFB2 pathway [237]. In ovarian cancer, the long noncoding RNA LINC00092 has been identified as a nodal driver of cancer associated fibroblast (CAF)-mediated metastasis. LINC00092 binds PFKFB2 thereby promoting metastasis by inducing a glycolytic phenotype and sustaining the local supportive function of CAFs [238].

A recent study in breast cancer cells reported that exposure of T47D cells to synthetic progestins (ORG2058 or norgestrel) induced rapid increase in Fru-2,6-$P_2$ levels. The cellular mechanism involves short- and a long-term activation of PFKFB3 via phosphorylation and increased protein levels, respectively. A PRE (progesterone response element) to which PR (progesterone receptor) binds is responsible for transactivation of the *PFKFB3* gene transcription. These findings can be further confirmed by inducing PR expression in the PR-negative cell line MDA-MB-231 which in turn induces endogenous expression of PFKPFB3 in response to norgestrel. This data

demonstrates a mechanism responsible for indirect regulation of Fru-2,6-$P_2$ to promote glycolysis in breast cancer cells [239].

*Role in prostate cancer*: The androgen receptor, a regulator of prostate growth, promotes glycolysis and anabolic metabolism via transcriptional regulation of *PFKFB2* [196], a regulator of Fru-2,6-$P_2$. Other studies have shown that *PFKFB4* is essential for prostate cancer survival by balancing the use of glucose for energy production and the synthesis of antioxidants [240]. Interestingly, genetic silencing of PFKFB4 results in increased levels of Fru-2,6-$P_2$ in LnCaP, PC3 and DU-145 prostate cancer cells suggesting a primary role of a phosphatase rather than a kinase in these cells [241].

*Clinical relevance: from diagnostic marker to therapeutic opportunities:* PFKFB and TIGAR control the Fru-6-P/Fru-2,6-$P_2$ and are overexpressed in cancer cells thus serving as potential prognostic markers. Given that Fru-2,6-$P_2$ is not part of a main metabolic pathway and is not a biosynthetic precursor or intermediate in energy production, its concentration needs to be controlled via the PFKFBs. The therapeutic target here are the *PFKFB2-4* genes which are overexpressed in various tumor types and activated by hypoxia and/or oncogenes. However, the expression of more than one PFKFB isoenzymes suggests redundancy in the activity of these enzymes. It is important to develop pan PFKFB kinase inhibitors to effectively reduce Fru-2,6-$P_2$ concentrations. PFKFB3 and PFKFB4 have been proposed as good targets because they are overexpressed in cancer cells [242]. These can be used in combination with hypoxia mimetics to enhance cellular dependency in glycolysis and PFKFBs.

### 2.2.2. Lactate

*Role in energy metabolism:* Lactate (2-hydroxypropanoic acid) is a hydroxycarboxylic acid present in the human body in two stereoisomers, D-lactate and, most predominantly, L-lactate [243]. Lactic acid is a metabolite resulting from pyruvate metabolism under anaerobic metabolism of glucose when oxygen is absent or in limited supply. Lactate dehydrogenase functions to catalyze the reversible conversion of lactate to pyruvate with the reduction of NAD+ to NADH and vice versa [244]. In aqueous solutions, lactic acid dissociates almost completely to lactate and $H^+$ (pKa at 7.4 = 3.9) [245]. Under normal conditions, lactate serves as a fuel source by the heart, brain and skeletal muscle as well as a substrate for gluconeogenesis in the liver [246]. Physiological concentrations of lactate in blood and tissues ranges from 1.5 to 3 mM [247] while plasma lactate concentration is estimated to be 0.3-1.3 mmol $liter^{-1}$ [245]. Interestingly, circulating lactate act as an inter-organ carbon shuttle in mammals [248]. Lactate plasma levels reflect a balance between lactate production and lactate metabolism. Aerobically, glucose can be catabolized to lactate via the glycolytic pathway, which serves as a nutrient for tissues and tumors [249]. Furthermore, a close examination at circulating metabolites found that circulating lactate could serve as a primary carbon source for the TCA cycle and a source of energy in both, normal and tumor tissues [250].

*Role in oncogenic metabolic reprogramming:* In 1926 German physiologist, Otto Warburg, described that tumor cells uptake high amounts of glucose producing large volumes of lactate even in the presence of oxygen [251], a term later coined as ‘Warburg effect’ or ‘aerobic glycolysis’, a far less efficient means of energy production than oxidative phosphorylation. The lactagenesis state observed in tumors is maintained via activation

of numerous transcriptional factors such as c-Myc, NF-kB, and Hypoxia-Inducible Factor 1-α (HIF1α) which activation has been attributed to the 'Warburg effect' [252-254]. Lactate, previously regarded as a 'metabolic waste product', is shuttled to the extracellular space via the MCTs causing acidification of the extracellular pH (6-6.5) thus favoring metastasis, angiogenesis, and an immunosuppressive state. Tumor secreted lactate is known to polarize tumor associated macrophages (TAM) in a HIF-dependent manner under normoxic conditions. TAMs shuttle lactate from the TME via the MCT1-4, which stabilizes the HIF-1α leading to transcription of *VEGF* and *ARG1,* a set of genes associated with M2 Macrophages [255]. Expression of VEGF and ARG1 support tumor growth, tissue remodeling and immune suppression [256]. Lactate also serves as a respiratory substrate and lipogenic precursor in some cultured cancer cells [257].

Pre-surgical imaging of human NSCLC using intra-operative infusion of $^{13}$C-labeled nutrients with postsurgical analysis of metabolic tumor features revealed concomitant glycolysis and glucose oxidation [258, 259]. Further analysis showed dilution of $^{13}$C labeling between glucose and TCA cycle intermediates, implying potential oxidation of alternative fuels such lactate [259]. Indeed, studies revealed that lactate also serves as a TCA cycle carbon source for human NSCLC, a distinguishing characteristic in tumors with high $^{18}$fluorodeoxyglucose uptake and aggressive oncological behavior. In these patients, evidence of extensive TCA cycle metabolite labeling upon infusion with $^{13}$C-lactate was observed. Furthermore, reduced labeling of tumor metabolites was observed in mice infused with [2-$^{13}$C] lactate bearing MCT-1 deficient HCC15 tumors suggesting the important role of MCT-1 in lactate transport. Remarkably, *in vivo* direct comparison between lactate and glucose metabolism revealed lactate as the predominant contributor

to the TCA cycle [248]. Furthermore, using intravenous infusion of $^{13}C$ labeled nutrients in mice, Hui et al. demonstrated the circulatory turnover flux of lactate to be the highest among all metabolites even exceeding that of glucose in fed and fasting mice [250]. Remarkably, $^{13}C$-lactate widely labeled TCA cycle intermediates in all tissues. Importantly, in fasting mice, circulating lactate primarily feeds the TCA cycle in all tissues except for the brain. In genetically engineered mouse models (GEMM) of lung and pancreatic tumors, the contribution of circulating lactate to tumor TCA intermediates was about two-fold greater than that of glucose. Therefore, the contribution of glucose to the TCA cycle is primarily through circulating lactate, a mechanism to decouple ATP production from glucose catabolism allowing glucose metabolism to serve more complex cellular processes (proliferation, NADPH production by the pentose phosphate pathway, brain activity, and systemic glucose homeostasis) [250].

*Role in prostate cancer*: The impact of lactate production/secretion in PCa cell survival and aggressiveness has been previously investigated. In the metastatic cell line DU-145 higher expression levels of MCT1/4 isoforms and glycolysis related markers GLUT1, HKII, LDHV and CAIX are observed compared to the primary tumor-derived 22RV1 cell line. MCT1/4 double knockdown had a detrimental effect on cell viability in both, DU-145 and 22RV1 cell lines under normoxia and hypoxia. Moreover, impaired cell migration was observed for both cells but only under hypoxic conditions. Pharmacological inhibition of the MCTs and LDHA by α-cyano-4-hydroxycinnamic acid (CHC) and oxamic acid (OA) lead to decrease DU-145 and 22RV1 tumor capacity formation in an *in vivo* model [260]. Interestingly, a meta-analysis study from 38 publications including records of 9,813 patients revealed a significant association between high levels of lactate dehydrogenase

(LDH) and poorer overall survival (OS) and progression free survival (PFS) in patients with metastatic Prostate cancer (mPCa) [261].

Bok et al. reported the use of a metabolic imaging approach with a dual agent [$^{13}$C-pyruvate and $^{13}$C-urea hyperpolarized (HP) $^{13}$C MRSI] to detect the metabolic flux of HP $^{13}$C-pyruvate to lactate catalyzed by lactate dehydrogenase in PCa. They investigated metabolic changes during prostate cancer development, progression from low-to-high grade disease and metastasis in the TRAMP mouse model [262]. Results evidenced a significant 2.4-fold increase in the 'Warburg effect' in high-grade versus low-grade prostate cancer as measured by the tumor HP lactate/pyruvate ratio (Lac/Pyr) and LDH activity. Interestingly, there was no significant difference in the HP Lac/Pyr ratio ('Warburg effect') in low-grade versus normal prostate tissue. This suggests that early stages /low-grade prostate cancers do not rely in the glycolytic phenotype for energy production but rather in lipids and other biological fuels. The 'Warburg effect' is rather a phenotype associated with the evolution of aggressive disease. Importantly, a significantly increased mRNA expression of the *Mct1* and *Mct4* was associated with high-grade PCa but not with low-grade and normal prostate tissue. Interestingly, genetic ablation of *Ldha* lead to a significant reduction in both, HP Lac/Pyr, and primary tumor growth, lymph node and visceral metastases [262].

*Clinical relevance: from diagnostic marker to therapeutic opportunities:* Serum lactate has been proposed as a biomarker to estimate the likelihood and extent of tissue hypoperfusion. Lactate measurements are made in blood and plasma, and they indicate the degree of lactic acidosis in patients resulting from inadequate perfusion and tissue hypoxia. Accordingly, lactate may serve as a bioanalyte for clinical screening (patients

at high risk of adverse outcome), as a risk-stratifying biomarker (i.e. identifying patients that may benefit or be harmed by a specific therapeutic intervention) and prognostic biomarker in critically ill patients [263]. A clinical report described a case from a patient suffering from lactic acidosis most likely caused by metastatic PCa. The authors suggest that increased production of lactate by tumor cells, among others may also have also contributed to the development of lactic acidosis. Further sequencing analysis revealed mutations in *TP53* and *PIK3CA* genes which likely contributed to the 'Warburg effect' in tumor cells with subsequent excess of lactate production [264].

### 2.2.3. Methylglyoxal (MG)

*Role in energy metabolism:* MG, a highly reactive α-oxoaldehyde and a thiol-reacting molecule, forms from various pathways in cells. MG primarily forms as a byproduct of glycolysis through spontaneous degradation of triose phosphate intermediates, glyceraldehyde-3-phosphate (G3P) and dihydroxyacetone phosphate (DHAP) (**Figure 3**) [265, 266]. Other sources of MG include protein and fatty acid metabolism; however, the glycolytic pathway represents the most important endogenous source of MG (**Figure 8**) [265, 267-270]. MG is a dicarbonyl compound and given its highly reactive nature, it is considered among the reactive carbonyl species (RCSs). RCSs have the ability to induce dicarbonyl stress when the rate of production is greater than that of detoxification [271]. Under normal conditions, cellular regulatory systems such as low concentrations of triose phosphates at steady-state and capping of the active site in triose phosphate isomerase maintain minimal levels of methylglyoxal (0.1-0.4% of glucose flux) [272]. Overall, per day production of MG has been estimated to be in the order of 125 μmol/kg cell mass [273].

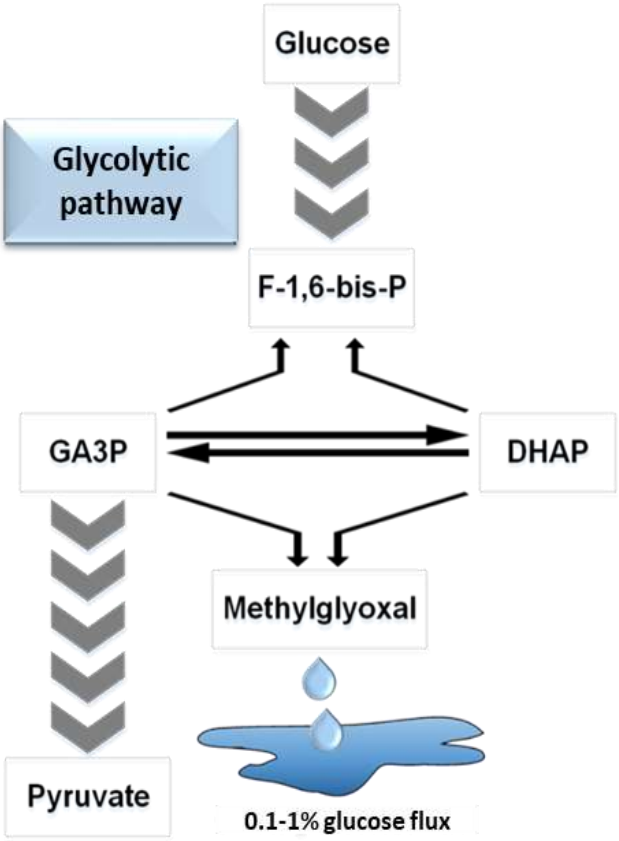


**Figure 3. Methylglyoxal (MG) formation in the glycolytic pathway.** MG forms as a byproduct of glycolysis through spontaneous degradation of triose phosphate intermediates G3P and DHAP. MG is maintained at minimal levels ranging from 0.1-0.4% of the total glucose flux in the cell. F-1,6-bis-P = Fructose 1,6, bisphosphate; GA3P= glyceraldehyde-3-phosphate; DHAP= dihydroxyacetone phosphate.

*Role in oncogenic metabolic reprogramming:* MG has high reactivity in glycation reactions *in vivo*, forming advanced glycation end-products (AGEs) of proteins, nucleotides, and basic phospholipids. MG is the principal intracellular precursor of AGEs [274] which concentrations are determined by the rates of formation and removal. In fact, MG is up to 10,000- 50,000 fold more active than glucose, as such MG is considered the most potent glycating agent [275]. MG primarily reacts with arginine residues to form MG-derived hydroimidazolones (MG-Hs), namely MG-H1, MG-H2 and MG-H3 [276, 277]. In addition to forming MG-Hs with arginine, MG also forms argpyrimidine and tetrahydropyrimidine

(THP) [278, 279]. MG also reacts with lysine residues to a lesser extent. These interaction results in formation of Nε-(1-carboxyethyl) lysine (CEL) [280], and the MG derived dimer 1,3-di(Nε-lysino)-4-methyl-imidazolium (MOLD; methylglyoxal-derived lysine dimer) [281]. MG interaction with one lysine and one arginine residue leads to formation of an adduct called MODIC (2-ammonio-6-([2-[(4-ammonio-5-oxido-5-oxopentyl)amino]-4-methyl-4,5-dihydro-1*H*-imidazol-5-ylidene]amino)hexanoate) [282] (**Figure 4** ). Arginine residues are commonly present in functional domains of proteins, hence AGEs from MG interactions with these residues can generate substantial cellular damage. The collective target proteins susceptible to post-translational modification by MG (RCS) constitute the ‘dicarbonyl proteome’ [283].

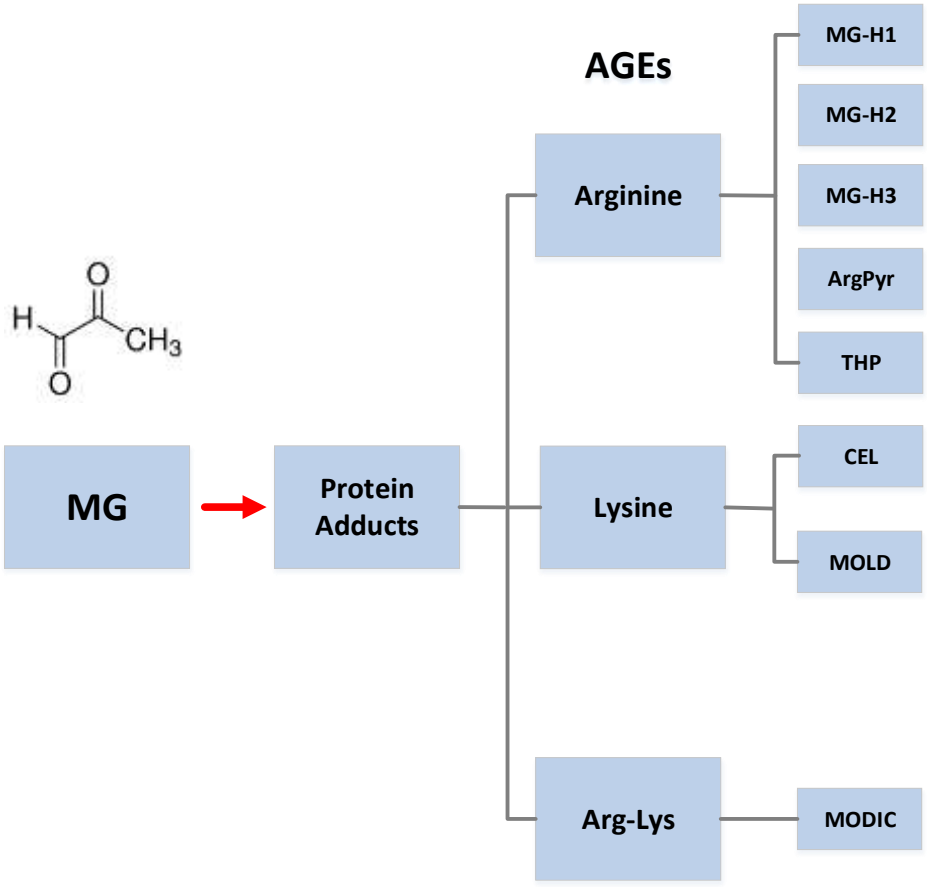


**Figure 4. MG has high reactivity in glycation reactions *in vivo*, forming advanced glycation end-products (AGEs) of proteins primarily.** MG can interact with arginine, lysine and a combination of both (Arg-Lys). MG primarily reacts with arginine residues to form MG-derived hydroimidazolones (MG-H1, MG-H2 and MG-H3). Arginine residues are common in functional domains of proteins thus MG can generate significant cell damage.

Glycation of proteins is a complex process occurring as a series of sequential reactions also known as the Maillard reaction. It is a process occurring in all tissues and body fluids, which primary targets include proteins lipids and nucleic acids, leading to formation of AGEs [271]. MG glycation of proteins, lipids and DNA leads to gradual accumulation of AGEs in cells and tissues. Importantly, AGE accumulation is now considered part of the pathogenesis of diseases including cancer thus MG is considered an emerging oncometabolite. In fact, studies have shown that patients with diabetes, where there is

high formation and accumulation of AGEs, are at a higher risk of developing cancer [271]. The major MG-derived AGE, MG-H1, is a known ligand with the ability to bind and activate the receptor of advanced glycation end products (RAGE). RAGE is a signal transduction receptor involved in oxidative stress and inflammatory, both of which contribute to carcinogenesis and various chronic inflammatory diseases including diabetes [284-286]. RAGE expression is reportedly overexpressed in various cancer types and associated to poor prognosis [287]. In addition to amino acids, MG has the ability to interact and modify nucleic acids to form genotoxic adducts. Glycation of DNA by MG leads to DNA strand breaks [288], nucleotide transversions [289], DNA-DNA crosslinks [290], DNA-protein crosslinks [291], and glycation of nucleosomal protein histone H2A [292]. Interestingly, auto-antibodies against these adducts can be detected in cancer patients, suggesting a pathophysiological importance in cancer development [293]. **Figure 5** summarizes MG-mediated effects in cellular components and functions.

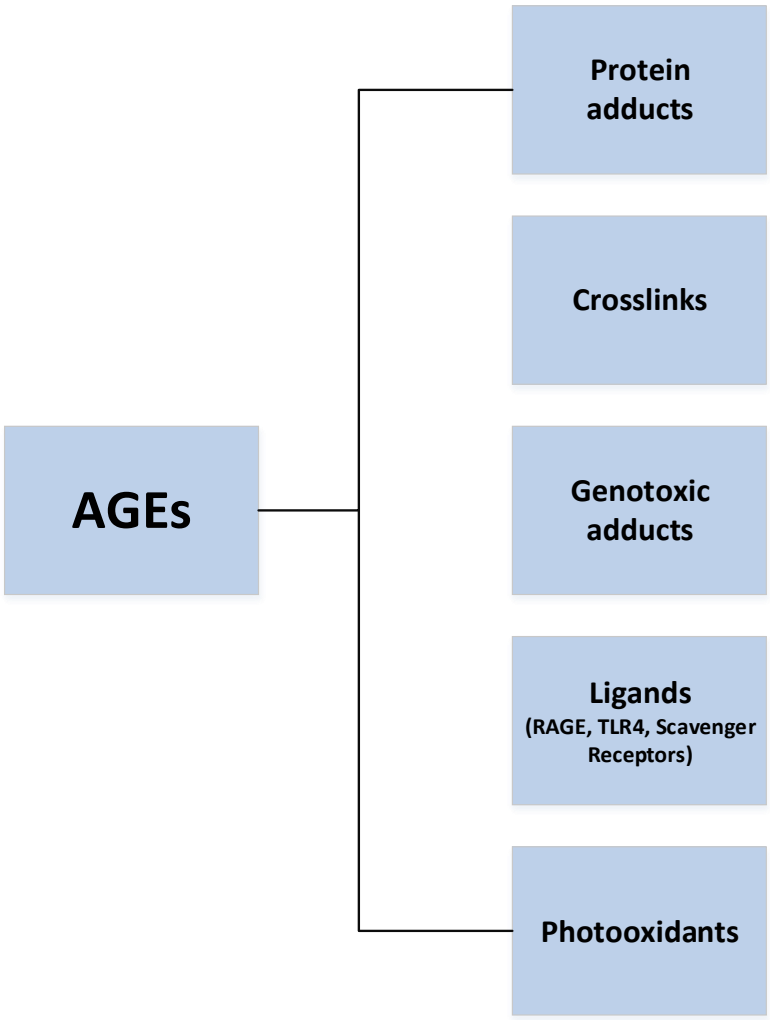


**Figure 5 . Effect of methylglyoxal-derived advanced glycation end products (AGEs) on cellular components and functions.** MG readily reacts with protein residues to form adducts [294] and proteins crosslinks; it can also target DNA leading to mutagenic adducts. In addition, MG-derived AGEs serve as receptor ligands [295] and can act as photooxidants if exposed to solar ultraviolet radiation.

MG plays a double role in the cell: at high levels, MG induces cellular toxicity via AGE formation while at steady levels, it mediates cellular processes involved with cell survival (**Figure 6**) [296, 297]. AGE modifications of DNA increases DNA strand breaks and frameshift mutations [298]. Protein modifications result in mitochondrial dysfunction with increased formation of ROS (reactive oxygen species) [299], cell detachment due to decreased integrin binding to the MG-modified ECM (extracellular matrix) proteins and

anoikis [300, 301]. A major target post-translational modifications by MG is the shock protein 27 (Hsp27) [302]. MG adduct on HSP27 was reported to inhibit Cyt c-mediated caspase activation thus preventing cell apoptosis in lung and gastrointestinal tumors and it is associated to chemotherapy resistance [303]. MG also play a role as modulator of the glyoxalase system. It was recently shown that in HT22 cells low concentrations of MG (0.3 mM) strongly induce GLO2 while at higher concentrations (0.75 mM), it is downregulated. Paradoxically, GLO1 is inhibited under high MG concentrations potentially due to GLO1 susceptibility to MG [304]. Additional targets of MG are listed on **Table 4.**

*In vitro* studies to evaluate the effect of MG in LNCaP and PC3 human prostate cancer cell line showed that it exerts cytotoxic via apoptosis control. Different apoptosis responses and susceptibilities to MG were observed on each of the cell lines. In LNCaP cells which showed the most sensitivity to MG-induced apoptosis, argpyrimidine (AP; MG adduct) intracellular accumulation triggered the mitochondrial apoptotic pathway via a decreased in NF-kB activation with subsequent downregulation of Bcl-2, Bcl-XL and upregulation of Bax proteins [305]. The detrimental effects of MG-derived adducts have also been reported in histones. Histones are rich in Arginine and Lysine residues, and they tend to be a target of MG. Arginine and Lysine MG post-translational modifications (PTMs) in histones are abundant and detected in all four core histones. Target sites of MG PTMs are critical residues involved in nucleosome stability and reader domain binding. This suggests a mechanism whereby an oncometabolite controls chromatin dynamics [306].

**Table 4.** Effect of Methylglyoxal on the cellular proteome. MG targets specific sites of critical proteins in the cellular proteome, a mechanism that promotes tumorigenesis. Adapted from Bellier et al. [271].

| Proteins | Target sites | Effect on the cellular proteome |
|---|---|---|
| Albumin | Majority Arg-410 Minority Arg-114, 186, 218, 428 | Inhibition of esterase activity and protein-ligand interactions |
| Hemoglobin | Alpha chain: Arg-31, 92, 141; Beta chain: Arg-30 40, 104 | Increased oxygen binding |
| Type IV collagen | Alpha1 chain: Arg-390; Alpha2 chain: Arg-889, 1452 | Decreased integrin binding |
| Alpha A-crystallin | Arg-12, 65, 157 and 163 | Increased chaperone function |
| HIF1-alpha co-activator protein P300 | Arg-354 | Decreased association with HIF1-alpha |
| 20S proteasome | Beta chain 2: Arg-85; Beta chain 4: Arg-224, 231; Beta chain 5: Arg-123, 128 | Impaired proteasome activity |
| HSP27 | Arg-75, 79, 89, 94, 127, 136, 140,188. Lys-123 | Prevents cytochrome c-mediated caspase activation and apoptosis |
| HSP90 | Arg-46-60-87-299-510-512-647 | Decreased ATPase activity |
| AKT | Cys-77 | Increased AKT activity |
| GAPDH | Not yet defined | Decreased GAPDH activity |
| FASN | Not yet defined | Increased FASN activity |
| PDGFR | Not yet defined | Inhibition of tyrosine kinase activity of PDGFR |

Indeed, a recent publication by Galligan et al. demonstrated that MG is a potent modulator of chromatin dynamics. MG-induced histone PTMs change the epigenetic landscape by regulating chromatin dynamics, accessibility to DNA and transcription. Strikingly, not only are MG histone modifications abundant on all four core histones, but they can be detected at critical residues related to nucleosome stability and reader domain binding. Importantly, changes induced by MG adduction of the histones can result in alteration of gene

transcription allowing for feedback and feedforward regulation of cellular metabolism [306, 307].

Interestingly, MG modulatory effects can be pro- and anti-tumorigenic depending on the concentration levels in the cell. This type of ‘bell curve’ relationship between metabolism-derived electrophile cellular levels and tumorigenesis-promoting phenotype has been established for numerous small molecules of relevance to carcinogenesis including superoxide ($O_2^-$) and $H_2O_2$ (**Figure 6**) [308].

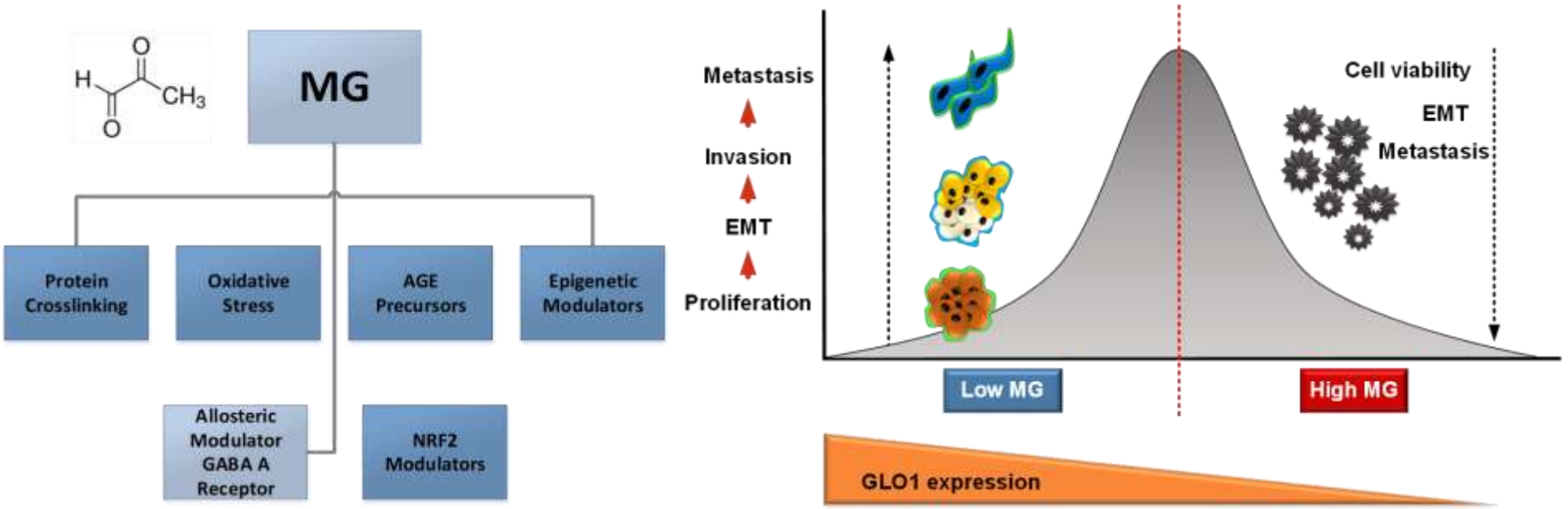


**Figure 6. Effect of methylglyoxal (MG) on the cell and cellular processes.**Right: MG has different biological and pathological functions in the cell; it mediates protein crosslinking, oxidative stress, serves as a precursor to AGEs, epigenetic modulator via adduction of specific histone residues in addition to modulating NRF2. MG is also a GABA A receptor agonist. Left: under low concentrations, MG can promote proliferation, invasiveness, and metastasis. Under high concentration MG induces cytotoxicity

### 2.2.4. The Glyoxalase System

The glyoxalase system was first discovered by Dakin and Dudley in 1913; a few years later, in 1920, Warburg described increased glycolytic activity in cancer cells [309]. However, the existence of the dual system, GLO1 and GLO2, was not elucidated until 1951 by Racker [310] (**Figure 7**). Several enzymatic pathways are involved in α-oxoaldehyde metabolism including aldose reductase, aldehyde dehydrogenase and the glyoxalase system [274]. The glyoxalase system is the main and most efficient enzymatic detoxification system that suppresses formation of MG and glyoxal-derived AGEs [311]. The glyoxalase system comprises two enzymes Glyoxalase 1 (GLO1), Glyoxalase 2 (GLO2) and a coenzyme, glutathione (GSH). GLO1, a lactoylglutathione lyase (EC: 4.4.1.5), exists in the cytosol of all mammalian cells and other species such as prokaryotes and plants [312-315].

Human GLO1 is localized to 6p21.3-p21.1, between HLA and the centromere. It is a $Zn^{2+}$ metalloenzyme, a dimer of 42 kDa containing 184-amino acid residues per monomer (21 kD). In the mammalian enzyme, each subunit has $Zn^{2+}$ bound to the active site [316, 317]. Substrates of GLO1 are potent glycating agents of proteins, nucleotides and basic phospholipids and they contribute to cytotoxicity *in vivo*. The glyoxalase system plays a crucial role in cellular detoxification of spontaneously formed hemithioacetal adducts between GSH and 2-oxoaldehydes such as MG. In this two-step reaction, GLO1 first catalyses the conversion of highly reactive MG to S-D-lactolylgluthatione. The resulting thioester, in the case of MG, is then hydrolyzed by GLO2 to produce D-lactate and reformed GSH (**Figure 8**) [315].

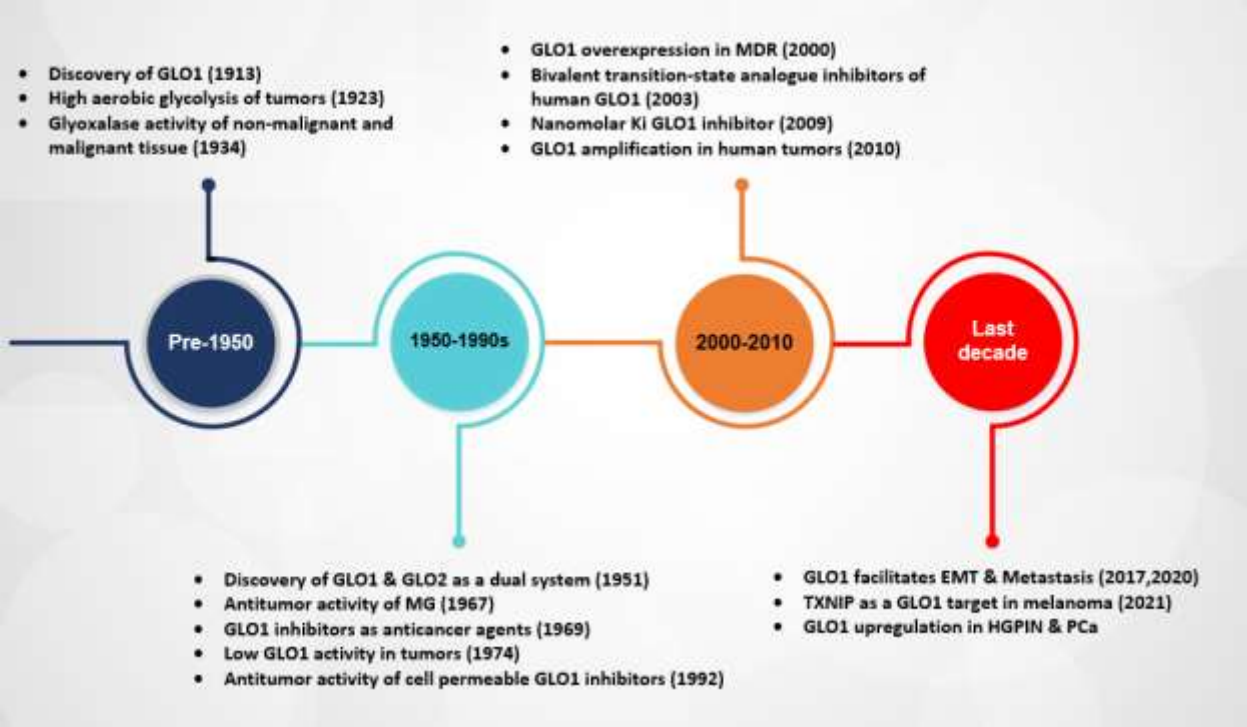


**Figure 7. Most relevant events in the discovery of the glyoxalase system and development of GLO1 inhibitors.** Since the discovery of the glyoxalase system most of the efforts have concentrated on GLO1, the rate limiting enzyme in the glyoxalase system. Current efforts have focused on developing GLO1-targeted inhibitors and understanding its role in cancer progression. GLO1 may also promote Epithelial to Mesenchymal Transition (EMT) and facilitate metastasis via TXNIP indirect downregulation. GLO1 is upregulated in early and during PCa progression. Adapted from Thornalley, et al. [288].

GLO1 specific substrates are MG, glyoxal and other acyclic α-oxoaldehydes; however, the major physiological substrate is MG. GLO1 is a GSH-dependent enzyme and thus the activity of GLO1 *in situ* is proportional to GSH in the cell. Glutathione reductase (GR) supplies the Glyoxalase system with reduced GSH to catalyze the transformation of MG and reduce protein glycation [318]. Depletion of GSH leads to an accumulation of MG with cytotoxic effects [319, 320]; therefore, the Glyoxalase system is key in cellular metabolism in health and disease. Preserving a homeostatic system in a normal cell is crucial to maintain physiological cellular functions while targeting this system in the transformed cancerous cells represents a therapeutic opportunity.

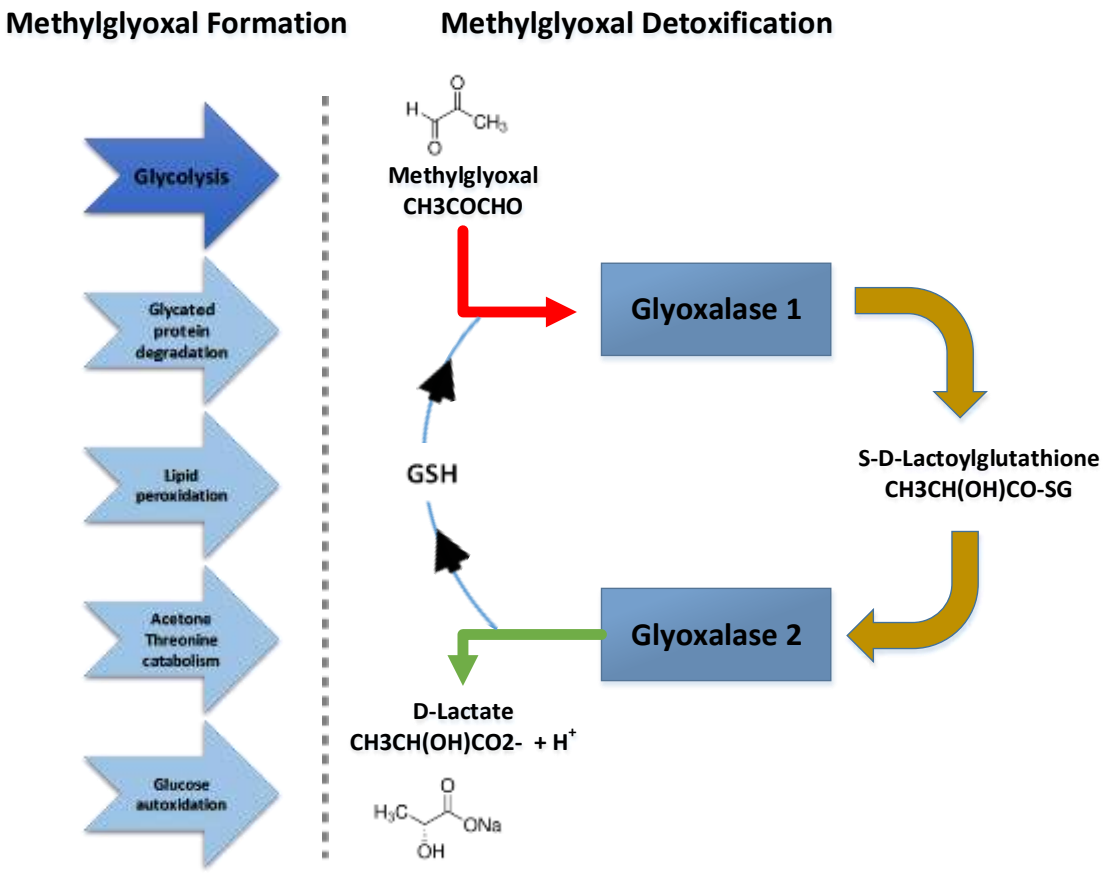


**Figure 8. Sources of Methylglyoxal and its detoxification via the Glyoxalase System**. MG primarily forms as a byproduct of glycolysis. Other sources of MG include protein and fatty acid metabolism. The Glyoxalase system (GLO1 and GLO2) detoxifies MG to D-Lactate in a two-step reaction. GLO1 first catalyzes the conversion of highly reactive MG, bound to GSH, to S-D-lactolylgluthatione. The resulting thioester is then hydrolyzed by GLO2 to produce D-lactate and reformed GSH. Adapted from Rabbani et al [321].

GLO1 efficient metabolism of α-oxolaldehydes represents an enzymatic defense against α-oxolaldehyde-mediated glycation [322]. A mouse model of GLO1 deficient (*GLO1*$^{-/-}$) is viable; however, some behavioral characteristics related to decreased anxiety and increased depression-like behavior observed in the animals are consistent with MG anxiolytic properties. As expected, the KO mice presents increased levels of AGEs [323]. There are reports of AGE protein modification (glycation) in a mouse model deficient in

laminin B receptor (i$c^J/ic^J$), a multifunctional inner nuclear membrane protein receptor. In this model, MG-derived argpyrimidine as well as pentosidine, markers of ageing, are increased with a concomitant increase of the AGE-preventing enzyme GLO1. Increased AGE formation is observed in the heart and the liver of the *Lbr* deficient mice, and this is accompanied with increased levels of *GLO1.* There appears to be a feedback loop which mechanism of activation is not yet clear, but it may resemble that of Yeast. In this model, MG accumulation is sensed by Slnl (osmosensor) and the signal transduced via the Hog1-Mapkinase pathway to the nucleus where Msn2/4 activates transcription of *GLO1* [324]. Therefore, *Lbr* deficiency may directly or indirectly affect physiological ageing via alteration on AGE metabolism, an effect that may be countered by GLO1 [325].

The Nrf2-Keap1 pathway is an emerging stress-responsive transcriptional regulator controlling MG-mediated dicarbonyl stress through positive modulation of GLO1 expression. Although the mechanism of induction remains unclear, the endogenous activation of the anti-stress gene response coordinated by Nrf2 (nuclear factor-erythroid 2 p45 subunit-related factor 2), an essential transactivator of genes associated with oxidative stress and electrophilic metabolite protection, increases the expression of GLO1 and thus protects the cell against the dicarbonyl stress. The specific mechanism relies on the presence of an ARE (antioxidant-response element) in the 5'-untranslated region of exon 1 of the mammalian *GLO1* gene. Binding of the Nrf2 to this ARE induces expression of GLO1 which in turn decreases cellular and extracellular concentration of MG and MG-derived protein adducts, mutagenesis and cell detachment. Decreased levels of *GLO1* mRNA and protein are observed in the liver, brain, heart, kidney ad lung of the Nrf2 deficient mice ($Nrf2^{-/-}$) [326]. Interestingly, MG was found to induce nuclear Nrf2 in HT22

nerve cells; however, GLO1 expression and activity was not increased and was even inhibited at high MG concentrations making the glyoxalase system a cellular target of MG [304]. One can speculate this inhibition to be associated with the ability of MG to react with GLO1 to form AGEs and subsequently impairing its activity. Additional regulatory elements such as the metal-response element (MRE) and insulin response element (IRE) are also present in the *GLO1* promoter region as depicted in **Figure 9** [327]

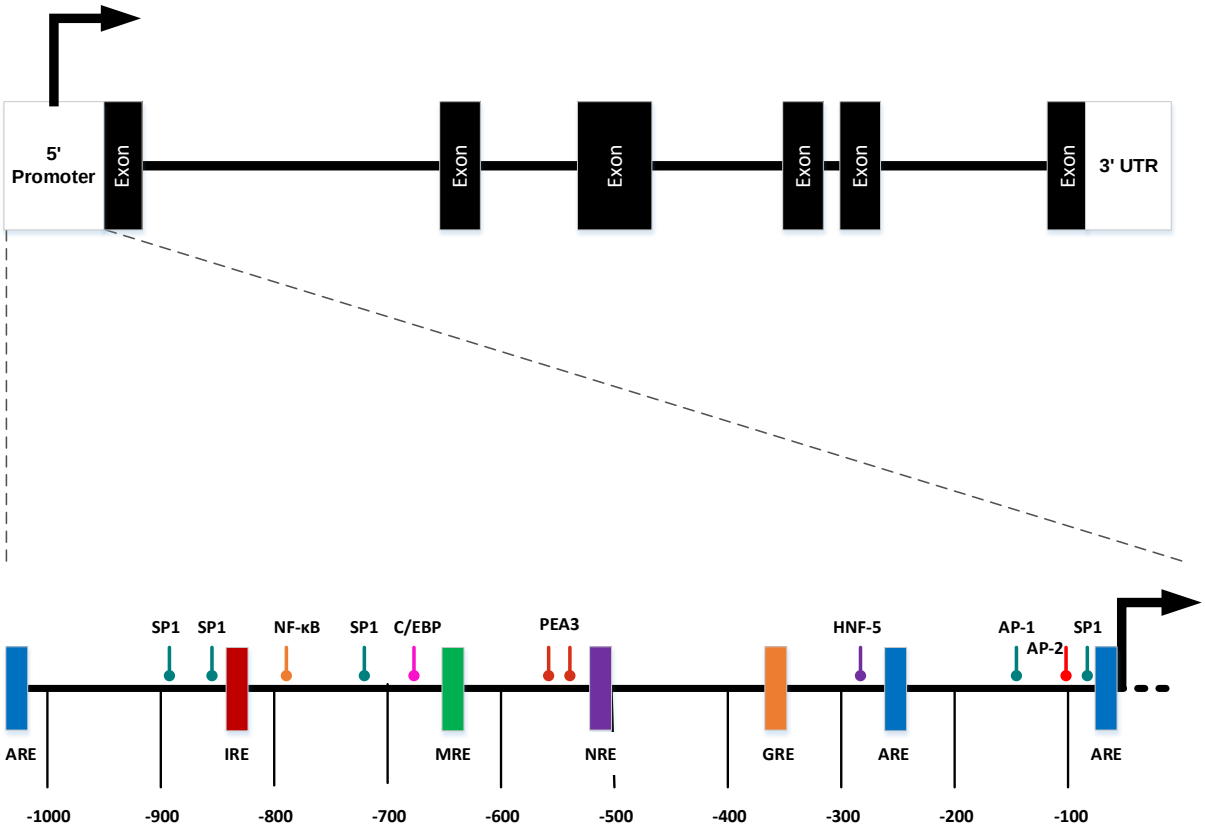


**Figure 9. Schematic representation of the human GLO1 promoter region.** Consensus sequences for the most notable regulatory elements are depicted including ARE (antioxidant response element), IRE (insulin response element), and MRE (metal response element), NRE (negative regulator element), GRE (glucocorticoid response element). Additional putative binding sites identified include SP1 (specificity protein 1), C/EBP (CCAAT-enhancer-binding protein), PEA3 (polyomavirus enhancer activator 3), HNF-5 (hepatocyte nuclear factor 5), AP-1 (activator protein 1), AP-2 (activator protein 1). Adapted from Bellahcène et al. [328].

GLO1 upregulation has been described in the context of metabolic and inflammatory stress *in vitro* and *in vivo* [329-332] serving as a cellular mechanism to detoxify high levels of MG. Human GLO1 is recognized as a hotspot for CNV (copy number variation) and it is associated with chemotherapy resistance. In tumors with high glycolytic rates, GLO1 CNV is a mechanism employed to counterbalance the increased levels of toxic MG. In gastro-entero-pancreatic neuroendocrine tumors (GEP-NET), for example, GLO1 copy-number positively correlates with increased GLO1 protein in tumor tissue and it is a predictor of tumor progression in specific GEP-NET cases. While increased copy number may not always translate to increased protein production, in the case of GLO1 these copies are functional and correlates with shorter time to tumor progression [333]. The potential mechanism for GLO1 CNV may be driven by hypoxia-activated histone demethylase (*KDM4A*/JMJD2A) allowing for more open chromatin thus promoting inappropriate recruitment of the MCM (mini-chromosome maintenance) proteins and DNA polymerase thus facilitating the repetitive DNA replication and copy number gain. Interestingly, GLO1 copy number can also be decreased in certain tumors [333] potentially due to allele deletion [333] . Patients with decreased copy number have increased time to tumor progression [333]. The growth inhibitory effect of Doxorubicin was potentiated when upon silencing of GLO1 in BON1 cells which supports the idea on the MDR role of GLO1 [333]. Chemotherapy resistance is linked to elevated levels of GLO1 thus inhibiting *GLO1* action represents an antitumor target [334-337].

Since the first reports in upregulation in cancer, GLO1 has gained more and more recognition as a suitable marker of cancer progression in solid tumors. Indeed, in human malignant melanoma GLO1 upregulation serves as the main antiglycation defense

against MG-induced dicarbonyl stress with downregulation of GLO1, rendering A375 and G361 human metastatic melanoma cell lines more sensitive to MG-induced apoptosis, oxidative stress and increased protein adduction [302]. Importantly, GLO1 overexpression has been reported in hormone-responsive breast and prostate cancer cells. In androgen responsive LNCaP cells, GLO1 expression and activity is induced upon testosterone treatment [338]. The same observation has been made in hormone responsive MCF7 breast cancer cells when treated with estrogen [339]. Importantly, hormone-insensitive prostate and breast cancer cells did not have an effect on basal expression levels of GLO1 suggesting that this is a hormone-mediated mechanism. In addition, treatment of estrogen-dependent and independent breast cancer cells with the estrogen receptor agonist, tamoxifen, decreased GLO1 expression and had a negative impact on cell proliferation likely due to accumulation of toxic levels of MG [339].

Molecular signatures are a promising area of study in trying to define risk or malignant tendencies of cancer cells. In this regard, GLO1 may serve as a prognostic marker for breast cancer (BCa) patients. A proteomic approach revealed that, in 79% of the cases, GLO1 expression positively correlated with tumor grade demonstrating the clinical relevance of this marker in the clinic [340]. In prostate, GLO1 upregulation is associated to aggressive prostate cancer, especially those characterized by *ERG* fusion and *PTEN* deletion. Upregulation of GLO1 correlates with unfavorable tumor phenotype including, Gleason grade, advanced pathological tumor stage and positive lymph node status. On invasive prostate cancers, GLO1 immunostaining was predominantly cytoplasmic and often accompanied by nuclear co-staining. The prognostic impact of GLO1 expression, however, was inconclusive. ERG positive tumors correlated with GLO1 upregulation and

given that the GLO1 promoter harbors an ETS transcription factor binding site, it may be that GLO1 is a target of ERG [341].

The active site of GLO1 is located where the two identical chains from the two dimers interface. Moreover, given that GLO1 is a homodimer, it has two similar active sites on opposite sides both of which contribute to its catalytic efficiency. The active sites have three structurally defined regions: positively charged entrance, a central zinc atom, and a deep hydrophobic pocket [342]. Given the pivotal role in the pathogenesis of different diseases, including cancer, GLO1 is now considered an emerging therapeutic target. In this regard, efforts to develop GLO1 inhibitors are undergoing (**Figure 10**). Current GLO1 inhibitors include Glutathione inhibitors and non-glutathione inhibitors. Although various glutathione inhibitors have been evaluated and their potency was already seeing at sub-micromolar concentrations, their metabolic instability among other issues, have forced researchers to find alternative compounds [309]. Among non-glutathione-based inhibitors, natural flavonoids and anthocyanidins have shown promising results as GLO1 inhibitors. In addition, curcumin derivatives were also reported potent GLO1 inhibitor. Interestingly, Indomethacin, a nonsteroidal anti-inflammatory drug (NSAID), was found to be a potent GLO1 inhibitor and has since propel the study of structurally similar Zopolrestat, an aldose reductase, as a GLO1 inhibitor. Zopolrestat currently in phase III clinical trials, is a highly potent competitive GLO1 inhibitor [343].

### 2.2.5. D-Lactate

The resulting product of the detoxification of MG is D-lactate, a metabolite largely modified in cancer cells, including prostate cells. Although lactate is metabolized to pyruvate by

lactate dehydrogenase (LDH), the enzyme is isomer-specific and metabolism of D-lactate to pyruvate requires D-LDH, an enzyme absent in mammalian cells. However, human cells have the ability to metabolize D-lactate to pyruvate via D-2-hydroxyacid-dehydroganse, a mitochondrial enzyme [344-346]. D-lactate is the less predominant form of lactate produced under normal physiological conditions. Unfortunately, this important metabolite has not been widely studied in the context of carcinogenesis. The general idea is that D-lactate is shuttled to the extracellular space [347] where it can be taken up by cells via the monocarboxylate transporter [348]. A study by Bari et al. sought to investigate the metabolic fate of D-lactate in both normal (PNT1A) and prostate cancer cells (PC-3) [349]. The study not only showed that mitochondrial D-lactate dehydrogenase, a membrane flavoprotein, can efficiently metabolize D-lactate but it also demonstrated that the activity and protein levels were higher in PC-3 cells compared to the normal prostate cells PNT1A. D-lactate enters the mitochondria via D-lactate/H+ symporters and where it is further oxidize by D-LDH to pyruvate which is suspected to produce malate via pyruvate carboxylase [350] and exit the mitochondria likely through the D-lactate/Malate carrier [351, 352]. Once in the cytosol, malate contributes to NAPDH formation via the cytosolic malic enzyme reaction. Therefore, oxidation of D-lactate in the mitochondria contributes to ROS scavenging and favor elimination of MG. Interestingly, this study also found cytosolic NADP-malic enzyme activity around five-fold higher in PC-3 versus PNT1A cells.

A recent study showed the immune modulatory effect of D-lactate on CD4 and CD8 T cells. Treatment of murine CD4 and CD8 T cells with sodium D-lactate resulted in marked impairment of cell proliferation. In fact, the effect on cells was more profound than that of

L-lactate. Importantly, treatment of $CD4^{+}CD25^{-}Foxp3^{-}$ T cells under polarizing conditions induced regulatory T cells (iTreg), a type of immune suppressive cells involved in tolerance. *In vivo* studies of mice treated with D-lactate showed significantly reduced (62.1%) T cell proliferation compared to controls [353]. These data evidence the role of D-lactate on immune cell suppression.

All in all, these study shows the importance of D-lactate in cancer cells, specifically prostate cancer, and the potential for the development of D-lactate anticancer therapies.

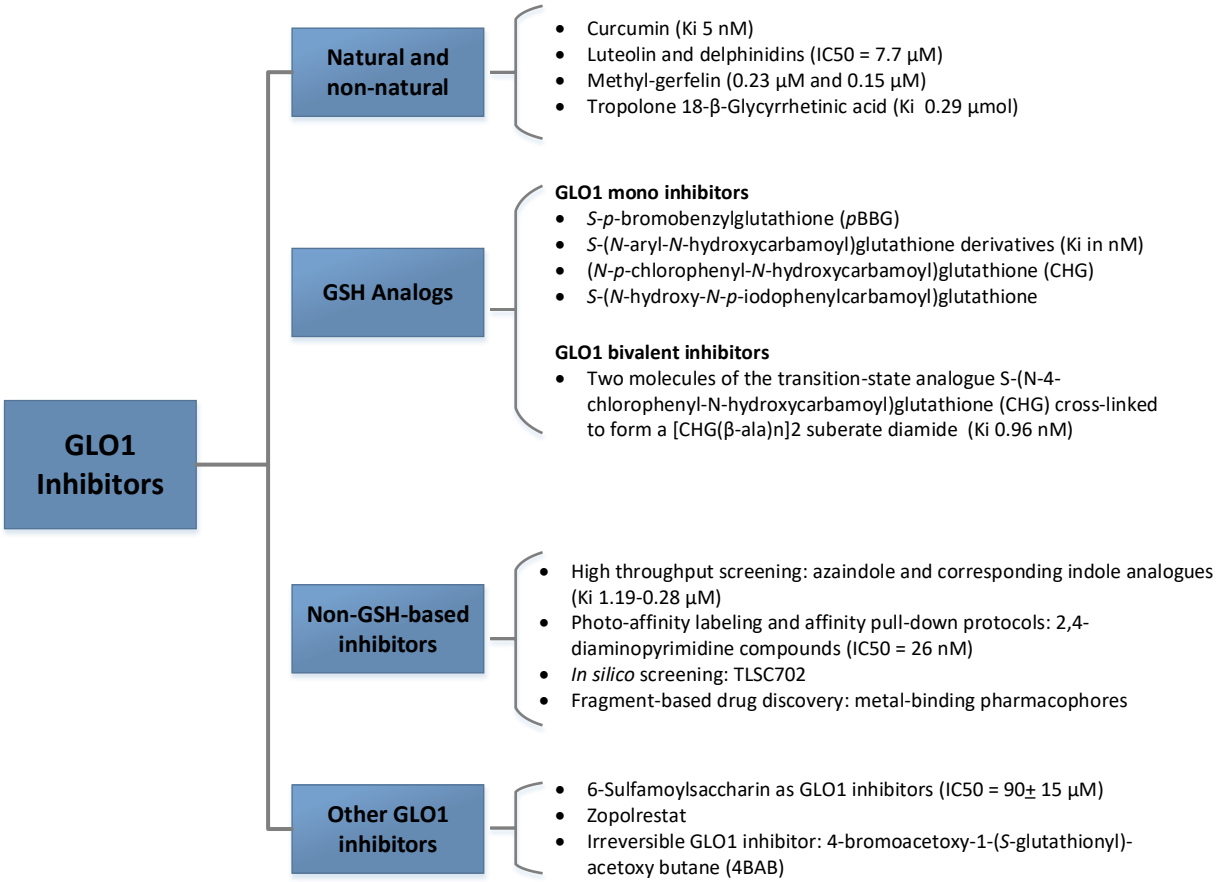


**Figure 10. Small molecule GLO1 inhibitors currently in research and early clinical development.** According to chemical structure and origin, GLO1 inhibitors can be classified as synthetic or natural product-derived including GSH analogs, non-GSH inhibitors, and others. Zopolrestat is currently undergoing phase III clinical trials testing,

serving as a highly potent structured-based competitive GLO1 inhibitor. TLSC702 is a potent non-GSH-based inhibitor employed in our *in vitro* studies.

# CHAPTER III

## Glyoxalase 1 Expression in Prostate Adenocarcinoma: Antibody Characterization and Assay Development

## 3.1. GLO1 Antibody Characterization

The first step in the development of the GLO1 immunohistochemical assay was the antibody selection. Previous studies [354] interrogating expression of GLO1 in formalin fixed paraffin embedded (FFPE) tissues described the use of an anti-GLO1 rabbit polyclonal antibody (Abcam; ab96032). The primary concern when using polyclonal antibodies is the potential for crossreactivity with proteins sharing homologous sites on the target epitope. Given that GLO1 and GLO2 share two sites with high homology (**Figure 11**), we sought out to investigate potential crossreactivity by probing both, cell line endogenous and human recombinant GLO1 (Abcam, ab87413) and GLO2 (Abcam, ab102019) proteins with the selected anti-GLO1 (ab96032, Abcam; RbpAb) and anti-GLO2 (Sino Biologicals, 12146-MM01) antibodies by immunoblotting. Using Genevestigator (mRNA database), we searched for two different cell lines with the highest expression of either GLO1 or GLO2 that could serve as positive controls. The searching criteria involved high expression of GLO1 and low expression of GLO2 and vice versa. We identified the human histiocytic lymphoma U-937 as a positive control for GLO1, and the human multiple myeloma OPM-2 as a positive control for GLO2. In addition, we resource to GLO1 and GLO1 human recombinant proteins as an additional set of positive controls.

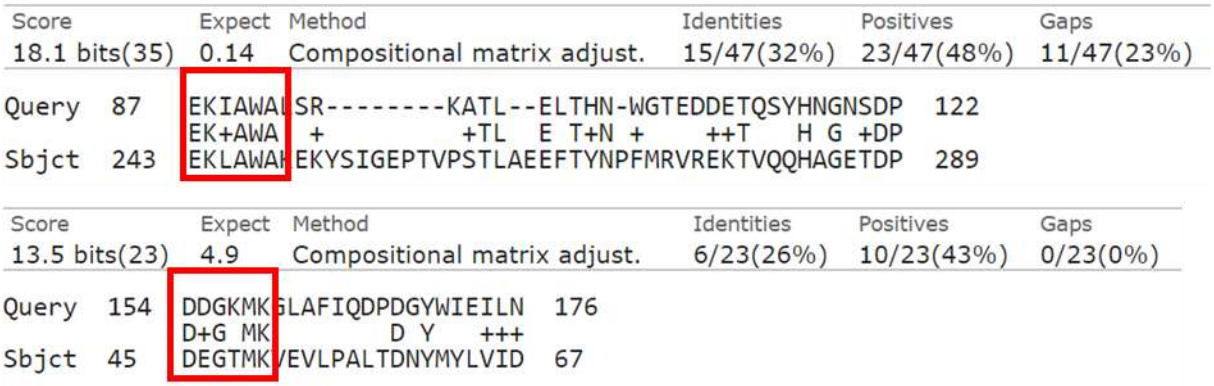


**Figure 11. Human GLO1 and GLO2 amino acid sequence alignment for identification of potentially shared epitopes.** Amino acid sequence alignment of GLO1 (top, 'Query') and GLOs (bottom, 'Sbjct') was performed using the NCBI Basic Local Alignment Search Tool (BLAST). Two sites sharing 48% and 43% sequence homology were identified.

As expected, our data showed reactivity of the anti-GLO1 antibody against the human recombinant and the endogenous (U-937) GLO1 proteins (**Figure 12A**; 21 kDa band). Likewise, there was specific reactivity of the anti-GLO2 antibody against the human recombinant and the endogenous (OPM-2) proteins (**Figure 12B**; 29 kDa band). Although there appeared to be some crossreactivity with the anti-GLO1 antibody against GLO2, the protein concentration used for this experiment was exceedingly high (40µg) and not representative of normal physiological levels. Therefore, we concluded that there was no risk for crossreactivity between the two antibodies of choice. In addition, we found very low levels of GLO2 expression by IHC (0 to 1+) in normal prostatic and prostate cancer tissues as shown on **Figure 13**, representative images from a small pilot study.

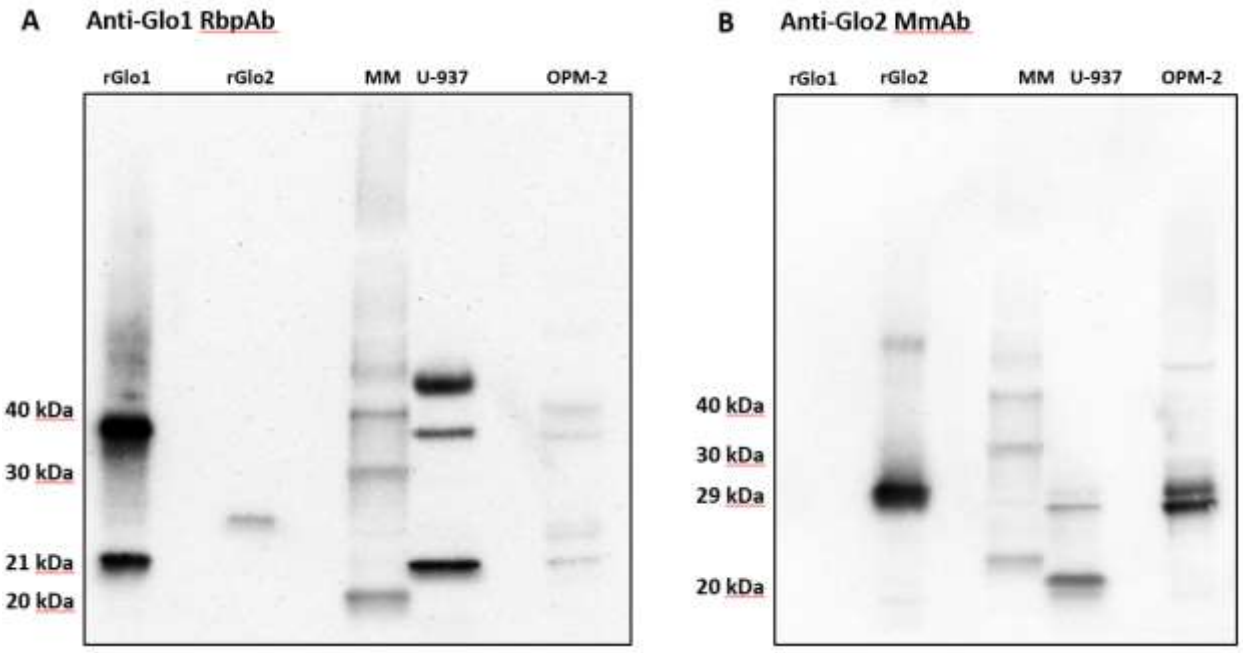


**Figure 12. GLO1 antibody characterization by immunoblotting.** U-937 and OPM-2 whole cell lysates (40µg) and human recombinant GLO1 (200ng) and GLO2 (200ng) proteins were analyzed by immunoblotting using the anti-GLO1 (1:1000) and anti-GLO2 (1:1000) antibodies. (A) The 21 kDa band shows reactivity of the anti-GLO1 antibody against the human recombinant GLO1 protein (rGlo1) and the U-937 whole cell lysate. (B) The 29 kDa band shows reactivity of the anti-GLO2 antibody against the human recombinant GLO2 protein (rGlo2) and the OPM-2 whole cell lysate.

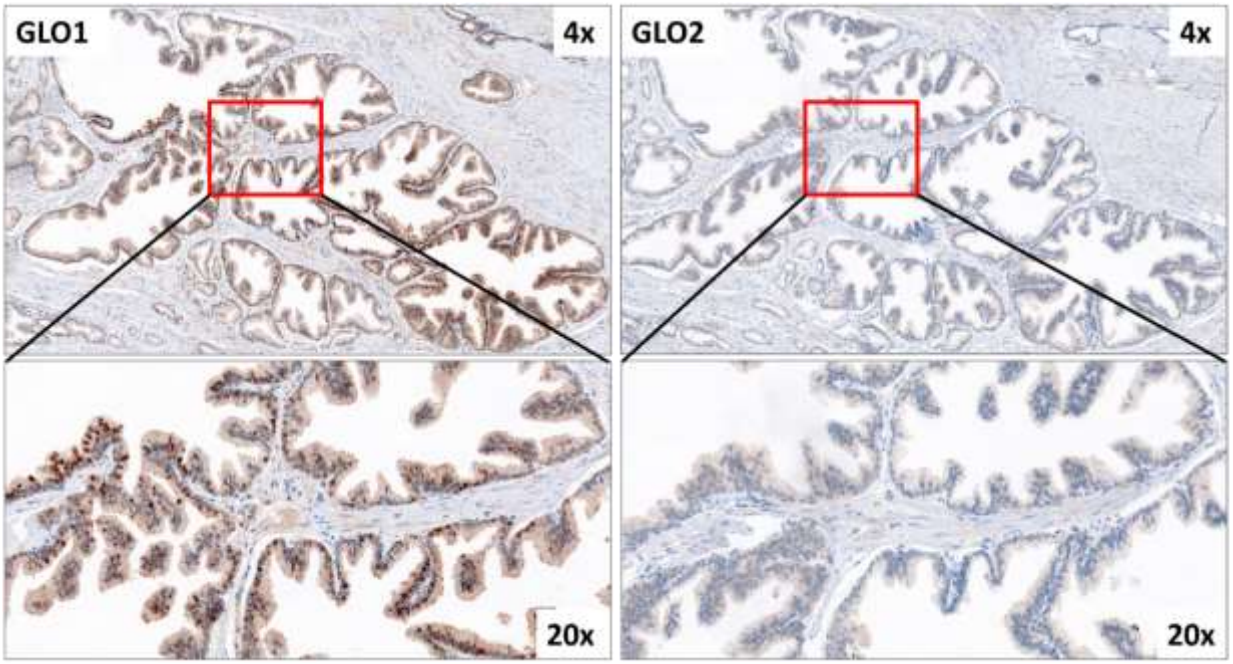


**Figure 13. Representative serial images immunohistochemically stained with GLO1 (left) and GLO2 (right) from a clinical tissue sample with both, normal and prostate cancer tissues.** Captured on the image (4x) is normal glandular tissue expressing moderate levels of GLO1 and very low levels of GLO2.

## 3.2. Assay Characterization

Next, we established the optimal conditions for the automated GLO1 immunohistochemical assay. Our work focused on selecting the appropriate antibody diluent, optimization of the antibody concentration and antigen retrieval from tissues. We aimed to develop the GLO1 IHC assay according to industry standards thus following the same rigor to that of a commercial IHC assay development.

We found that an antibody concentration of 2.5 µg/mL was optimal for the IHC assay yielding the best quality of staining with minimal background staining. Our final assay conditions are listed on **Table 5**. Using the Genevestigator mRNA expression database, we then performed a thorough *in silico* screening of over 1,000 cell lines to identify

potential candidates that could serve as system level controls. From our screen, we identified three cell lines with low, moderate, and high GLO1 mRNA expression. Staining intensity was designated with a numeric value of 1+, 2+ and 3+ which indicated the level of GLO1 expression. As shown on **Figure 14**, CAPAN-2 (1+), BT-483 (2+) and U-937 (3+) served as the low, moderate, and high system level controls, respectively. In addition, we identified a breast cancer case which also served as a positive control, and which allowed us to monitor background staining level in stromal tissue during assay optimization.

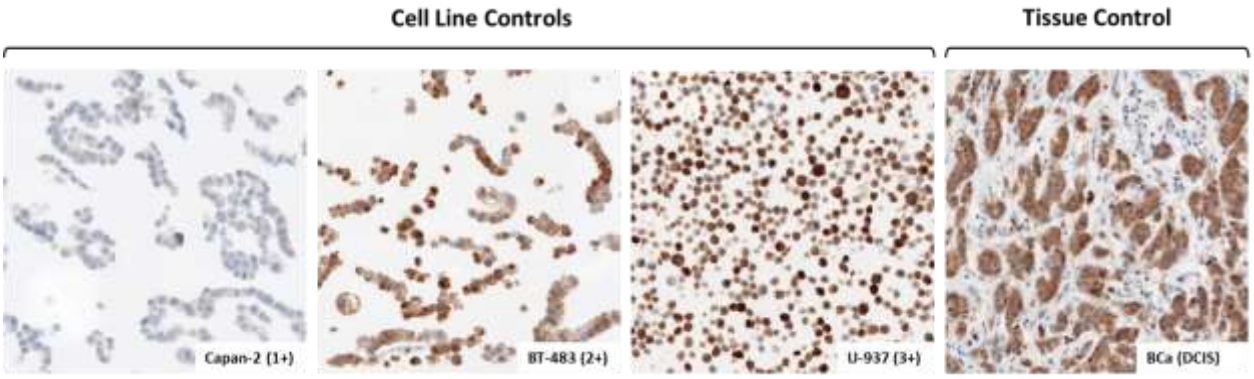


**Figure 14. System level controls and tissue controls used during GLO1 assay optimization**. Three cell lines were carefully chosen following an *in silico* mRNA expression analysis using the Genevestigator database. Left: cell lines with low (CAPAN-2; 1+), moderate (BT-483; 2+) and high (U-937; 3+) GLO1 expression. Right: breast cancer (DCIS= ductal carcinoma *in situ*) specimen used to assess staining background.

**Table 5.** Recommended staining protocol for the GLO1 (ab96032) assay and negative control with OptiView DAB IHC Detection Kit on a BenchMark ULTRA instrument.

| **GLO1 Staining Procedure<br>OptiView DAB IHC Detection Kit** | |
|---|---|
| **Procedure Parameter** | **Selection** |
| **Deparaffinization** | Selected |
| **Cell Conditioning** | CC1 Cell Conditioning 64 minutes |
| **Pre-primary Antibody Peroxidase** | Unselected |
| **Antibody (Primary)** | GLO1 (Ab96032)<br>or<br>No Antibody Control<br>16 minutes, 36°C |
| **OptiView HQ Linker** | 8 minutes |
| **OptiView HQ Multimer** | 8 minutes |
| **Counterstain** | Hematoxylin II, 4 minutes |
| **Post Counter Stain** | Bluing Reagent, 4 minutes |

## 3.3. GLO1 Expression in PCa: Pilot Study

Following IHC assay optimization, we sought to interrogate expression of GLO1 in various tumor types. First, we turned to two databases for an *in silico* analysis of the expression of GLO1 in various cancers. Interestingly, we identified prostate adenocarcinoma as a type of cancer with the highest *GLO1* mRNA expression (**Figure 15A**). Furthermore, when comparing GLO1 transcript levels in PCa to that of normal prostatic tissue, we found significantly higher expression in PCa (**Figure 15B**). With this premise in mind, we set out to interrogate GLO1 expression levels in normal and PCa tissues using our optimized IHC assay. We identified a PCa cohort available at the University of Arizona (U of A) Tissue Acquisition and Cellular/Molecular Analysis Shared

Resource (TACMASR) comprised of 200 prostate tissues from patients who underwent radical prostatectomies between the years of 1995 and 2007. Upon resection, full prostate tissues were shipped to the U of A TACMASR for fixation and processing. The certified pathologist along with a team of qualified histotechnicians took care of fixing,

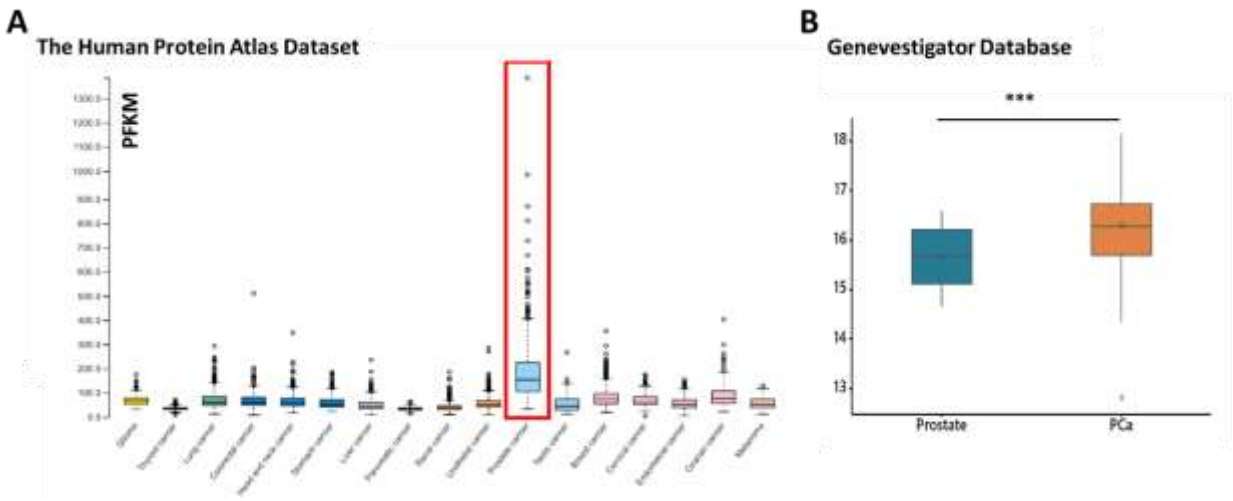


**Figure 15. GLO1 mRNA expression in normal and prostate cancer.** (A) Glo1 mRNA expression in various cancers obtained from The Human Protein Atlas dataset. FKPM denotes reads per kilobase million. (B) GLO1 mRNA expression in normal prostate compared to PCa from the Genevestigator database. Statistical analysis of mRNA data sets was done using two-tailed t-test (***p<0.0005). PFKM= Fragments per kilobase of transcript per million mapped reads.

Processing, and scoring the tissues as well as creating tissue multiarrays (TMAs). The preanalytical phase is a critical step in the preservation of tissue epitopes; poor fixation techniques can yield false IHC results. Given the preanalytical phase on this cohort was executed with the outmost quality, we were certain the GLO1 epitope was preserved properly.

To further investigate expression of GLO1 in PCa and to determine any potential association between invasive and non-invasive PCa, we decided to run small pilot study. The study included a total of 20 samples; ten samples where the carcinoma was still

confined to the prostate organ (‘organ confined’; non-invasive) and ten with capsular penetration (‘capsular penetration’; invasive). Three different staining protocols were deployed for this study: H&E, GLO1 and dual stain comprised of an antibody cocktail targeting normal prostatic epithelium (HMWCK and p63) and the p504s (racemase) antibody. All tissue histologies including normal, HGPIN and PCa within a given case were scored by a board-certified Pathologist. Histologic scores (H-score) were calculated for each individual tissue core as previously described [355].

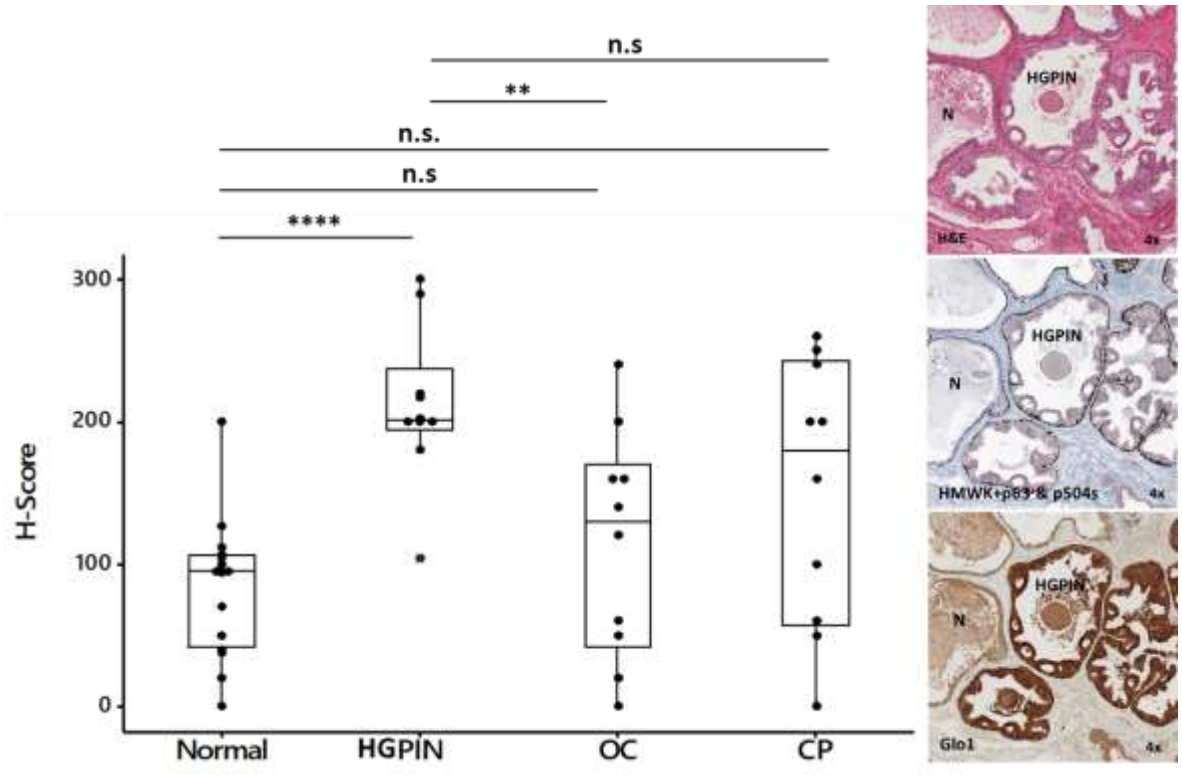


**Figure 16. GLO1 immunohistochemical analysis in a small prostate cancer patient cohort of organ confined (OC) and cases with capsular penetration (CP).** Left: GLO1 H-score on Normal, HGPIN, OC, and CP cases. GLO1 expression on HGPIN lesions is significantly overexpressed compared to normal and PCa on OC cases. A trend towards increase in GLO1 expression in OC and CP cases is observable and warranted further investigation. Right: Representative images of HGPIN and normal prostate. High GLO1 expression is observed on HGPIN lesions but not in adjacent normal prostate glands.

As shown in **Figure 16** we observed high expression of GLO1 in HGPIN. Further statistical analysis demonstrated that HGPIN was not only differentially expressed but it was highly significant when compared to normal and PCa. Our analysis did not reveal statistically significant difference between GLO1 expression in normal and PCa cases with organ confined (OC) or those with capsular penetration (CP) or between cases with organ confined and those with capsular penetration. This was likely due to the small sample size. However we observed a trend towards an increase in GLO1 expression in PCa, regardless of the status.

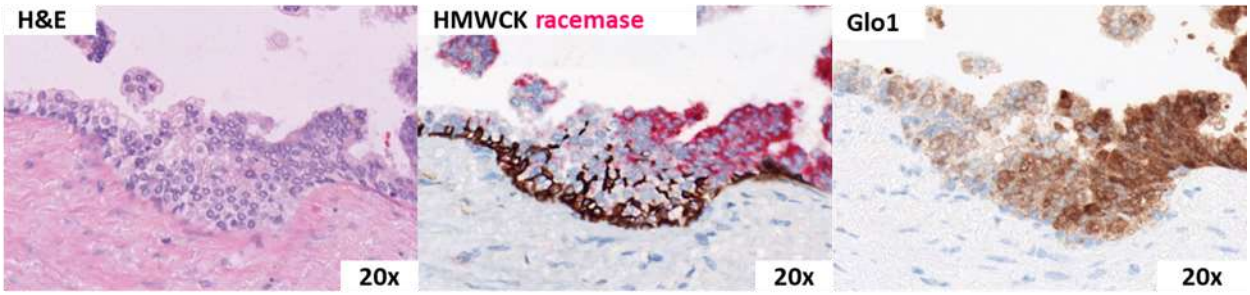


**Figure 17. GLO1 expression in malignant transition zones in prostate tissues.** Serial sections stained with H&E (left), HWMCK racemase (dual; middle), and GLO1 (right) showed zones of transition towards malignancy as evidenced by the overexpression of racemase concomitant with GLO1 overexpression.

Interestingly, we also observed zones of transition (**Figure 17**) where we could appreciate malignant transformation as evidenced by the upregulation of racemase and histological features. Strikingly, these zones also show upregulation of GLO1. These findings suggest a role for GLO1 in malignant transformation in the prostatic epithelium. Although the pilot study did not show evidence of GLO1 overexpression in PCa (OC and CP), our results showed high expression in HGPIN, a widely accepted precursor lesion to invasive PCa.

# CHAPTER IV

## Glyoxalase 1 Expression as a Novel Diagnostic Marker of High-Grade Prostatic Intraepithelial Neoplasia in Prostate Cancer

## 4.1. Introduction

Prostate cancer (PCa) is the most commonly diagnosed cancer and the second leading cause of cancer-associated deaths in men in the USA. It is estimated that in the year of 2021, a total of 248,530 new cases will be diagnosed and 34,130 of those men will succumb to the disease [60]. The etiology of PCa is not well understood, although some risk factors including inflammation, metabolic factors, hormonal influences and genetic variation [27] have been associated with it. Prostatic intraepithelial neoplasia (PIN) is the only widely accepted histological condition preceding PCa, although it is unclear whether PIN arises from normal prostatic tissue or dysplastic epithelial cells [34-37]; also, high-grade PIN lesions (HGPIN) are now considered the most likely precursor of invasive PCa [33, 356].

PCa is a disease with a disproportionate burden afflicting the elderly, and risk prediction is crucial. Most patients present with low-risk, relatively indolent tumors; however, 20–30% of patients present with tumor characteristics associated with high-risk PCa, more likely to progress and relapse [61]. In this group of men, early-stage intervention may limit the development of prostate cancer, and identification of this subpopulation of patients is critical for optimal therapy. Therefore, a lack of molecular markers with clinical utility for early detection and prediction of tumor progression represents an unmet medical need. Hence, effective intervention requires identification and development of improved diagnostic assays allowing early detection of disease progression.

Standard diagnostic immunohistochemistry of PCa currently involves detection of a-methylacyl-CoA racemase (AMACR; also referred to racemase) together with basal cell

markers including p63 and high-molecular-weight cytokeratin (34βE12, HMWCK). However, the diagnostic value and correct interpretation of these markers require a distinct assessment of their morphological context [357]. For example, racemase overexpression is a molecular hallmark already detectable in HGPIN, thereby limiting the value of this marker to discriminate between precursor and advanced PCa [358, 359]. There is continuous clinical interest in identification of additional markers that may prove helpful where AMACR staining is insufficient or ambiguous including fatty acid synthase (FAS), Golgi membrane protein 1 (GOLM1, also known as GOLPH2 or GP73), and ETS-related gene (ERG), useful in the context of transmembrane protease, serine 2 (TMPRSS2)-ERG gene translocation [357].

High glycolytic activity is an oncometabolic hallmark of cancer cells [5, 8, 9]. Indeed, dysregulated energy metabolism is an important driver in oncogenesis. Cancer cells turn to aerobic glycolysis for energy production in a process referred to as ‘the Warburg effect’ leading to accumulation of methylglyoxal (MG), a cytotoxic glycolytic byproduct that causes adduction of macromolecules by formation of advanced glycation end-products (AGEs). Glyoxalase 1 (GLO1), also known as lactoylglutathione lyase (EC: 4.4.1.5), is part of the glyoxalase system, playing a crucial role in cellular detoxification of spontaneously formed MG. In a two-step reaction, GLO1 first catalyzes the conversion of highly reactive MG to S-D-lactoylgluthatione. The resulting thioester, in the case of MG, is then hydrolyzed by GLO2 to produce D-lactate and reformed glutathione (GSH) [315]. The cytoprotective glyoxalase system prevents formation of AGEs and promotes cell survival. GLO1 upregulation has been described in the context of metabolic and inflammatory stress in vitro and in vivo [329-332], serving as a cellular mechanism to

detoxify high levels of MG, particularly in cancer, where high glycolytic rates as a result of the Warburg effect are observed. Previous reports have shown upregulation of GLO1 in various cancers including melanoma [302], breast cancer [340, 360, 361], prostate cancer [341, 362], gastric cancer [337, 363], pancreatic cancer [364] and renal carcinoma (clear cell carcinoma) [365].

Interestingly, previous studies have reported GLO1 upregulation in PCa patient tissue samples detecting a wide range of staining intensity [341, 362]. GLO1 displayed a strong association with Gleason grade, pathological tumor stage, and early biochemical recurrence (BCR). In addition, a positive correlation between circulating plasma GLO1 and TGFβ levels was identified in metastatic PCa patients, suggestive of a role of GLO1 in TGFβ-driven EMT was also confirmed by cell-based mechanistic studies [366]. Moreover, GLO1 upregulation appears to be a feature of prostate cancers characterized by *ERG* fusion and *PTEN* deletion [341, 362]. In spite of significant variability in GLO1 prevalence in PCa specimens, these prior studies strongly indicate that GLO1 upregulation is associated with progression and aggressiveness.

Given the critical role of GLO1 as an enabler of disease progression via MG detoxification, it is important to further investigate and provide more evidence on the status of this marker, especially in PCa, where the mechanism of disease progression and aggressiveness is still poorly understood. In this study, we have evaluated GLO1 expression by immunohistochemistry in a tissue microarray cohort consisting of 882 prostate cancer specimens obtained from 187 cases with associated clinical data. GLO1 expression was identified as a distinct molecular marker characteristic of early PCa

development as substantiated by high expression levels observed in HGPIN for the first time.

## 4.2. Materials and Methods

### 4.2.1. Patients

**Table 6**. Characteristics of the arrayed prostate cancer tumors and clinical data.

| **Characteristics** | **Total** | **%** |
|---|---|---|
| No. of cases | 187 | 100 |
| No. unique cases w/evaluable cores | 170 | 90.9 |
| No. of cores | 882 | 100 |
| No. of evaluable cores | 797 | 90.4 |
| Age (years) | 41-79 years old | |
| 41-49 | 6 | 3.5 |
| 50-59 | 44 | 25.9 |
| 60-69 | 76 | 44.8 |
| 70-79 | 39 | 22.9 |
| Unknown | 5 | 2.9 |
| Mean | 63.4 | |
| Pathologic stage | | |
| 2a | 4 | 2.4 |
| 2b | 2 | 1.2 |
| 2c | 47 | 28.3 |
| 3a | 109 | 65.7 |
| 3b | 4 | 2.4 |
| Unknown | 4 | 2.4 |
| **PSA** (pre-radical prostatectomy) | 165 cases | |
| Unknown | 5 cases | |
| Range | 1-120 ng/mL | |
| Mean | 11.56 ng/mL | |
| **PSA** (post-radical prostatectomy) | 136 cases | |
| Unknown | 34 cases | |
| Range | 0-163 ng/mL | |
| Mean | 2.43 ng/mL | |
| Biochemical recurrence | $\geq$0.2 ng/mL (77 cases) | |

Prostate specimens from 200 patients undergoing radical prostatectomies between the years of 1995-2007 at the University of Arizona Medical Center (UMC) and the Tucson Medical Center (TMC) were available at the Tissue Acquisition and Cellular/Molecular Analysis Shared Resource (TACMASR) at the University of Arizona Cancer Center, University of Arizona, Tucson, AZ (**Table 6**).

The clinical database associated with this tissue cohort was originally generated from information obtained from de-identified pathology reports. Histopathological data included patient age, pre- and postoperative prostate specific antigen (PSA), Gleason assessment at biopsy, and pathologic stage (T2 = organ confined tumor; T3 = capsular penetrating tumor). Gleason score and grade, as defined by the International Society of Urological Pathology [367], were revalidated and used for data analysis. Biochemical recurrence (BCR) was defined as postoperative PSA $\geq$ 0.2 ng/mL [368]. Specifically, upon resection, whole prostate specimens were placed on ice and transported to the TACMASR facility where they were dissected, sliced at 10 mm intervals, and placed in 10% neutral buffered formalin for at least 24 h. Prostate specimens were finally sectioned at (5 mm), processed and embedded to produce 20-50 formalin fixed paraffin embedded (FFPE) blocks per specimen. An H&E section per block was evaluated by a board-certified pathologist to generate maps of the tumor-containing areas. Multiple cores (3 mm) from selected tumor areas and adjacent normal tissue for each prostate specimen were used to assemble a total of 17 tissue microarrays (TMAs). Each TMA was composed of 59 randomly assigned specimen cores and one orientation tissue from a normal organ different from prostate. All steps during the pre-analytical phase including sample preparation and processing were monitored carefully to preserve tissue integrity and avoid degradation of tissue

biomarkers. This study was reviewed by the University of Arizona, Institutional Review Board (IRB) and was determined to be exempt from the need for approval.

### 4.2.2. Immunohistochemistry

Immunohistochemical (IHC) detection of the various epitopes in human prostate cancer tissues was performed using the BenchMark ULTRA automated slide stainer (Ventana Medical Systems, Inc.). All TMAs were stained using an anti-GLO1 polyclonal rabbit antibody (ab96032, Abcam). At the same time, to discern normal prostatic tissue from prostate carcinoma, a dual standard stain [consisting of (*i*) a basal cell-directed antibody cocktail (34βE12+p63, VENTANA) and (*ii*) a rabbit monoclonal anti-p504s (racemase, SP116 clone, VENTANA), referred to as Rac/p63/HMWCK], was employed [48, 369, 370]. Sections from TMAs previously cut (4 µm) and stored were baked at 60°C (60 min) prior to IHC staining. All steps thereon were performed on the VENTANA automated staining platform. Briefly, TMA sections were deparaffinized, pretreated with Cell Conditioning 1 for antigen retrieval, followed by inactivation of endogenous peroxidase. Specimens were incubated with anti-GLO1 rabbit polyclonal antibody (2 µg/ml) for 16 min at 37°C. Immunoreactions were visualized using the OptiView DAB IHC Detection Kit (Ventana Medical Systems, Inc.). Following the chromogenic detection, all slides were counterstained with Hematoxylin II and Bluing Reagent (Ventana Medical Systems, Inc) for 4 min each and coverslips were applied. System level controls from cell line-derived FFPE included CAPAN-2, BT-474 and U-937 for weak, moderate and strong GLO1 expression, respectively. In addition, breast cancer tissue was used to monitor unspecific background staining on stromal cells. As a negative control, staining was performed in the absence of primary antibody. All reagents and incubation times on the dual staining

assay were used as directed by the manufacturer. Although cytoplasmic and nuclear GLO1 staining was observable, only cytoplasmic staining was scored for biomarker expression. Intensity and prevalence of staining were assessed by a board-certified pathologist, and histologic scores (H-score) were calculated for each individual tissue core as previously described [355]. In the case of GLO1, complete absence of staining was considered ‘negative’, while an H-score of 1-100, 101-200, and 201-300 corresponded to ‘weak’, ‘moderate’ and ‘strong’ GLO1 expression, respectively.

### 4.2.3. Inclusion/ Exclusion Criteria

Tissue cores were excluded based on the occurrence of staining artifacts (e.g. due to lack of reagent reaching the tissue or tissue cores detaching during the staining run). Additional exclusion criteria included tissue cores with folds due to poor adherence to the tissue slide. The final analysis included 797 tissue cores from 170 patient cases (**Table 6**). The majority of the cases had at least three evaluable tissue cores (with <10% displaying two or less evaluable tissue cores). Staining intensity and percent positive staining were scored for different tissue histologies (adjacent normal, HGPIN, PCa) and the calculated H-score was used for final analysis.

### 4.2.4. Statistical Analysis

GraphPad Prism 9.1.0 software (Prism Software Corp., Irvine, CA) was used for statistical analysis. Tissue data sets were analyzed employing non-parametric analysis using the Mann–Whitney test or Kruskal-Wallis test (performed to evaluate associations between GLO1 expression and clinical variables); *$p<0.05$; ***$p<0.0005$; ****$p<0.0001$.

## 4.3. Results

### 4.3.1. GLO1 Immunodetection during Tumorigenic Progression in Arrayed Prostate Patient Specimens.

In order to comprehensively profile GLO1 expression during tumorigenic progression, tissue specimens originating from PCa (stage 2 and stage 3) patients were analyzed in TMA format (**Figure 18A** and **18B**). For comparison, tissue was also analyzed using H&E and Rac/p63/HMWCK staining, performed according to established clinical standard procedures. Overall, as expected, racemase staining was highly elevated as a function of clinical occurrence of prostate adenocarcinoma and almost absent from normal tissue. Moreover, racemase was upregulated in HGPIN lesions as compared to normal control tissue and displaying a moderate staining intensity as compared to PCa (**Figure 18A** and **18C**). A broad distribution of staining intensities detectable in HGPIN lesions was visualized by violin plot depiction, whereas the same analysis revealed a uniform expression characteristic of PCa specimens (**Figure 18C**, right panel). Remarkably, GLO1 was upregulated in HGPIN lesions displaying a higher staining intensity (uniform among tissue specimens) than PCa lesions as visualized by violin plot analysis (**Figure 18D**). Specifically, all HGPIN positive cores (120/120) demonstrated positive GLO1 staining and 79/120 (65.8%) displayed strong GLO1 staining (**Table 7**).

**Table 7**. GLO1 immunodetection during tumorigenic progression in arrayed prostate patient specimens.

| Staining scores[1] | Adjacent normal (n=286) | HGPIN (n=120) | Tumor (n=569) |
|---|---|---|---|
| Negative | 12 (4.2%) | 0 (0%) | 3 (0.5%) |
| Weak | 100 (35.2%) | 18 (15%) | 152 (27%) |
| Moderate | 127 (44.7%) | 23 (19.2%) | 240 (42.6%) |
| Strong | 45 (15.8%) | 79 (65.8%) | 169 (30%) |
| Total | 284 | 120 | 564 |

[1] H-score: weak (1-100); moderate (101-200); strong (201-300)

Remarkably, out of 564 PCa cores most displayed weak to moderate levels of GLO1 expression [weak: 152 (27%); moderate: 240 (42.6%)] and almost one third of tissue cores demonstrated strong staining (169 cores; 30%) (**Table 7**). Taken together these data indicate that whereas racemase expression increases linearly with tumorigenic progression, GLO1 expression is more characteristic of HGPIN lesions indicative of early progression.

Among these observations, pronounced GLO1 upregulation characteristic of HGPIN lesions is of particular interest given the role of HGPIN in PCa tumorigenesis. Morphological features of HGPIN as revealed by H&E staining include features such as a pronounced increase in nuclear size and chromatin as well as prominent nucleoli [33, 356, 371]. Indeed, the occurrence of HGPIN lesions is widely recognized as being indicative of carcinoma *in situ* with high predictive value of subsequent carcinogenesis, and HGPIN lesions are now considered being the most likely precursor of invasive PCa [33, 356].

### 4.3.2. GLO1 Immunodetection in HGPIN as a Determinant of Adjacent Tissue GLO1 Expression.

Next, we evaluated GLO1 expression in adjacent normal and PCa cores from cases with either strong or weak-moderate GLO1 immunostaining status detectable in HGPIN lesions. We also assessed the frequency of normal and PCa tissue adjacent to HGPIN. Although the number of HGPIN cores with weak-moderate expression of GLO1 was considerably lower to those displaying strong GLO1 staining, the proportion of PCa in both categories remained the same (60% vs 65%) (**Figure 19A**). Of note, in the same tissue core, there were also cases displaying all three histologies (normal, HGPIN, PCa) adjacent to each other (see **Figure 19A**, top image). Importantly, PCa tissue adjacent to HGPIN displayed a similar H-score for GLO1 expression, independent of GLO1 expression status (weak-moderate or strong) observed in HGPIN tissue (Figure 18B). In contrast, normal tissue adjacent to HGPIN characterized by strong GLO1 expression exhibited high GLO1 expression, while GLO1 expression of normal tissue adjacent to HGPIN expressing weak-moderate GLO1 showed a significantly lower H-score (**Figure 19C**).

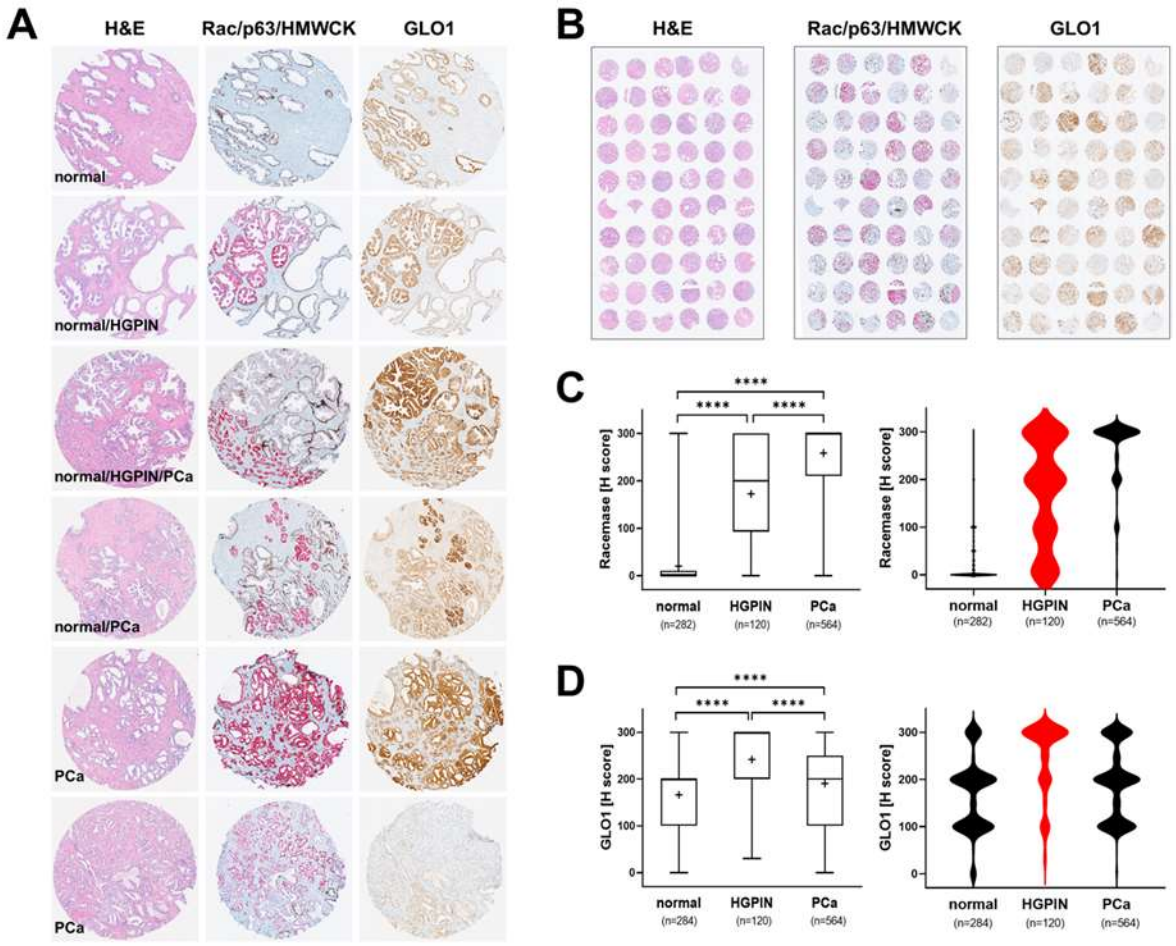


**Figure 18. Comparative immunohistochemical analysis in prostate cancer tissue specimens: GLO1 versus standard (Rac/p63/HMWCK; 'racemase') staining.** (**A**) Representative cores: H&E (left column), Rac/p63/HMWCK (middle column) and GLO1 (right column). (**B**) Representative TMAs stained as in panel A. (**C**) Racemase H-score comparison between adjacent normal, HGPIN, and PCa tissues (left: box and whisker plot; right: violin plot). (**D**) GLO1 H-score comparison between adjacent normal, HGPIN, and PCa tissues (left: box and whisker plot; right: violin plot). Statistical analysis of data was performed using the Kruskal-Wallis test (****p<0.0001); '+' signifies the mean; HGPIN data depicted in red.

Due to the rare occurrence of HGPIN characterized by weak GLO1 expression (4/42) statistical analysis was limited by the small sample size of low GLO1 expressing HGPIN. However, strikingly, analysis of a limited number of these specimens available to us revealed a clear trend suggesting a positive correlation between upregulation of GLO1 in normal tissue adjacent to HGPIN lesions displaying strong GLO1 expression (**Figure**

**19C**). Taken together these data indicate that GLO1 status detectable in HGPIN correlates with GLO1 expression in adjacent normal tissue, a relationship not observable in PCa.

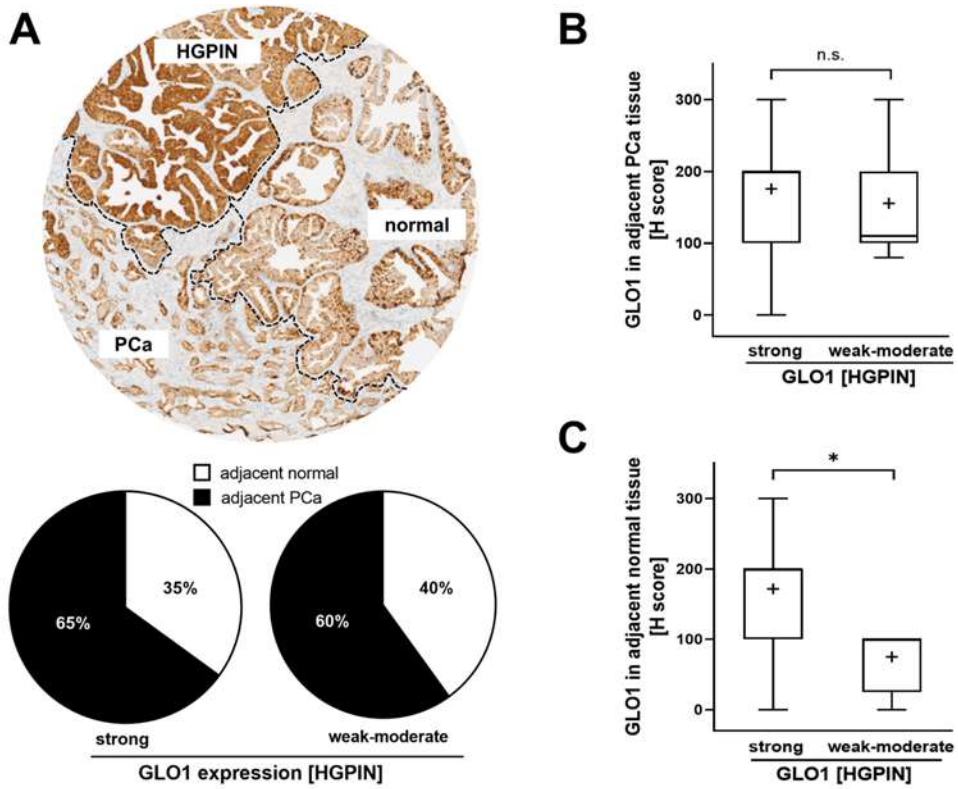


**Figure 19. GLO1 immunohistochemical staining in HGPIN as a determinant of adjacent tissue GLO1 expression.**(**A**) A representative core with HGPIN, adjacent normal, and PCa tissue (top panel). The pie chart (bottom panel) assesses the frequency (i.e. percentage of total cores scored) of normal and PCa tissue occurring adjacent to HGPIN [stratified by GLO1 expression status in HGPIN tissue; (strong GLO1: H-score 200-300; weak-moderate GLO1: H-score <200)]. (**B**) GLO1 H-score in PCa adjacent to HGPIN with altered GLO1 expression (strong versus weak-moderate). (**C**) GLO1 H-score in normal tissue adjacent to HGPIN with altered GLO1 expression (strong versus weak-moderate). Statistical analysis was done using the Mann–Whitney test (*p<0.05); '+' signifies the mean.

### 4.3.3. Association of GLO1 Expression with Gleason Grade, Pathological Stage, and BCR.

Next, we examined the potential association of GLO1 expression with clinical patient parameters. First, a potential relationship between Gleason grade and GLO1 expression status was examined (**Figure 20A**). Indeed, from Gleason 6 [3+3 (‘grade 1’)] to Gleason 7 [3+4 (‘grade 2’); 4+3 (‘grade 3’)] a significant increase of GLO1 H-score was observed. Violin plot analysis revealed that frequency of highest GLO1 expression (H-score = 300) was observed in Gleason 7 (4+3), clinically referred to as ‘intermediate high-risk’ (Figure 19B, right panel). Gleason 7 (3+4), clinically referred to as ‘intermediate low-risk’ displayed diminished GLO1 expression as compared to Gleason 7 (4+3) yet elevated as compared to Gleason 6 (3+3) clinically referred to as ‘low risk’. Remarkably, GLO1 expression in tissue displaying Gleason >7 (‘grade 4/5’) was not statistically different from Gleason 6 and was characterized by a broad range of GLO1 expression (**Figure 20B**). In contrast, racemase immunodetection of the same tissue cores revealed high (H-score >200) expression levels irrespective of Gleason score, and violin frequency analysis indicated the uniformity of this expression pattern (H-score = 300) (**Figure 20C**). In contrast to the remarkable correlation between GLO1 expression and Gleason grade, patient-associated parameters [including pathological stage and biochemical recurrence (BCR)] did not display a statistically significant difference as a function of tissue GLO1 expression levels (**Figure 20D** and **20E**).

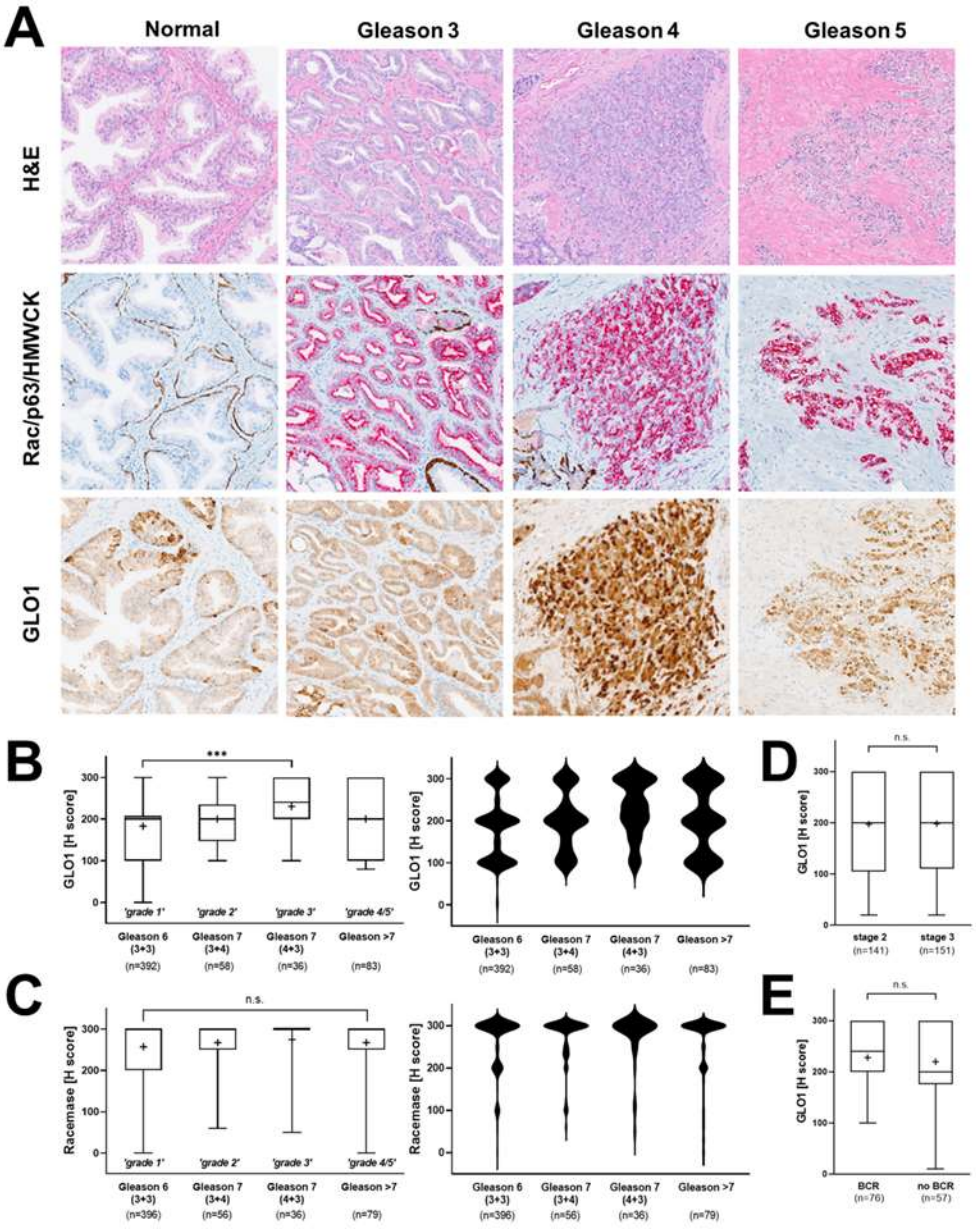


**Figure 20. Association of GLO1 immunohistochemical staining with clinical parameters of PCa.** (**A**) Representative images depicting different Gleason patterns from the tissue cohort; H&E (top row); Rac/p63/HMWCK (middle row); GLO1 (bottom column). (**B**) GLO1 expression as a function of Gleason grade (left: box and whisker plot; right: violin plot). (**C**) Racemase detection as a function of Gleason grade (left: box and whisker plot; right: violin plot). (**D**) GLO1 immunohistochemical detection as a function of pathologic stages 2 (organ confined) and 3 (capsular penetration). (**E**) GLO1 detection as a function of biochemical recurrence (BCR). Statistical analysis of tissue data sets was done using Mann–Whitney and Kruskal-Wallis tests (***$p<0.0005$); '+' signifies the mean.

## 4.4. Discussion

PCa is a progressive malignant disease with poor treatment outcomes when detected at late stages. Even though highly informative molecular markers exist that allow clinical detection of advanced malignancy (for example racemase- and cytokeratin-based markers), there is an urgent need for improved molecular biomarkers with diagnostic value that will allow detection of early-stage disease. Indeed, availability of a valid biomarker indicative of precancerous stages would be expected to change current intervention paradigms that interfere with progression of PCa.

Here, we show for the first time that pronounced GLO1 immunostaining is a distinct characteristic of HGPIN lesions analyzed in representative stage 2 and stage 3 prostate tissue specimens embedded in TMAs (**Figure 18**). Furthermore, GLO1 expression in HGPIN correlated with GLO1 expression in adjacent normal tissue (**Figure 19**). In addition, it was observed that GLO1 expression occurred as a function of Gleason grade up to 7 (‘intermediate–high risk’) with high statistical significance (**Figure 20**). Strikingly, we found that GLO1 upregulation is a consistent and specific molecular characteristic of HGPIN (precursor lesion to invasive PCa), and it is differentially expressed compared to PCa unlike the widely accepted biomarker, racemase with expression indistinguishable between HGPIN and PCa [34]. Thus, since current pathological assessment of HGPIN status solely depends on morphological features, our data suggest that GLO1 after further molecular and clinical validation may have utility as a novel diagnostic marker.

GLO1 upregulation in HGPIN lesions is of particular interest given the clinical role of HGPIN, widely considered as a premalignant state preceding PCa characterized by

morphological features such as marked increase in nuclear size and chromatin, prominent nucleoli, and genomic instability [7,8,38]. Cumulative research supports the hypothesis that HGPIN represents early carcinoma in situ with high likelihood of this premalignant lesion progressing towards invasive PCa, a premalignant condition serving a comparable role as observed in other premalignancies such as hyperplastic polyposis in colorectal cancer (CRC), actinic keratosis in squamous cell carcinoma (SCC) and dysplastic nevi in melanoma [8,39,40,41]. Indeed, genomic analysis indicates that HGPIN and PCa share common genetic alterations [42]. Interestingly, upregulated GLO1 expression is a molecular characteristic observable even during later stages of PCa progression as documented by us as a function of Gleason grades 1 through 3 ('low risk' to 'intermediate–high risk') (**Figure 20**). Nevertheless, in contrast to the uniformity of elevated GLO1 expression in HGPIN, PCa specimens were characterized by a wide range of GLO1 expression levels, an observation with particular relevance to high Gleason grades (grade 4/5) (**Figure 20**).

Reprogramming of energy metabolism has now been identified as a hallmark of tumorigenic progression, and changes in GLO1 expression observable in precancerous and cancerous lesions of PCa patients must be interpreted in this context [31,43,44,45]. Strikingly, our observations indicate that advanced PCa specimens display a wide range of GLO1 immunoreactivity. It may therefore be hypothesized that metabolic adaptations associated with GLO1 expression serve an essential oncometabolic role during early stages of tumorigenesis (HGPIN), yet become dispensable at later stages of tumorigenic progression (**Figure 18**). Indeed, association of GLO1 expression observed in low to intermediate Gleason grade suggests that this occurrence represents an early

oncometabolic switch relevant to PCa that becomes non-essential during later progressional stages of the disease.

Additionally, it has been shown that even though normal prostatic epithelial cells rely on aerobic glycolysis ('Warburg effect') for energy production, reversion to mitochondrial OXPHOS-based energy metabolism during late stages of PCa progression has been documented [15]. Moreover, metabolic reprogramming in cancer cells might also occur in the context of crosstalk with the surrounding stroma and tumor microenvironment [46,47]. Thus, it is no surprise that normal tissue (adjacent to HGPIN lesions overexpressing GLO1) displays high expression of GLO1 consistent with the occurrence of molecular crosstalk and stromal support of malignant cells (**Figure 19**). In order to resolve these relevant questions, we are currently pursuing an experimental approach involving CRISPR/Cas9-based genetic target elimination that we have implemented successfully to explore the role of GLO1 in cancer cell lines including A375 malignancies melanoma and DU-145 PCa cells [21,44,45]. Concordantly, a recent publication has provided strong evidence that genetic modulation of GLO1 expression by siRNA impairs metastasis of PCa cell lines (DU-145, PC3). It was proposed that GLO1 antagonism, through elevation of cellular MG levels, causes TGFβ inactivation with suppression of TGF-β1/Smad EMT upstream of mesenchymal markers including vimentin, N-cadherin, MMP2, and MMP9 [31]. The availability of potent small-molecule drug-like GLO1 inhibitors currently used as pre-clinical therapeutics might also provide a powerful tool supporting mechanistic and clinical studies targeting GLO1 in PCa animal models and patients [48].

In summary, these data suggest that GLO1 may serve as a novel diagnostic biomarker of early PCa progression. Future research with inclusion of additional molecular

parameters will substantiate the validity of GLO1 expression that selectively identifies HGPIN lesions in clinical samples and will also explore the mechanistic role of GLO1 as a causative effector in PCa progression that might also serve as a novel target for chemotherapeutic intervention at the early stage of the disease.

## 4.5. Conclusions

In conclusion, we have identified GLO1 as a distinct molecular marker characteristic of early PCa development, as substantiated by high expression levels observable in HGPIN. Given its crucial role in regulation of glycolytic energy metabolism, GLO1 association with low to intermediate Gleason grade may be indicative of an early oncometabolic adaptation in PCa. Taken together, our data suggest that GLO1 may serve as a novel diagnostic marker for HGPIN detection during early PCa progression. Our ongoing research aims at substantiating the biomarker role of GLO1 that might also serve as a novel molecular target in PCa tumorigenesis.

# CHAPTER V

## Genetic Target Modulation by CRISPR/Cas9 Substantiates the Role of GLO1 as a Molecular Enabler of EMT in Prostate Cancer Cells

## 5.1. Introduction

Having demonstrated that GLO1 is overexpressed in HGPIN and PCa tissue samples, we further investigated the role of GLO1 in prostate cancer at the mechanistic level. The prostate cancer field is in need or biomarkers that can, a) predict aggressive disease, and b) serve as therapeutic targets; GLO1 may be of clinical utility. Recently, our laboratory generated CRISPR/Cas9 *GLO1* knock-out isogenic clones from DU-145 prostate carcinoma cells, a molecular target modulation approach already implemented successfully in A375 malignant melanoma cells as published recently [372]. Here, we demonstrate successful *GLO1* elimination on DU-145 (*GLO1*_KO_A16, A26 and A29 isogenic clones) confirmed at the genomic, transcript, protein and at the enzymatic levels. Recently published data generated in our laboratory using Nanostring™ nCouter gene expression analysis showed that, in A375 human malignant melanoma cells, *GLO1* genetic deletion resulted in upregulation of *TXNIP* (encoding thioredoxin-interacting protein) a master regulator of cellular energy metabolism and redox homeostasis. Similarly, upregulation of *TXNIP* was confirmed in the DU-145-*GLO1*_KO as a function of *GLO1* status. The same effect was observed with *GLO1* genetic deletion following treatment of A375 wild type (WT) cells with methylglyoxal (MG) or a pharmacological GLO1 inhibitor (TLSC02). These results suggest that *GLO1* antagonizes *TXNIP* expression via control of cellular MG levels. Metastatic prostate cancer (mPCa) is presently incurable with a direct effect on quality of life and patient survival. The molecular mechanism involved in the progression to metastatic disease is still not well understood. We previously identified GLO1 as a novel molecular determinant of invasion and metastasis in malignant melanoma. Furthermore, a previous study using modulation of

GLO1 by siRNA identified this glycolytic enzyme as a key player in sustaining the metastatic phenotype in PCa. To further investigate the role of GLO1 in promoting invasion and metastasis we performed a human EMT expression array analysis comparing DU-145 WT versus *GLO1*_KO isogenic cells. Using this approach, we identified *MMP-3* (encoding matrix metalloproteinase-3) and *SPP1* (encoding secreted phosphoprotein 1) as the two genes displaying the most significant downregulation in response to *GLO1* elimination. Strikingly, MMP-3 and SPP1 are two effectors implicated in the development of prostate cancer in the bone, tumor-associated inflammation, facilitating metastasis, and promoting drug resistance. Furthermore, based on TCGA data, decreased survival probability correlated with high MMP-3 mRNA expression levels in tissue from prostate cancer patients suggesting that GLO1 expression status is a novel and underappreciated determinant of PCa invasiveness and patient survival.

## 5.2. Materials and Methods

### 5.2.1. Prostate Carcinoma Cell Culture

Human DU145 prostate carcinoma cells (ATCC, HTB-81) and engineered isogenic variants CRISPR/Cas9-derived *GLO1*_KO cells (DU145 *GLO1*_KO-A16; DU145 *GLO1*_KO-A29) were cultured in EMEM (Corning Inc., Corning, NY), supplemented with 10% FBS and 2 mM L-glutamine. Cells were maintained in a humidified incubator (37 °C, 5% $CO_2$ and 95% air).

### 5.2.2. CRISPR/Cas9-based Engineering of DU145 GLO1_KO Prostate Carcinoma Cells

Homozygous *GLO1* gene knock-out in human DU145 prostate carcinoma *GLO1*_KO cells was performed using genetic engineering. Briefly, double strand breaks were generated on both sides of exon 2 (chromosome 6, positions: 38, 687, 313 bp; 38,685,738 bp) with guide CRISPR RNAs (5′-ACCCTCATGGACCAATCAGT-3′ and 5′-TGATCATAGGTGTATACGA G-3′). Parental cells were transfected with Cas9 protein, crRNAs, and *trans*-activating crRNA (Integrated DNA Technologies, San Diego, CA) using the Lipofectamine RNAiMAX reagent (Thermo Fisher Scientific, Waltham, MA). Next, single cells were deposited in 96-well plates and once single cell colonies expanded (after approximately three weeks), individual clones were screened by PCR. Clones that were negative for a sequence inside the targeted deletion and negative for the undeleted chromosomal sequences but positive for ligation-junction fragment were scored as potentially homozygous for *GLO1* exon 2 deletion. Absence of *GLO1* expression was confirmed by single RT-qPCR, immunoblot, and enzymatic activity assays.

### 5.2.3. Single RT-qPCR Analysis

Total RNA was isolated using the Qiagen RNeasy Mini Kit (Qiagen) according to the manufacturer's protocol. RNA integrity was checked by the RNA 6000 Nano chip kit using Agilent 2100 Bioanalyzer (Agilent Technologies, Santa Clara, CA). Human 20X primer/probes [*GLO1* (Hs_02861567_m1), *TXNIP* (Hs_01006900_m1) *RPS18* (housekeeping gene; Hs_01375212_g1)] were obtained from Thermo Fisher Scientific, Waltham, MA. 500 ng of total RNA was used for cDNA synthesis using following cycling conditions: 25 °C for 10 min; 48 °C for 30 min and 95 °C for 5 min performed in MJ Thermocycler PTC-200 (MJ Research, Watertown, MA). Then, 10 ng of cDNA was used for amplification of target genes by quantitative PCR using following conditions: 95 °C for 10 min followed by 95 °C for 15 s and 60 °C for 1 min for a total of 40 cycles performed in the ABI7500 Real-Time PCR System (Applied Biosystems, Foster City, CA). PCR amplification of human housekeeping gene *RPS18* was used to control quality of the cDNA. Non-template controls were included on each PCR plate. Expression levels of target genes were normalized to the *RPS18* control [ΔCt = Ct (gene of interest) – Ct (housekeeping gene)]. Amplification plots were generated and the Ct values (cycle number at which fluorescence reaches threshold) recorded as published before [373, 374].

### 5.2.4. Immunoblot Analysis

After cellular protein extraction using RIPA buffer (50 mM Tris, pH 7.4, 150 mM NaCl, 1 mM EDTA, 1% Triton N- 100, 1% sodium deoxycholate and 0.1% sodium dodecyl sulfate) supplemented with protease inhibitor mixture (leupeptin, aprotinin, PMSF), equal

amounts of total protein were separated using 4%–15% SDS-PAGE gel (Bio-Rad laboratories, Irvine, CA) transferred to PVDF membrane, and developed. Detection of proteins was conducted using the GLO1 (ab96032, Abcam) primary antibody. HRP-conjugated goat anti-rabbit antibody (Jackson ImmunoResearch Laboratories, West Grove, PA, USA) was used as a secondary antibody. The membrane was incubated with ECL Western Blotting Detection Reagents (Amersham Biosciences, Piscataway, NJ) and exposed to BioMax XAR film (Kodak, Rochester, NY). Equal protein loading was examined by β-actin detection using a mouse anti-actin monoclonal antibody (Sigma Aldrich, St. Louis, MO, USA). For quantification, densitometric image analysis was performed using Image Studio™ Lite quantification software (LI-COR Biosciences, Lincoln, NE) [373, 375].

### 5.2.5. Enzymatic Activity Assay

Glyoxalase 1-specific enzymatic activity in prostate adenocarcinoma DU-145 and engineered isogenic variants [CRISPR/Cas9-derived *GLO1*_KO cells (DU-145 *GLO1*_KO-A16, *GLO1*_KO-A26 and *GLO1*_KO-A29)] cytosolic fractions was analyzed using a colorimetric glyoxalase 1 assay kit (241019; Abcam, Cambridge, UK) according to the manufacturer's instructions [376]. Briefly, pelleted cells (~1–2 x $10^6$) were homogenized with 300 µL of ice-cold GLO1 Assay Buffer containing protease inhibitor PMSF and centrifuged (12,000 g; 4 °C; 10 min). Supernatant cytosolic fractions were analyzed for protein content (Pierce. BCA Protein Assay Kit, Thermo Fisher Scientific, Waltham, MA, USA); equal amounts (10 µg protein) were mixed with substrate and then examined for enzymatic activity by measuring absorbance at 240 nm in kinetic mode (room temperature; 10–20 min).

### 5.2.6. Cell Proliferation Assay and Population Doubling Time

Cells (50,000 per 100 mm dish) were seeded followed by culture in fresh growth medium (72 h). Viable cells (as determined by an acridine orange/DAPI-based assay) were counted (d0 and d3) using the Nucleocounter NC-200 automated cell counter (ChemoMetec, Denmark). Population doubling time (DT) was then calculated as follows: DT = T x log n2/log n1 (Xe/Xb) [T is the incubation time (72 h), n is the number of cells, Xb is the cell number at the beginning of the incubation time, and Xe is the cell number at the end of the incubation time] [373].

### 5.2.7. Colony Forming Assay

Cells were seeded in a six-well plate (500 cells per well; Falcon, USA) followed by culture in fresh growth medium for a period of 9 days followed by media medium removal. Colonies were stained with crystal violet (Sigma-Aldrich, St. Louis, MO, USA) and individual colonies (larger than 1 mm) manually counted.

### 5.2.8. Transwell Invasion Assay

Matrigel-coated (invasion) 8 µm pore size translucent 24-well plate transwell chambers (BD Biosciences, San Jose, CA, USA) were used to evaluate the invasion potential of DU-145 cells following a published standard procedure [377]. Briefly, 700 µL of normal growth medium (10% FBS) was added to the bottom of each well and a total of $5 \times 10^4$ cells resuspended in 250 µL of migration buffer (normal growth medium; 0.5% FBS; 0.1% BSA) were seeded on top. After 24 h incubation at 37 °C, 5% $CO_2$, non-invading cells were removed by wiping the upper side of the membrane, and invading cells fixed with

methanol and stained with crystal violet (Sigma-Aldrich, St. Louis, MO, USA). Ten random fields at 10x magnification per filter were considered for final quantification.

### 5.2.9. Human RT$^2$ Profiler™ PCR Expression Array

Total cellular RNA from DU-145 cells and their isogenic variants was isolated according to a standard procedure using the RNeasy Mini kit (Qiagen, Valencia, CA, USA). Reverse transcription was performed using the RT$^2$ First Strand kit (Qiagen, Valencia, CA, USA) from 500 ng total RNA. For expression profiling, the RT$^2$ PCR expression array technology (Qiagen, Valencia, CA, USA) was used as published before [45,46]. For EMT-related gene expression changes, Human Epithelial Mesenchymal Transition array was used. Quantitative PCR was run using the following conditions: 95 °C for 10 min, followed by 40 cycles of 95 °C for 15 s alternating with 60 °C for 1 min (Applied Biosystems, Carlsbad, CA, USA). Gene-specific products were normalized to a group of 5 housekeeping genes including ACTB, B2M, GAPDH, HPRT1 and RPLP0 and quantified using the comparative (DDCt) Ct method as described in the ABI Prism 7500 sequence detection system user guide. Expression values were averaged across three independent array experiments, and standard deviation was calculated for graphing and statistical analysis as published before [378]. Volcano plot depiction displays each gene's p-value and fold expression difference (log2 scale) with the selected covariate. Thus, statistically significant gene alterations occur at the top of the plot [(above the horizontal cut-off line (p-value threshold: 0.05)], and differentially expressed genes are depicted on either side (beyond the 2-fold cut-off line).

### 5.2.10. Database

The open source The Human Protein Atlas (TCGA-based) database (https://www.proteinatlas.org/) was used to perform a survival analysis in a prostate cancer cohort of patients with high and low MMP3 expression.

## 5.3. Results

### 5.3.1. Characterization of the DU-145 Human Prostate Adenocarcinoma Cells with Genetic GLO1 Deletion (DU-145-GLO1_KO).

Previous studies evaluating the role of GLO1 in human prostate cancer cells relied on the use of siRNA knock-out cell lines. Our rigorous approach employed genetic elimination of the *GLO1* gene using CRISPR/Cas9- mediated exon 2 deletion (**Figure 21A**). Successful *GLO1* elimination on clones DU-145-*GLO1*_KO_A16, A26 and A29 was confirmed by PCR analysis of genomic DNA (Figure **21B**) and further substantiated by RT-qPCR and immunodetection. Results on **Figure 21C** show complete absence of the *GLO1* mRNA transcript and protein, respectively, from all analyzed *GLO1*_KO clones as compared to DU-145 WT cells. Consistent with complete ablation of *GLO1* mRNA and proteins levels, GLO1 enzymatic activity, as assessed by an enzymatic activity assay, in two selected DU-145-*GLO1*_KO clones (A16 and A29) was almost completely absent (**Figure 21D**).

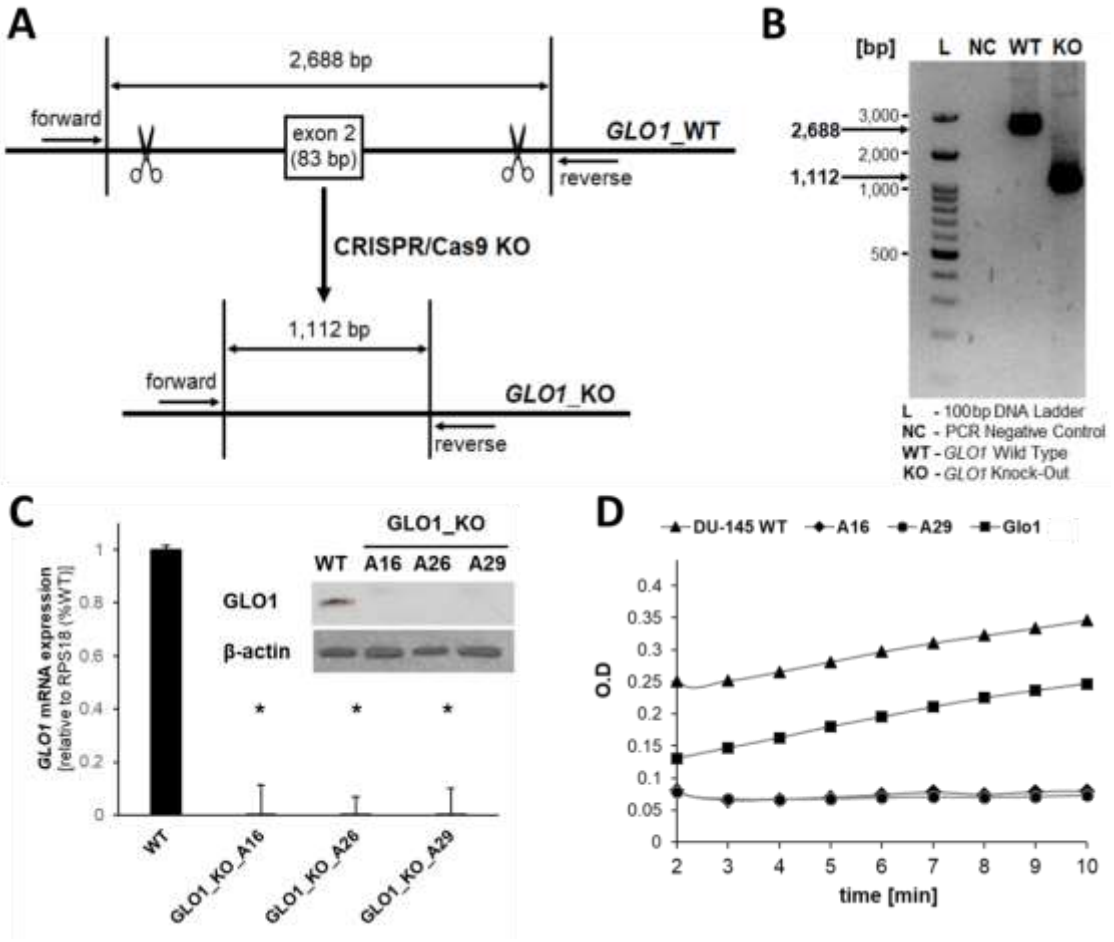


**Figure 21. Genomic deletion of *GLO1* in DU-145 human prostate carcinoma**.(**A**) Exon 2-directed CRISPR/Cas9-dependent GLO1 deletion (**B**) was confirmed by PCR analysis of genomic DNA as compared to wild type (WT) allele. KO status of DU-145-*GLO1*_KO clones (A16, A26, A29) was validated at the (**C**) mRNA (RT-qPCR) and protein (immunoblot analysis) levels (Inset). (**D**) Loss of GLO1 enzymatic activity was determined in DU-145-*GLO1*_KO (A16, A29) clones used for further experimentation.

### 5.3.2. The Tumor Suppressor TXNIP is Upregulated upon GLO1 Genetic Deletion in the A375 Malignant Melanoma and DU-145 Prostate Carcinoma, and Pharmacological Modulation with the GLO1 Inhibitor TLSC702 Mimics GLO1 Genetic Deletion.

Previous studies using Nanostring nCounter™ analysis revealed *TXNIP* (encoding the thioredoxin-interacting protein; tumor suppressor gene) as the gene with the most pronounced upregulation as a result of *GLO1* genetic deletion in the A375 human malignant melanoma cell line (**Figure 22A**) [372]. In line with this observation, immunoblot analysis showed upregulation of TXNIP at the protein level (**Figure 22B**). Importantly, *TXNIP* upregulation in the A375 *GLO1*_KO cell lines was associated with attenuated glucose uptake and metabolism (data not shown) [59]. Furthermore, treatment of the A375 WT cells with MG, the metabolite inactivated by GLO1, or treatment with TLSC702, a pharmacological GLO1 inhibitor, induced *TXNIP* upregulation in a dose- dependent manner. Importantly, these results reproduced the effect observed with genetic deletion of *GLO1*, suggesting an indirect modulatory role of *GLO1* on *TXNIP* via MG control. Given the role of TXNIP as a tumor suppressor, we became interested in investigating the status of *TXNIP* in the newly generated DU-145 *GLO1*_KO prostate carcinoma cells using transcript and immunoblotting analysis. In line with our previous observations in the A375 malignant melanoma cells, *TXNIP* transcript (**Figure 22D**) and protein (**Figure 22E**) levels were significantly upregulated in the *GLO1*_KO clones with higher expression observable in the *GLO1*_KO_A29 cell line.

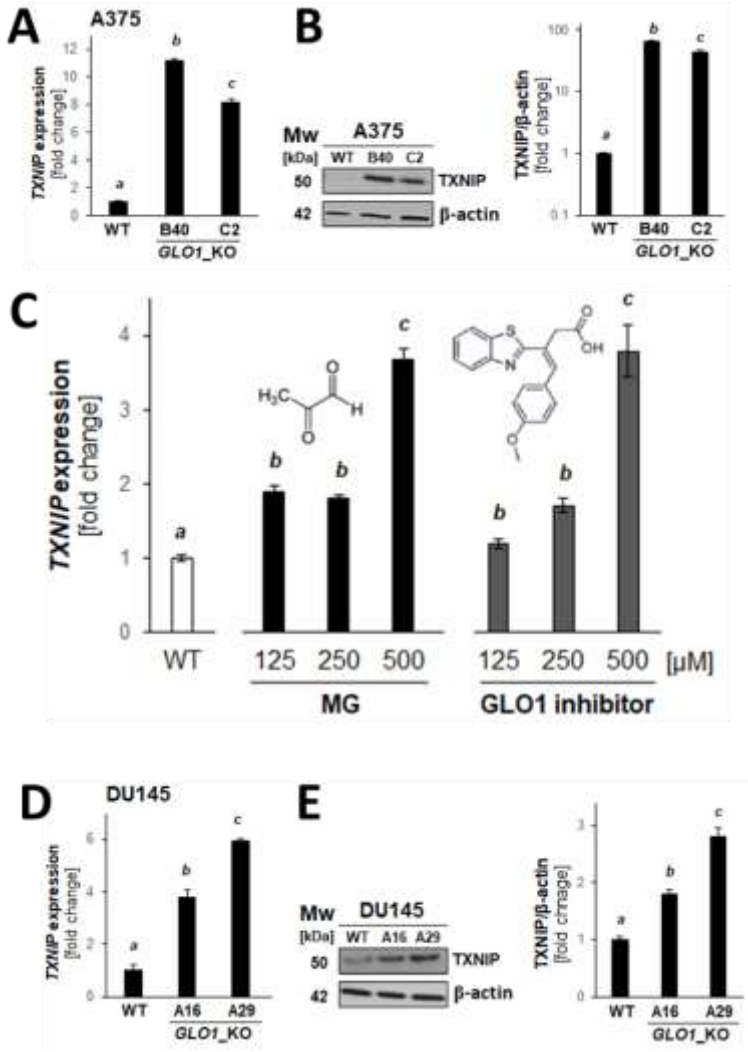


**Figure 22. GLO1 genetic deletion leads TXNIP upregulation in A375 melanoma cells and DU-145 prostate carcinoma cells, a reproducible effect observed following MG or a GLO1 inhibitor treatment.**(**A**) A significant upregulation of TXNIP at the mRNA and (**B**) protein levels is observed on A375 melanoma cells with GLO1 genetic deletion (GLO1_WT versus GLO1_KO clones [B40 and C2]). (**C**) *TXNIP* can also be upregulated upon treatment of A375 WT melanoma cells with MG or TLSC702, a GLO1 inhibitor. (**D**) A significant upregulation of TXNIP at the mRNA and (**E**) protein levels is observed on DU-145 prostate cancer cells with GLO1 genetic deletion (GLO1_WT versus GLO1_KO clones [A16 and A29]). [372].

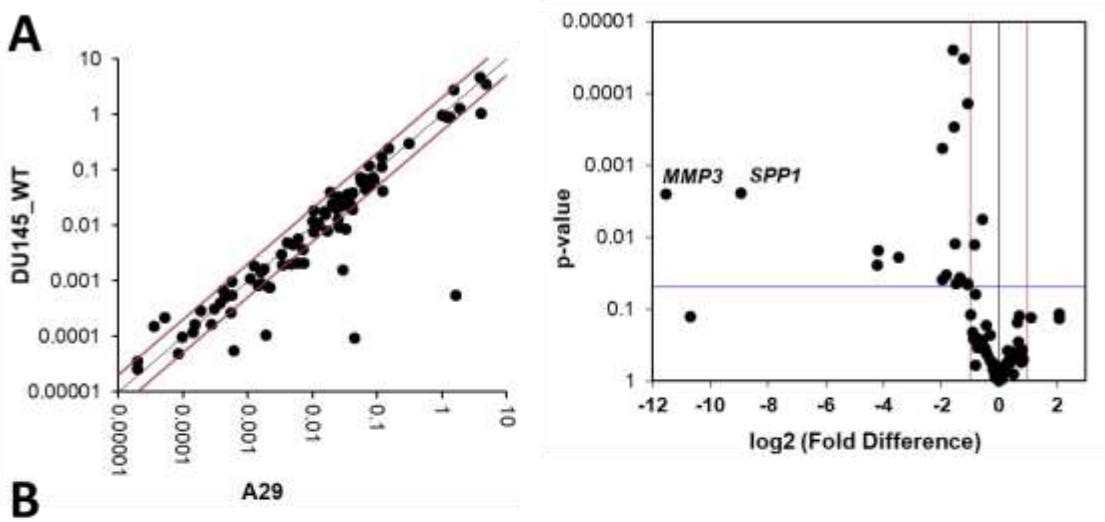


| gene symbol | description | p-value | fold change |
|---|---|---|---|
| ***MMP3*** | Matrix metallopeptidase 3 (stromelysin 1, progelatinase) | 0.00250 | **-2986.00** |
| ***SPP1*** | Secreted phosphoprotein 1 | 0.00245 | **-487.41** |
| ***DSP*** | Desmoplakin | 0.02481 | **-18.69** |
| ***COL5A2*** | Collagen, type V, alpha 2 | 0.01538 | **-17.99** |
| ***BMP7*** | Bone morphogenetic protein 7 | 0.01895 | **-11.27** |
| ***STAT3*** | Signal transducer and activator of transcription 3 | 0.03907 | **-3.87** |
| ***CALD1*** | Caldesmon 1 | 0.00058 | **-3.86** |
| ***SNAI2*** | Snail homolog 2 | 0.03342 | **-3.55** |
| ***MAP1B*** | Microtubule-associated protein 1B | 0.00003 | **-3.02** |
| ***ZEB1*** | Zinc finger E-box binding homeobox 1 | 0.00030 | **-2.97** |
| ***GNG11*** | Guanine nucleotide binding protein (G protein), gamma 11 | 0.01234 | **-2.90** |
| ***TFPI2*** | Tissue factor pathway inhibitor 2 | 0.04442 | **-2.84** |
| ***JAG1*** | Jagged 1 | 0.03648 | **-2.53** |
| ***FN1*** | Fibronectin 1 | 0.00003 | **-2.31** |
| ***WNT5B*** | Wingless-type MMTV integration site family, member 5B | 0.00014 | **-2.14** |
| ***ERBB3*** | V-erb-b2 erythroblastic leukemia viral oncogene homolog 3 | 0.04421 | **-2.13** |
| ***SNAI1*** | Snail homolog 1 | 0.04498 | **-2.12** |

**Figure 23. RT-qPCR gene expression array analysis indicates downregulation of epithelial to mesenchymal transition (EMT)-related genes in human DU-145 prostate carcinoma cells with genomic *GLO1* deletion.**(**A**) Left: Scatter plot depiction; Right: Volcano plot depicting differential gene expression (DU145_WT versus A29 (*GLO1*_KO) as detected by the RT$^2$ Profiler™ PCR expression array technology; (cut-off criteria: expression differential > 2; p value $\leq$ 0.05; n = 3). (**B**) Numerical expression changes [A29 (*GLO1*_KO) versus WT] revealing modulation of EMT-related genes as a function of *GLO1* deletion.

### 5.3.3. Differential Array Analysis Reveals Pronounced Modulation of EMT-related Gene Expression in DU-145-GLO1_KO Cells.

Recent studies from our laboratory identified GLO1 as a novel molecular determinant of invasion and metastasis in malignant melanoma [372, 373]. In addition, a previous

publication reported a mechanism whereby GLO1 sustains the metastatic phenotype of PCa cells. Their findings showed that by preventing adduction of *TGF-β*, GLO1 contributes to the TGF-β1/Smad signaling which controls the EMT phenotype [366]. To further identify tumorigenesis-related changes resulting from genomic *GLO1* deletion and the impact on the EMT phenotype, we performed differential gene expression analysis comparing DU-145-*GLO1*_KO (A26) with DU-145-*GLO1*_WT cells (**Figure 23**). Using the $RT^2$ Profiler™ PCR expression array technology, we interrogated expression of 80 genes. Significant changes at the mRNA level affecting seventeen EMT-related genes were identified to be downregulated ($p < 0.05$) (**Figure 23B**). Some of the genes with the most striking fold change included *MMP3*, *SPP1*, *CALD1*, *MAP1B*, *ZEB1*, *FN1* and *WNT5B*. Specifically, the *MMP3* gene had close to a three-thousand-fold change compared to the WT clone. The *SPP1* was also differentially expressed by a nearly five hundred-fold. Importantly, both, MMP3 and SPP1, have been associated with bone metastatic prostate cancer progression, tumor inflammation, and drug resistance [379-382]. SPP1, mediates interaction between tumor and stromal cells thus promoting tumor progression, angiogenesis and drug resistance [382].

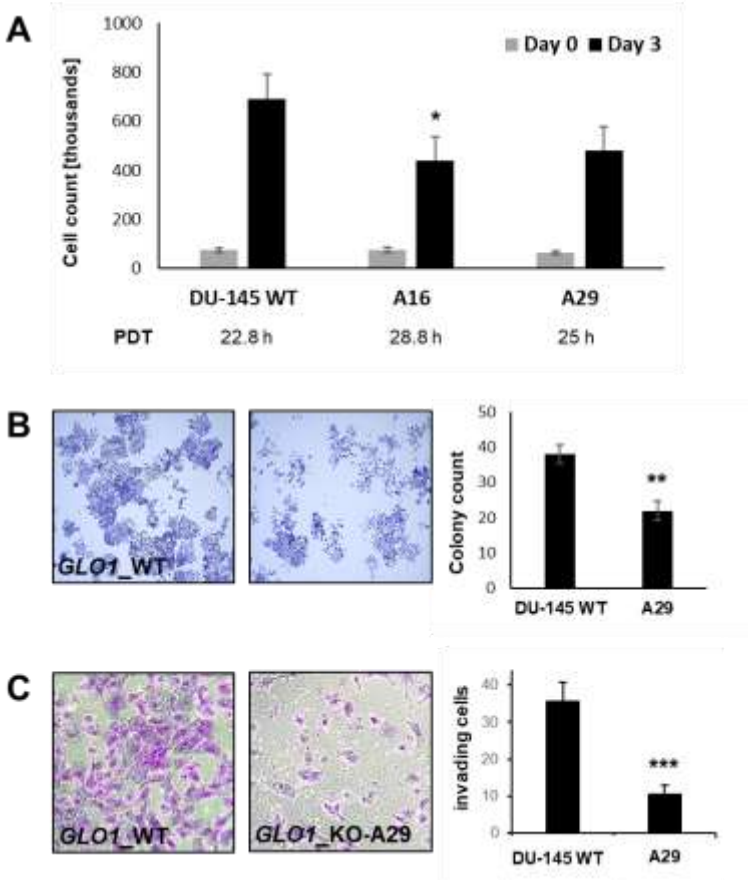


**Figure 24. Human DU-145 prostate carcinoma cells with GLO1 genomic deletion display impaired clonogenic and invasive capacity.**(A) Cell proliferation assay comparing the DU-145 wild type (WT) to the A16 and A29 with GLO1 genomic deletion shows significantly reduced proliferation ability on the A16 cells but not the A29 clone. (B) GLO1 genetic deletion significantly impairs (B) clonogenic and (C) invasive capacity. Left panel: representative images (10x magnification); right panel: bar graphs with statistical analysis. Statistical analysis of the data sets was done using T-test (*p <0.05, **p <0.005, ***p<0.0005).

### 5.3.4. GLO1 Genetic Deletion has a Detrimental Effect in Clonogenicity and Cell Invasion in DU-145 Cells.

Next, we performed phenotypic characterization of selected *GLO1*_KO-A16 and A29 clones (**Figure 24**). Genomic deletion of *GLO1* expression resulted in decreased cell proliferation in the two selected clones (**Figure 24A**); however, this effect was only statistically significant in clone *GLO1*_KO-A16. Given the proliferating defect observed in

the *GLO1*_KO-A16, we pursuit further studies using the *GLO1*_KO-A29 clone. Remarkably, genetic deletion of *GLO1* caused a decrease in the ability of this clone to form colonies as shown on **Figure 24B**. Furthermore, *GLO1*_KO-A29 cells appeared more elongated and disperse compared to the more uniform colonies in the DU-145 WT parental cell line (**Figure 24B**; right image). Additionally, when we compared the invasive capacity of the *GLO1*_KO-A29 clone versus the DU-145 WT cells on a transwell invasion assay using matrigel-coated inserts, we observed a significant decrease in the ability of the *GLO1*_KO-A29 cells to invade (**Figure 24C)**. These results suggest a role of GLO1 as an important molecular effector and critical player involved in the metastatic capacity of DU-145 human prostate carcinoma cells.

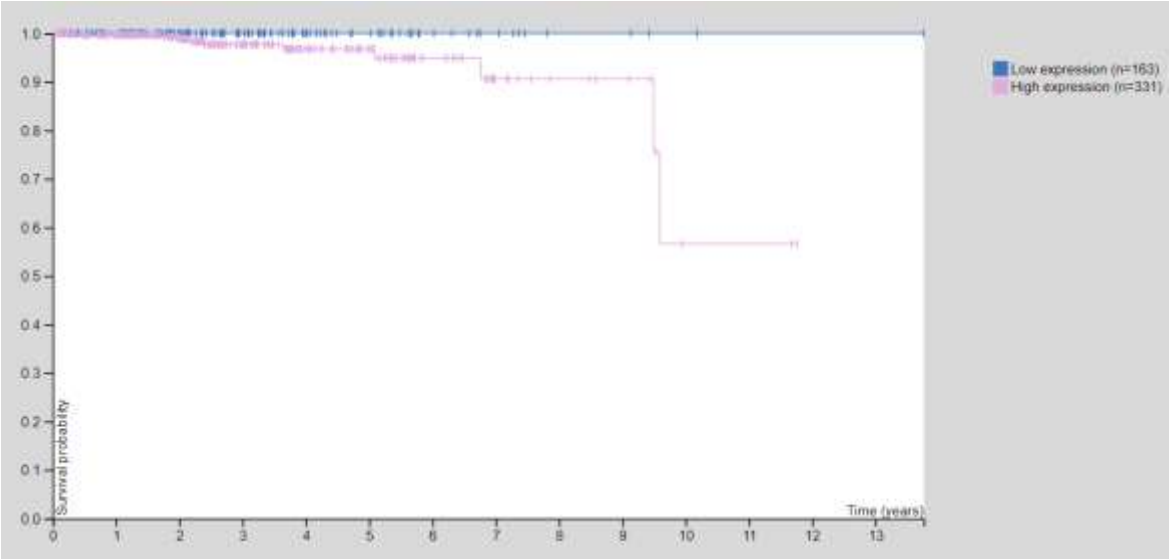


**Figure 25. Survival probability of prostate cancer patients as a function of MMP-3 tissue expression at the mRNA level.** Kaplan-Meier survival analysis distinguishes two cohorts of prostate cancer patients with low (n=163) and high (n=331) MMP-3 tissue expression as a determinant of patient survival. Decreased survival probability correlates with high MMP-3 mRNA expression levels [383].

### 5.3.5. MMP3 Overexpression in Prostate Cancer Patients Negatively Impacts Survival Probability.

The gene expression array analysis revealed MMP3 as the gene with the most profound downregulation in the *GLO1*_KO-A26 clone compared to the parental DU-145 WT. It was reported that MMP3 plays a critical role during prostate cancer progression by remodeling the extracellular matrix (ECM) and directly contributing to changes in the tumor microenvironment thus promoting prostate cancer development. Given that the DU-145 cell line is derived from a brain metastasis and that tumor-derived MMP-3 contributes to bone metastatic prostate cancer progression, we investigated the association of MMP3 with survival in prostate cancer patients. We turned to The Human Protein Atlas database to examine the association of MMP-3 expression with patient survival. As shown on **Figure 25**, MMP-3 tissue expression is a determinant of patient survival as observed on the Kaplan-Meier survival analysis of two prostate cancer patient cohorts with low and high *MMP3.*

## 5.4. Discussion

Metastatic prostate cancer, resulting from the dissemination of the disease, is presently incurable and the primary cause of death in PCa patients. Prevention and treatment of aggressive disease requires better understanding of the molecular enablers driving prostate cancer cells towards a more malignant phenotype. We recently reported upregulation of GLO1, a glycolytic enzyme part of the Glyoxalase system critical to the detoxification of a reactive glycolytic byproduct methylglyoxal, in HGPIN and prostate cancer [59]. Although our data showed higher GLO1 expression in HGPIN, GLO1

expression also occurred as a function of Gleason Grade. The present work further investigated the mechanistic role of GLO1 upregulation in prostate cancer.

Here, using genetic target modulation via the CRISPR/Cas9 system, we provide further evidence suggesting that GLO1 plays a critical role as a molecular determinant of invasion and metastasis. Importantly, other groups have demonstrated that GLO1 sustains the metastatic phenotype of prostate cancer cells via EMT control in *GLO1* knock-down cell lines. Our approach relied on the genetic deletion of *GLO1* via the CRISPR/Cas9 system (**Figures 21A** & **21B**). To confirm *GLO1* target modulation, we performed mRNA and protein-directed assays including RT-qPCR, immunoblotting (**Figure 21C**) and enzymatic activity (**Figure 21D**).

In addition, we demonstrated upregulation of *TXNIP* (encoding the thioredoxin-interacting protein) in the DU-145 *GLO1*_KO-A16 and *GLO1*_KO-A29 clones (**Figures 22D** and **2E**), a finding previously observed in malignant melanoma cells (**Figures 22A** and **22B**) [372]. Importantly, treatment of the A375 WT cell line with either MG, the metabolite inactivated by GLO1, or TLSC702, a pharmacological GLO1 inhibitor, reproduced the effect observed in the *GLO1* genetically deleted clones, suggesting an antagonistic role of *GLO1* on *TXNIP* via MG control (**Figure 22C**) [372]. TXNIP inhibits the antioxidative role of thioredoxin, a thiol-oxidoreductase that protects cells from oxidative stress, resulting in accumulation of reactive oxygen species (ROS) and cellular stress. TXNIP is also a regulator of cellular metabolism by negatively regulating glucose uptake and endoplasmic reticulum (ER) stress. TXNIP is considered a tumor suppressor gene because it mediates oxidative stress, inhibits proliferation, and induces apoptosis via thioredoxin inhibition [384]. Importantly, TXNIP expression is downregulated in a wide range of tumors [384,

385] and it has become an emerging target in the field of prostate cancer. A recent study reported a significant decrease in TXNIP expression in PCa tumors and this was associated with clinicopathological features. In line with these observations, overexpression of TXNIP in PC-3 cells significantly inhibited proliferation, migration, invasion and glucose uptake in addition to promoting apoptosis by stalling the cell cycle in the G0/G1 phase [385].

Acquisition of metastatic potential in cancer cells is dependent on EMT [386], yet the mechanism is still not well understood in prostate cancer. We previously identified GLO1 as a novel molecular determinant of invasion and metastasis in malignant melanoma, a premise that led us to study the role of GLO1 in the EMT phenotype in PCa. As observed in melanoma, differential gene expression array analysis (DU-145 WT versus DU-145-*GLO1*_KO-A29) revealed profound modulation of EMT-related genes (**Figure 23**). Two, among all downregulated genes, displayed striking fold change compared to the WT cell line, the matrix metalloproteinase 3 (*MMP-3*) and the secreted phosphoprotein 1 (*SPP1*). These two genes encode for modulators of the ECM and tumor-associated inflammation during prostate cancer development, both of which facilitate metastasis [380, 381].

Matrix metalloproteinases (MMPs) are well established mediators of tumor progression due to their ability to degrade extracellular matrix components and regulate growth factor and cytokine bioactivity [379]. The invasive capacity of cancer cells relies on their ability to cleave the extracellular matrix (ECM) and basement membranes surrounding epithelial cells as well as to remodel ECM components. MMPs are responsible for the dynamic regulation of micrometastasis [387, 388]. Recently, it was reported that tumor-derived MMP-3 contributes to bone metastatic prostate cancer progression via intrinsic and

extrinsic routes. Intrinsically, genetic silencing of MMP-3 in prostate cancer cell lines significantly reduced *in vitro* growth. Moreover, the lack of MMP-3 not only decreased AKT and ERK phosphorylation but also total VEGFR1 and FGFR3 protein levels. In line with the *in vitro* observations, *in vivo* studies showed that MMP-3 ablated tumors had a reduced growth rate and were significantly less vascularized due to a downregulation of a wide array of angiogenic factors. Furthermore*, in vitro* endothelial tube formation assays using conditioned media from MMP-3 silenced cells resulted in slower rates of tube formation further demonstrating the extrinsic role of MMP-3 in angiogenesis. These findings further evidence the crucial role MMP-3 plays in the development of prostate cancer in the bone. Bone metastatic prostate cancer is presently incurable with a direct effect on quality of life and patient survival and the unmet need for improved treatment options. Selective inhibition of MMP-3 may prove efficacious for the treatment of bone metastatic prostate cancer [379].

Another important gene significantly downregulated in our screening was the Secreted phosphoprotein 1 (SPP1), also recognized as osteopontin (OPN). SPP1 is a secreted chemokine-like glycophosphoprotein and a key mediator of tumor-associated inflammation and facilitates metastasis [389]. SPP1 is produced by tumor cells and multiple host cells including immune cells, osteoclasts, fibroblasts, endothelial, smooth muscle, and epithelial cells [390]. Interestingly, SPP1 mediates interaction between tumor and stromal cells thus promoting tumor progression, angiogenesis, and drug resistance [381]. Until recently, the role of SPP1 in PCa was not well understood, although it was thought that it could promote bone metastasis progression by stimulating and activating host resident cells on the bone microenvironment (immune cells, endothelial cells and

fibroblasts), in addition to regulating osteoclast and osteoblast bone formation and resorption [391]. Pang et al., using a bioinformatics approach coupled with *in vitro* functional testing, identified SPP1 as a key signature factor central to PCa metastasis and drug resistance development [381]. To this end, organoid models derived from mCRPC showed remarkably increased SPP1 mRNA and protein levels compared to hormone sensitive prostate cancer. Further studies on either SPP1-overexpressing or SPP1-depleted cell lines demonstrated a strong relationship between SPP1 upregulation and malignant progression of CRPC as well as enzalutamide resistance. As expected, given its critical role in drug resistance, *SPP1* knockdown enhanced enzalutamide sensitivity and had a detrimental effect on cell invasion and migration. Attenuation of the EMT phenotype was also observed in SPP1-deficient cells while upregulating SPP1 promoted EMT via the PI3K/AKT and ERK1/2 signaling pathways [382].

Phenotypic characterization of the *GLO1*-depleted clones showed no impact to cell proliferation on the *GLO1*_KO-A29 clone, however, we did observe a statistically relevant difference on the *GLO1*_KO-A16 clone in its ability to proliferate (**Figure 24A**). Given the proliferation defect and to eliminate the confounding effect of proliferative capacity, we decided to pursuit the *GLO1*_KO-A29 clone for further experiments. In line with previous studies and the results observed in our melanoma studies [373], *GLO1* elimination had a profound detrimental effect in the ability of the *GLO1*_KO-A29 clone to form colonies and invade (**Figures 26B** and **26C**). These results, in conjunction with previous reports [366, 373], provide further evidence to substantiate the critical role of GLO1 in sustaining the metastatic phenotype. Moreover, the observed modulation of factors that critically control the EMT-phenotype (such as MMP3) led to further transcriptomic-based investigations

using The Human Protein Atlas which substantiated the role of MMP3 expression in patient survival. As shown in **Figure 25**, the survival probability over time in prostate cancer patients with high MMP3 mRNA levels of expression strikingly decreases compared to patients with low expression levels.

## 5.5. Conclusions

Taken together, our data provides further evidence for the crucial role of *GLO1* by modulating key effectors such *MMP-3*, *SPP1* and TXNIP likely via MG control thus promoting aggressive disease and metastasis. Based on the data presented here, our previous reports and others, we propose that GLO1-mediated modulation of prostate cancer progression and maintenance of metastatic disease is dependent on its ability to prevent MG from targeting critical effectors involved in EMT. Furthermore, the upregulation of *TXNIP*, a master regulator of cellular energy metabolism and redox homeostasis, upon *GLO1* genetic deletion suggests yet another role of GLO1 in modulating tumor suppressors. **Figure 26** is a depiction of the proposed mechanism whereby GLO1 promotes prostate cancer aggressiveness by modulating the epithelial to mesenchymal (EMT) phenotype via TXNIP and other molecular effectors such as TGFβ. Our ongoing research aims at further elucidating the mechanistic role of GLO1 in prostate cancer progression and its potential as a therapeutic target in early and advanced PCa.

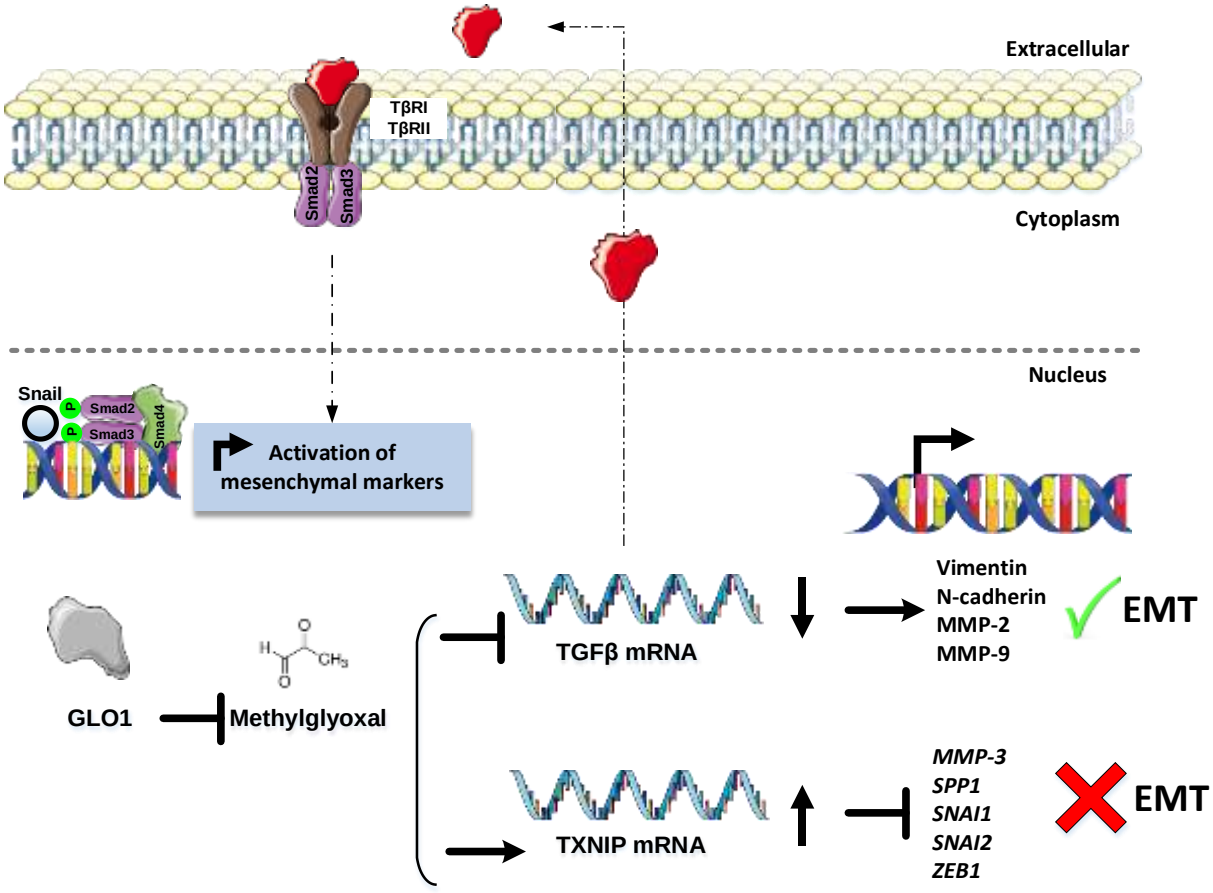


**Figure 26. Glyoxalase 1 expression promotes prostate cancer progression sustaining the metastatic phenotype by modulating epithelial to mesenchymal (EMT)-related gene expression.** GLO1-dependent detoxification prevents MG-modulation of key molecular effectors involved in tumorigenesis. On one hand, GLO1-dependent upregulation of TGFβ mRNA expression allows further protein translation and activation of pro-EMT markers: Vimentin, N-cadherin, MMP-2, MMP-9 (as recently substantiated in prostate carcinoma by the Antognelli group [366]). On the other hand, GLO1-dependent control of cellular MG levels antagonizes expression of TXNIP, a tumor suppressor and inhibitor of glucose metabolism that downregulates pro-EMT gene expression of *MMP-3*, *SPP1*, *SNAI1*, *SNAI2*, *ZEB1.* Taken together GLO1-dependent control of MG levels enables maintenance of high glycolytic flux during tumorigenesis without impairment of EMT, invasion, and metastasis.

# CHAPTER VI

## Future Directions

## 6.1. *In Vitro* and *In Vivo* Studies

In Chapter IV we identified GLO1 as a distinct molecular marker characteristic of early PCa development, as substantiated by high expression levels observable in HGPIN. In addition, GLO1 association with low to intermediate Gleason grade may be indicative of an early oncometabolic adaptation in PCa. From this work, we proposed that GLO1 may serve as a novel diagnostic marker for HGPIN detection during early PCa progression. Although this work largely focused on early PCa development, it is important to mention that GLO1 upregulation was also observable in PCa and it was significantly differentially expressed compared to normal prostatic tissue. Although we reported a wide range of GLO1 expression in high grade PCa cases (‘Grade 4/5’), our cohort lacked enough representation of such cases therefore making it difficult to assess the status of this biomarker in late PCa stages. Thus, it became important to further investigate the role of GLO1 in PCa.

To address questions regarding the role of GLO1 in prostate cancer progression, we resourced to the widely used DU-145 human prostate carcinoma cell line and the state-of-the-art CRISPR/Cas9 system to genetically engineer *GLO1*-deleted isogenic variants. In Chapter V, using an *in vitro* approach, we phenotypically characterized the DU-145 cells with *GLO1* genetic deletion to further investigate the role of GLO1 in PCa. Our data showed that genetic modulation of GLO1 in DU-145 cells significantly impacts their invasive and clonogenic capacity. Furthermore, genes associated with the EMT phenotype including MMP-3 and SPP1, were profoundly downregulated upon *GLO1* genetic deletion. We also found upregulation of TXNIP, a tumor suppressor gene which

mediates oxidative stress, inhibits proliferation, and induces apoptosis, in the *GLO1*-deleted isogenic variants. Although we showed we could reproduce the same antagonistic effect on TXNIP with MG treatment or pharmacologically inhibiting GLO1 in the A375 human malignant melanoma cells, we did not perform this study in the DU-145 prostate carcinoma cells. All in all, we and others, have reported solid evidence to substantiate the role of GLO1 in promoting aggressive disease and metastasis; however, further studies are required to substantiate the role of GLO1 in prostate cancer development and progression. In the following sections, we discuss questions that remain to be answer and how we can approach them as our future directions. In addition, **Figure 27** depicts in a sequential manner the proposed experiments as part of our future directions.

First, we would like to discuss the mechanism of GLO1 modulation. Although we show that genetic deletion of *GLO1* results in reduced invasive and clonogenic capacity in addition to significantly reduce expression of key genes involved in the EMT phenotype, our data did not elucidate the molecular mechanism. To this end, we believe this effect is related to the ability of GLO1 to prevent MG from targeting effectors involved on activation of EMT, such is the case of the important tumor suppressor TXNIP [372] and other effectors (TGF-β) as previously reported [366].

Next, we are interested in testing TLSC702, a GLO1 inhibitor, *in vitro* to determine whether the effects observed upon genetic inhibition of GLO1 are associated with lack of the *GLO1* gene or the functional protein. To this extent, the studies performed in the A375 human malignant melanoma cell lines whereby treatment with TLSC702, in addition to treatment with MG, resulted in *TXNIP* upregulation suggest this is merely related to the

ability of the cells to detoxify MG, thus associating this effect to the lack of a functional GLO1 enzyme. These studies will inform whether we can pharmacologically inhibit GLO1 in the DU-145 cell line.

Furthermore, the specific and consistent upregulation of GLO1 in HGPIN leads us to believe metabolic changes in early prostate cancer development are not only different than those observed in more advance stages but may also permit the changes needed for the cells to adopt a more malignant and invasive phenotype. As discussed before, HGPIN lesions are associated with aggressive prostate cancer, perhaps early metabolic changes enable the aggressive phenotype. Understanding the role of GLO1 in early and late stages during prostate cancer development and progression towards metastatic disease becomes crucial in devising therapeutic interventions. In this regard, we propose testing the GLO1 inhibitor TLSC702 in an *in vitro* model of HGPIN. This is of particular importance because the question that remains is whether inhibition of GLO1 via pharmacological intervention can serve a preventive measure for tumorigenesis, specifically in the context of HGPIN. To answer this question, we propose the use of a HGPIN model previously developed by Wang et al. [371]. This model relies on modulation of expression of α6β4 integrin via shRNA in RWPE-1 human normal prostate epithelial cells, and displays the characteristic invasive budding phenotype observed in HGPIN lesions from clinical specimens. The use of this model of early prostate cancer development will allow us to study molecular changes upon pharmacological inhibition of GLO1, particularly those associated with changes in genes associated with the EMT phenotype such as MMP-3.

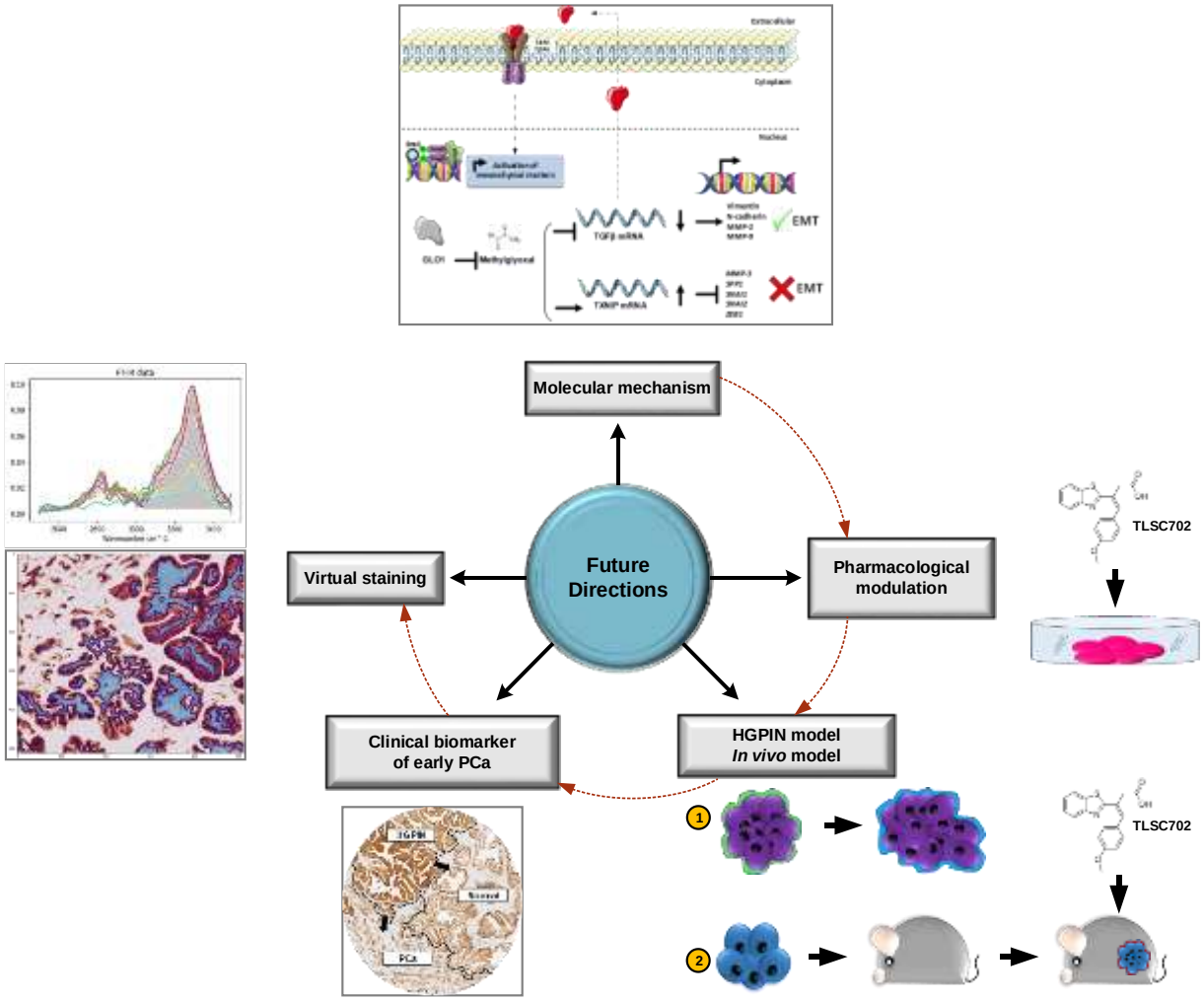


**Figure 27. Graphical depiction of proposed future directions**. The exploratory research presented here promises to impact the following fields related to prostate cancer. 1. A better understanding of molecular mechanisms underline oncometabolic dysregulation in PCa. 2. An improved understanding of the molecular basis underlying early PCa with a focus on HGPIN lesions pursued in relevant murine models. 3. Identification of improved molecular therapeutics that allow early interventions targeting HGPIN and mPCa. 4. Development of powerful prognostic and diagnostic biomarkers identifying HGPIN and PCa. 5. Discovery and development of novel optics-based technologies for the antibody independent diagnosis and prediction of PCa grade and progression.

Our *in vitro* results will become the foundation for the next step, a) compare the ability of the DU-145 WT versus the GLO1_KO cells in the SCID (severe combine immunodeficient) mouse model to form tumors and invade. For the invasion studies, we propose the use of a previously reported model of tumor cell invasion using the SCID mouse diaphragm [392]. The prostate organ is surrounded by fibromuscular tissue of smooth muscle cells, namely the 'capsule', directly connected to the prostatic stroma; therefore, invading prostate tumor cells must penetrate the muscular layer. It is known that capsular penetration is associated with significantly higher risk of lymph node metastasis [392]. We plan to inject DU-145 cells (WT or GLO1_KO) intraperitoneally (i.p.) and harvest cells three to five weeks later to assess the ability of the cells to invade and penetrate the muscle layer and form colonies on the inferior surface of the mouse diaphragm. To further test the GLO1 inhibitor, TLSC702, in early prostate cancer development *in vivo*, we propose the use of a previously describe transgenic mice expressing human *c-Myc* in the mouse prostate [393]. These mice develop murine PIN (mPIN) followed by invasive prostate adenocarcinoma. These results will provide further evidence to support the use of GLO1 as a therapeutic target as well as to further substantiate its use as a biomarker in early prostate cancer lesions associated with aggressive PCa.

Finally, an interesting finding for us was the wide range of GLO1 tissue expression in high grade ('Grade 4/5'). The diversity of expression perhaps is in line with the lack of differentiation and function on the highly malignant cells at that stage. As mentioned before, we need to screen a larger cohort of patients with 'Grade 4/5' in order to confirm our findings and to provide more statistical power to our study. Our novel findings

associating GLO1 expression to HGPIN and its specificity are worth pursuing in the context of biomarker development. In this regard, our recent publication on the role of GLO1 as novel diagnostic marker of HGPIN caught the attention of a team at Roche Tissue Diagnostics. The current interest of the team is to develop a technology to collect data from H&E stained tissues to identify malignant signatures as well as potential biomarkers to identify patients at risk of aggressive disease in PCa. Collectively, this technology is what we will refer to as ‘virtual staining’. In the next section we provide background information on the technology and application. We acknowledge the information provided is limited; however, this is due to the intellectual property surrounding this project.

## 6.2. Virtual Staining to Detect Signatures in the Development of Aggressive PCa

Tissue staining and morphological pattern recognition, namely histopathology, is a method which has remained essentially unchanged in over 140 years [394]. Although the method of choice, it is time-consuming, subjective and with limited statistical confidence due to operator variability. Processing to visualize specific biomarkers requires dyes or molecular probes, in addition to the constrained amount of information obtained, adds to its limitations. The idea of automation in this field has gained much interest and new methods promising approaches have surface and are gaining much interest. One of this approaches, vibrational spectroscopy, provides non-perturbing molecular descriptors based on the intrinsic chemical constitution of the tissue.

Vibrational spectroscopy is defined as the oscillating changes in bond lengths (stretching) and angles between the bonds (deformation) triggered by the interaction of electromagnetic radiation and the irradiated molecules (**Figure 28**) [395]. There are two types of vibration spectroscopy, Fourier transform infrared (FTIR) and Raman. FTIR measures the absorption and transmission of the infrared (IR) light on a given vibrating molecule. IR spectroscopy refers to the infrared region of the electromagnetic spectrum-light with a longer wavelength and lower frequency than visible light. IR can be used to identify and study chemicals. The IR portion of the electromagnetic spectrum can be divided into three regions; the near-, mid- and far- infrared based on the relation to the visible spectrum. Raman, on the other hand, measures the light scatterings caused by the vibrations of the molecule [396]. These are methods with high chemical specificity thus allowing for full construction of a chemical image of the sample including distribution of compounds at the cellular and subcellular levels. The major advantage of these methods is their non-destructive approach with minimal sample processing. Moreover, the identified chemicals in the sample can be used as biomarkers [395].

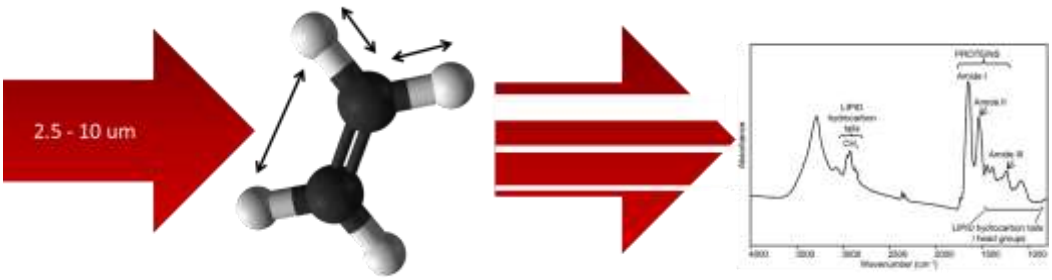


**Figure 28. Vibrational spectroscopy and oscillating changes in a molecule.** In vibrational spectroscopy oscillating changes in bond lengths (stretching) and angles between the bonds (deformation) triggered by the interaction of electromagnetic radiation (mid-IR= 2.5- 10 μm wavelength) and the irradiated molecules is used to generate a spectral signature. Spectral signatures can be used to identify specific molecules in a sample. Graphic courtesy: Christian Davila-Peralta.

Vibrational infrared spectroscopy is a non-destructive photonic technique that can rapidly measure the chemical components in a tissue sample [397]. Infrared spectroscopy has been previously used to analyze a wide range of biomedical samples [397], providing growing evidence for its potential use in the clinical setting. High-throughput FTIR spectroscopic imaging coupled with statistical pattern recognition of spectral signatures of endogenous molecules has been previously used to analyze prostate tissue microarrays. This new approach does not require the use of dyes or molecular probes to interrogate tissue composition and incorporates well-defined tests of statistical significance [398].

Infrared spectral histopathology has gained much interest and promises to become a great tool in the field of cancer diagnostics in particular. Our recent publication on GLO1 upregulation in HGPIN, a precursor of aggressive PCa, called the attention of a team seeking to develop and algorithm to detect early PCa lesions associated with poor patient outcomes using mid-IR spectroscopy. Given the ability of GLO1 to detect HGPI, the team

set out to further investigate the feasibility to detect GLO1 in a subset of tissue cores from the cohort used in our previously published study [59]. One of the aims of the project is to detect GLO1 in tissue for potential use as biomarker of HGPIN for early detection of aggressive PCa using spectroscopic imaging. Most importantly, the primary goal is to define specific biochemical signatures in patient tissues bearing normal, HGPIN and PCa tissue histologies. These signatures can be used to predict aggressive disease, and patient stratification to guide therapeutic intervention. Development of this novel methodology relies on the use of previously stained tissue cores with the traditional H&E stain to train the algorithm that will ultimately identify normal and malignant areas (**Figure 29**) thus aiding the Pathologist and decreasing the patient results turnaround time in the clinical setting.

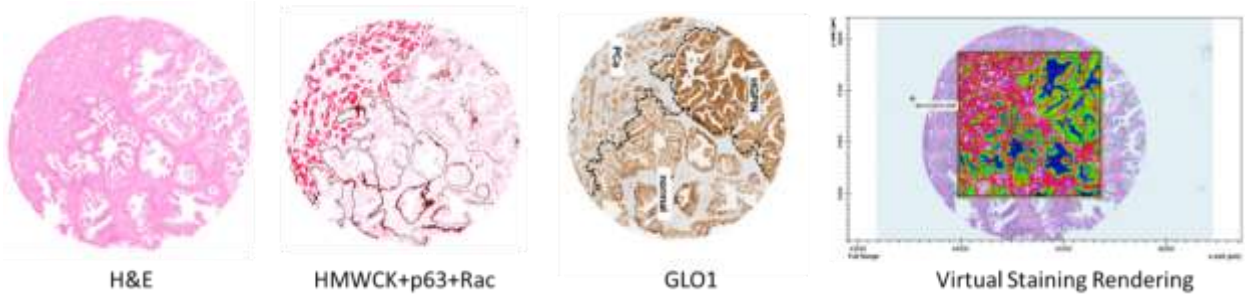


**Figure 29. Comparison between 3 mm prostate cores with the traditional H&E and immunohistochemical stains and the resulting virtual staining rendering.** The H&E stained prostate cancer core from a tissue microarray was subjected to spectroscopic imaging coupled with statistical pattern recognition of spectral signatures of endogenous molecules to generate a virtually stained rendering. Virtually stained render shows the high fidelity of the developed algorithm to identify the three different histologies present on the tissue core (normal, HGPIN and PCa) as identified by traditional staining methods. From left to right: H&E, Dual (HWMCK+p63+Rac), and GLO1 stains. Photo courtesy: Christian Davila-Peralta.

The path to develop the methodology for spectroscopic imaging involves measurement of large number of spectral profiles from every tissue subtype (normal, HGPIN and PCa), identification of potentially relevant spectral markers by identifying spectral signatures (**Figure 30**), organization of markers into a prediction algorithm and, the statistical validation of the process. Three critical aspects of consideration include: acquisition of high-fidelity microspectroscopic imaging data; development of robust algorithm that can serve as statistical controls for the tissue classification process, and large-scale validation of the algorithms [398].

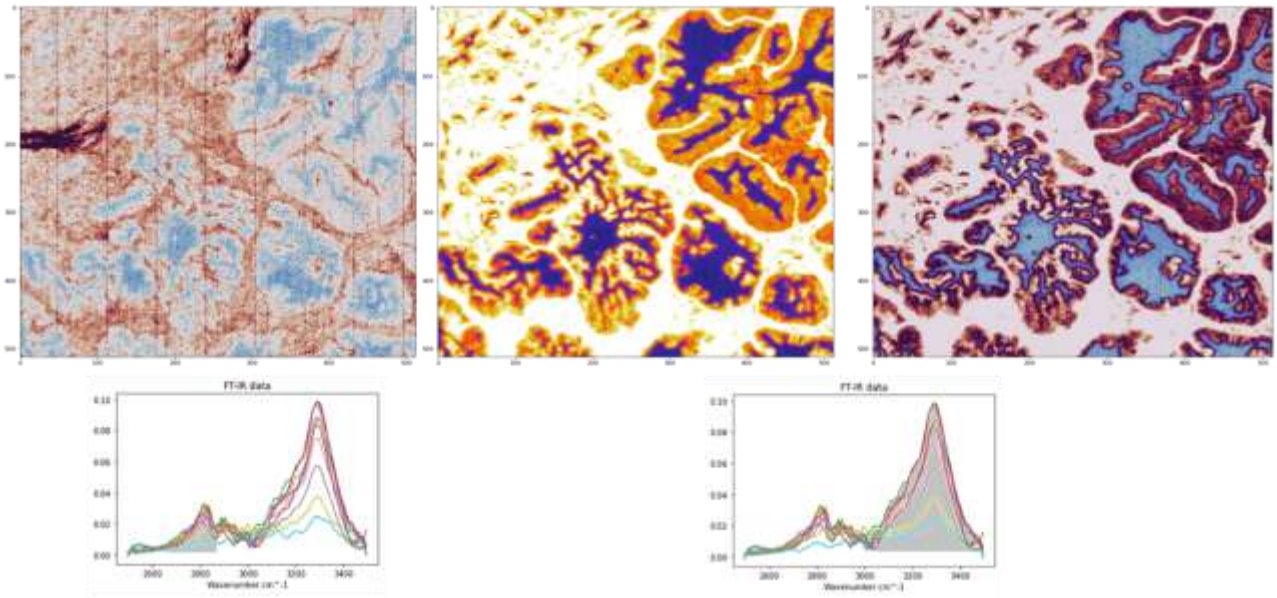

**Figure 30. Virtual Stain rendering tuning of a prostate cancer core.** The Integration area, color and intensity on the virtually generated image can be tuned to accentuate areas or markers in the various tissue histologies (normal, HGPIN and PCa). Blue indicates empty spaces; orange and dark red indicate epithelial tissue. Graphs below the virtually stained images correspond to chemical tissue signatures from the selected regions of interest. Photo courtesy: Christian Davila-Peralta.

# REFERENCES


1. Cunha, G.R., et al., *The endocrinology and developmental biology of the prostate.* Endocr Rev, 1987. **8**(3): p. 338-62.
2. Cunha, G.R., et al., *Development of the human prostate.* Differentiation, 2018. **103**: p. 24-45.
3. Partin, A.W., *High-grade prostatic intraepithelial neoplasia on a prostate biopsy-what does it mean?* Reviews in urology, 2002. **4**(3): p. 157-158.
4. Kronz, J.D., et al., *Predicting cancer following a diagnosis of high-grade prostatic intraepithelial neoplasia on needle biopsy: data on men with more than one follow-up biopsy.* Am J Surg Pathol, 2001. **25**(8): p. 1079-85.
5. Verze, P., T. Cai, and S. Lorenzetti, *The role of the prostate in male fertility, health and disease.* Nat Rev Urol, 2016. **13**(7): p. 379-86.
6. Costello, L.C. and R.B. Franklin, *The intermediary metabolism of the prostate: a key to understanding the pathogenesis and progression of prostate malignancy.* Oncology, 2000. **59**(4): p. 269-82.
7. Lowsley, O.S., *The development of the human prostate gland with reference to the development of other structures at the neck of the urinary bladder.* American journal of Anatomy, 1912. **13**(3): p. 299-349.
8. Vander Heiden, M.G., L.C. Cantley, and C.B. Thompson, *Understanding the Warburg effect: the metabolic requirements of cell proliferation.* Science, 2009. **324**(5930): p. 1029-33.
9. Cutruzzola, F., et al., *Glucose Metabolism in the Progression of Prostate Cancer.* Front Physiol, 2017. **8**: p. 97.
10. Franz, M.C., et al., *Zinc transporters in prostate cancer.* Mol Aspects Med, 2013. **34**(2-3): p. 735-41.
11. Franklin, R.B., et al., *Zinc and zinc transporters in normal prostate and the pathogenesis of prostate cancer.* Front Biosci, 2005. **10**: p. 2230-9.
12. Wang, Y., et al., *Cell differentiation lineage in the prostate.* Differentiation, 2001. **68**(4-5): p. 270-9.
13. Szczyrba, J., et al., *Neuroendocrine Cells of the Prostate Derive from the Neural Crest.* J Biol Chem, 2017. **292**(5): p. 2021-2031.
14. Cunha, G.R., P.S. Cooke, and T. Kurita, *Role of stromal-epithelial interactions in hormonal responses.* Arch Histol Cytol, 2004. **67**(5): p. 417-34.
15. Ishii, K., et al., *Role of Stromal Paracrine Signals in Proliferative Diseases of the Aging Human Prostate.* J Clin Med, 2018. **7**(4).
16. Deslypere, J.P., et al., *Testosterone and 5 alpha-dihydrotestosterone interact differently with the androgen receptor to enhance transcription of the MMTV-CAT reporter gene.* Mol Cell Endocrinol, 1992. **88**(1-3): p. 15-22.
17. Adams, J.Y., et al., *Expression of estrogen receptor beta in the fetal, neonatal, and prepubertal human prostate.* Prostate, 2002. **52**(1): p. 69-81.
18. Shapiro, E., et al., *Immunolocalization of estrogen receptor alpha and beta in human fetal prostate.* J Urol, 2005. **174**(5): p. 2051-3.

19. Prins, G.S., et al., *The role of estrogens in normal and abnormal development of the prostate gland.* Ann N Y Acad Sci, 2006. **1089**: p. 1-13.
20. Lorenzetti*, S. and L. Narciso, *Chapter 1 Nuclear Receptors: Connecting Human Health to the Environment*, in *Computational Approaches to Nuclear Receptors*. 2012, The Royal Society of Chemistry. p. 1-22.
21. Ficarra, V., et al., *The role of inflammation in lower urinary tract symptoms (LUTS) due to benign prostatic hyperplasia (BPH) and its potential impact on medical therapy.* Curr Urol Rep, 2014. **15**(12): p. 463.
22. Ribal, M.J., *The Link Between Benign Prostatic Hyperplasia and Inflammation.* European Urology Supplements, 2013. **12**(5): p. 103-109.
23. Nickel, J.C., et al., *The relationship between prostate inflammation and lower urinary tract symptoms: examination of baseline data from the REDUCE trial.* Eur Urol, 2008. **54**(6): p. 1379-84.
24. Sfanos, K.S. and A.M. De Marzo, *Prostate cancer and inflammation: the evidence.* Histopathology, 2012. **60**(1): p. 199-215.
25. McNeal, J.E.B.W.C., *The prostate gland, morphology and pathobiology*. 1983, Princeton, NJ: Published for Burroughs Wellcome Co. by Custom Pub. Services.
26. Chang, R.T., R. Kirby, and B.J. Challacombe, *Is there a link between BPH and prostate cancer?* Practitioner, 2012. **256**(1750): p. 13-6, 2.
27. Orsted, D.D. and S.E. Bojesen, *The link between benign prostatic hyperplasia and prostate cancer.* Nat Rev Urol, 2013. **10**(1): p. 49-54.
28. Guess, H.A., *Benign prostatic hyperplasia and prostate cancer.* Epidemiol Rev, 2001. **23**(1): p. 152-8.
29. Sommers, S.C., *Endocrine changes with prostatic carcinoma.* Cancer, 1957. **10**(2): p. 345-58.
30. McVary, K.T., *BPH: epidemiology and comorbidities.* Am J Manag Care, 2006. **12**(5 Suppl): p. S122-8.
31. DeMarzo, A.M., et al., *Pathological and molecular aspects of prostate cancer.* Lancet, 2003. **361**(9361): p. 955-64.
32. Montironi, R., R. Mazzucchelli, and M. Scarpelli, *Precancerous lesions and conditions of the prostate: from morphological and biological characterization to chemoprevention.* Ann N Y Acad Sci, 2002. **963**: p. 169-84.
33. Bostwick, D.G. and J. Qian, *High-grade prostatic intraepithelial neoplasia.* Mod Pathol, 2004. **17**(3): p. 360-79.
34. Montironi, R., et al., *Prostatic intraepithelial neoplasia: its morphological and molecular diagnosis and clinical significance.* BJU Int, 2011. **108**(9): p. 1394-401.
35. Davidsson, S., et al., *Inflammation, focal atrophic lesions, and prostatic intraepithelial neoplasia with respect to risk of lethal prostate cancer.* Cancer Epidemiol Biomarkers Prev, 2011. **20**(10): p. 2280-7.
36. Merrimen, J.L., et al., *Multifocal high grade prostatic intraepithelial neoplasia is a significant risk factor for prostatic adenocarcinoma.* J Urol, 2009. **182**(2): p. 485-90; discussion 490.
37. De Marzo, A.M., et al., *Prostate cancer: New answers prompt new questions regarding cell of origin.* Nat Rev Urol, 2010. **7**(12): p. 650-2.

38. Zhou, M., C. Magi-Galluzzi, and J.I. Epstein, *Chapter 2 - Neoplasms of the Prostate and Seminal Vesicles*, in *Genitourinary Pathology*, M. Zhou and C. Magi-Galluzzi, Editors. 2007, Churchill Livingstone: Philadelphia. p. 56-108.
39. Keetch, D.W., et al., *Morphometric analysis and clinical followup of isolated prostatic intraepithelial neoplasia in needle biopsy of the prostate.* J Urol, 1995. **154**(2 Pt 1): p. 347-51.
40. Shepherd, D., et al., *Repeat biopsy strategy in men with isolated prostatic intraepithelial neoplasia on prostate needle biopsy.* J Urol, 1996. **156**(2 Pt 1): p. 460-2; discussion 462-3.
41. Brawer, M.K., et al., *Significance of prostatic intraepithelial neoplasia on prostate needle biopsy.* Urology, 1991. **38**(2): p. 103-7.
42. Weinstein, M.H. and J.I. Epstein, *Significance of high-grade prostatic intraepithelial neoplasia on needle biopsy.* Hum Pathol, 1993. **24**(6): p. 624-9.
43. Häggman, M.J., et al., *The relationship between prostatic intraepithelial neoplasia and prostate cancer: critical issues.* J Urol, 1997. **158**(1): p. 12-22.
44. Qian, J., R.B. Jenkins, and D.G. Bostwick, *Genetic and chromosomal alterations in prostatic intraepithelial neoplasia and carcinoma detected by fluorescence in situ hybridization.* Eur Urol, 1999. **35**(5-6): p. 479-83.
45. Davidson, D., et al., *Prostatic intraepithelial neoplasia is a risk factor for adenocarcinoma: predictive accuracy in needle biopsies.* J Urol, 1995. **154**(4): p. 1295-9.
46. Ashida, S., et al., *Molecular features of the transition from prostatic intraepithelial neoplasia (PIN) to prostate cancer: genome-wide gene-expression profiles of prostate cancers and PINs.* Cancer Res, 2004. **64**(17): p. 5963-72.
47. Rubin, M.A., et al., *alpha-Methylacyl coenzyme A racemase as a tissue biomarker for prostate cancer.* Jama, 2002. **287**(13): p. 1662-70.
48. Luo, J., et al., *Alpha-methylacyl-CoA racemase: a new molecular marker for prostate cancer.* Cancer Res, 2002. **62**(8): p. 2220-6.
49. Xia, C., et al., *Identification of a prostate-specific G-protein coupled receptor in prostate cancer.* Oncogene, 2001. **20**(41): p. 5903-5907.
50. Thomas, T. and T.J. Thomas, *Polyamines in cell growth and cell death: molecular mechanisms and therapeutic applications.* Cell Mol Life Sci, 2001. **58**(2): p. 244-58.
51. Doll, J.A., et al., *Pigment epithelium-derived factor regulates the vasculature and mass of the prostate and pancreas.* Nat Med, 2003. **9**(6): p. 774-80.
52. Peng, S., et al., *Decreased expression of serine protease inhibitor family G1 (SERPING1) in prostate cancer can help distinguish high-risk prostate cancer and predicts malignant progression.* Urol Oncol, 2018. **36**(8): p. 366.e1-366.e9.
53. Raviv, G., et al., *Do prostate specific antigen and prostate specific antigen density enhance the detection of prostate carcinoma after initial diagnosis of prostatic intraepithelial neoplasia without concurrent carcinoma?* Cancer, 1996. **77**(10): p. 2103-8.
54. Ramos, C.G., et al., *The effect of high grade prostatic intraepithelial neoplasia on serum total and percentage of free prostate specific antigen levels.* J Urol, 1999. **162**(5): p. 1587-90.

55. Obralic, N. and B. Kulovac, *High grade intraepithelial neoplasia of prostate is associated with values of prostate specific antigen related parameters intermediate between prostate cancer and normal levels.* Bosn J Basic Med Sci, 2011. **11**(4): p. 223-7.
56. Tosoian, J.J., et al., *Managing high-grade prostatic intraepithelial neoplasia (HGPIN) and atypical glands on prostate biopsy.* Nature Reviews Urology, 2018. **15**(1): p. 55-66.
57. Sakr, W.A., et al., *The frequency of carcinoma and intraepithelial neoplasia of the prostate in young male patients.* J Urol, 1993. **150**(2 Pt 1): p. 379-85.
58. Emmert-Buck, M.R., et al., *Allelic loss on chromosome 8p12-21 in microdissected prostatic intraepithelial neoplasia.* Cancer Res, 1995. **55**(14): p. 2959-62.
59. Rounds, L., et al., *Glyoxalase 1 Expression as a Novel Diagnostic Marker of High-Grade Prostatic Intraepithelial Neoplasia in Prostate Cancer.* Cancers (Basel), 2021. **13**(14).
60. Siegel, R.L., et al., *Cancer Statistics, 2021.* CA Cancer J Clin, 2021. **71**(1): p. 7-33.
61. Cooperberg, M.R., et al., *High-risk prostate cancer in the United States, 1990-2007.* World J Urol, 2008. **26**(3): p. 211-8.
62. Gonthier, K., R.T.K. Poluri, and É. Audet-Walsh, *Functional genomic studies reveal the androgen receptor as a master regulator of cellular energy metabolism in prostate cancer.* J Steroid Biochem Mol Biol, 2019. **191**: p. 105367.
63. Jividen, K., et al., *Genomic analysis of DNA repair genes and androgen signaling in prostate cancer.* BMC Cancer, 2018. **18**(1): p. 960.
64. Labrie, F., *Combined blockade of testicular and locally made androgens in prostate cancer: A highly significant medical progress based upon intracrinology.* The Journal of Steroid Biochemistry and Molecular Biology, 2015. **145**: p. 144-156.
65. Audet-Walsh, É., et al., *Inverse Regulation of DHT Synthesis Enzymes 5α-Reductase Types 1 and 2 by the Androgen Receptor in Prostate Cancer.* Endocrinology, 2017. **158**(4): p. 1015-1021.
66. Davey, R.A. and M. Grossmann, *Androgen Receptor Structure, Function and Biology: From Bench to Bedside.* Clin Biochem Rev, 2016. **37**(1): p. 3-15.
67. Wyce, A., et al., *Research Resource: The Androgen Receptor Modulates Expression of Genes with Critical Roles in Muscle Development and Function.* Molecular Endocrinology, 2010. **24**(8): p. 1665-1674.
68. Pihlajamaa, P., et al., *Tissue-specific pioneer factors associate with androgen receptor cistromes and transcription programs.* Embo j, 2014. **33**(4): p. 312-26.
69. Watson, P.A., V.K. Arora, and C.L. Sawyers, *Emerging mechanisms of resistance to androgen receptor inhibitors in prostate cancer.* Nature Reviews Cancer, 2015. **15**(12): p. 701-711.
70. Wyatt, A.W. and M.E. Gleave, *Targeting the adaptive molecular landscape of castration-resistant prostate cancer.* EMBO Molecular Medicine, 2015. **7**(7): p. 878-894.
71. Quigley, D.A., et al., *Genomic Hallmarks and Structural Variation in Metastatic Prostate Cancer.* Cell, 2018. **174**(3): p. 758-769.e9.

72. Viswanathan, S.R., et al., *Structural Alterations Driving Castration-Resistant Prostate Cancer Revealed by Linked-Read Genome Sequencing.* Cell, 2018. **174**(2): p. 433-447.e19.
73. Robinson, D., et al., *Integrative Clinical Genomics of Advanced Prostate Cancer.* Cell, 2015. **161**(5): p. 1215-1228.
74. Taylor, B.S., et al., *Integrative Genomic Profiling of Human Prostate Cancer.* Cancer Cell, 2010. **18**(1): p. 11-22.
75. Cooper, J.F. and I. Farid, *THE ROLE OF CITRIC ACID IN THE PHYSIOLOGY OF THE PROSTATE. 3. LACTATE/CITRATE RATIOS IN BENIGN AND MALIGNANT PROSTATIC HOMOGENATES AS AN INDEX OF PROSTATIC MALIGNANCY.* J Urol, 1964. **92**: p. 533-6.
76. Samaratunga, H., et al., *From Gleason to International Society of Urological Pathology (ISUP) grading of prostate cancer.* Scand J Urol, 2016. **50**(5): p. 325-9.
77. Cagney, D.N., et al., *The FDA NIH Biomarkers, EndpointS, and other Tools (BEST) resource in neuro-oncology.* Neuro Oncol, 2018. **20**(9): p. 1162-1172.
78. Gerdes, J., et al., *Production of a mouse monoclonal antibody reactive with a human nuclear antigen associated with cell proliferation.* Int J Cancer, 1983. **31**(1): p. 13-20.
79. Sun, X. and P.D. Kaufman, *Ki-67: more than a proliferation marker.* Chromosoma, 2018. **127**(2): p. 175-186.
80. Miller, I., et al., *Ki67 is a Graded Rather than a Binary Marker of Proliferation versus Quiescence.* Cell reports, 2018. **24**(5): p. 1105-1112.e5.
81. Tao, M., et al., *Ki-67 labeling index is a predictive marker for a pathological complete response to neoadjuvant chemotherapy in breast cancer: A meta-analysis.* Medicine (Baltimore), 2017. **96**(51): p. e9384.
82. Klöppel, G., *Neuroendocrine Neoplasms: Dichotomy, Origin and Classifications.* Visc Med, 2017. **33**(5): p. 324-330.
83. Lotan, T.L., et al., *Report From the International Society of Urological Pathology (ISUP) Consultation Conference on Molecular Pathology of Urogenital Cancers. I. Molecular Biomarkers in Prostate Cancer.* Am J Surg Pathol, 2020. **44**(7): p. e15-e29.
84. Berlin, A., et al., *Prognostic role of Ki-67 score in localized prostate cancer: A systematic review and meta-analysis.* Urol Oncol, 2017. **35**(8): p. 499-506.
85. Bubendorf, L., et al., *Ki67 labeling index in core needle biopsies independently predicts tumor-specific survival in prostate cancer.* Hum Pathol, 1998. **29**(9): p. 949-54.
86. Hoogland, A.M., C.F. Kweldam, and G.J. van Leenders, *Prognostic histopathological and molecular markers on prostate cancer needle-biopsies: a review.* Biomed Res Int, 2014. **2014**: p. 341324.
87. Kammerer-Jacquet, S.-F., et al., *Ki-67 is an independent predictor of prostate cancer death in routine needle biopsy samples: proving utility for routine assessments.* Modern Pathology, 2019. **32**(9): p. 1303-1309.
88. Zellweger, T., et al., *Tumour growth fraction measured by immunohistochemical staining of Ki67 is an independent prognostic factor in preoperative prostate*

*biopsies with small-volume or low-grade prostate cancer.* Int J Cancer, 2009. **124**(9): p. 2116-23.
89. Jamaspishvili, T., et al., *Clinical implications of PTEN loss in prostate cancer.* Nature Reviews Urology, 2018. **15**(4): p. 222-234.
90. Lotan, T.L., et al., *Analytic validation of a clinical-grade PTEN immunohistochemistry assay in prostate cancer by comparison with PTEN FISH.* Mod Pathol, 2016. **29**(8): p. 904-14.
91. Picanço-Albuquerque, C.G., et al., *In prostate cancer needle biopsies, detections of PTEN loss by fluorescence in situ hybridization (FISH) and by immunohistochemistry (IHC) are concordant and show consistent association with upgrading.* Virchows Arch, 2016. **468**(5): p. 607-17.
92. Lotan, T.L., et al., *PTEN loss detection in prostate cancer: comparison of PTEN immunohistochemistry and PTEN FISH in a large retrospective prostatectomy cohort.* Oncotarget, 2017. **8**(39): p. 65566-65576.
93. Lotan, T.L., et al., *PTEN protein loss by immunostaining: analytic validation and prognostic indicator for a high risk surgical cohort of prostate cancer patients.* Clin Cancer Res, 2011. **17**(20): p. 6563-73.
94. Raap, M., et al., *Quality assurance trials for Ki67 assessment in pathology.* Virchows Arch, 2017. **471**(4): p. 501-508.
95. Yoshimoto, M., et al., *FISH analysis of 107 prostate cancers shows that PTEN genomic deletion is associated with poor clinical outcome.* British journal of cancer, 2007. **97**(5): p. 678-685.
96. Krohn, A., et al., *Genomic deletion of PTEN is associated with tumor progression and early PSA recurrence in ERG fusion-positive and fusion-negative prostate cancer.* Am J Pathol, 2012. **181**(2): p. 401-12.
97. Lotan, T.L., et al., *PTEN Loss as Determined by Clinical-grade Immunohistochemistry Assay Is Associated with Worse Recurrence-free Survival in Prostate Cancer.* Eur Urol Focus, 2016. **2**(2): p. 180-188.
98. Mehra, R., et al., *Association of ERG/PTEN status with biochemical recurrence after radical prostatectomy for clinically localized prostate cancer.* Med Oncol, 2018. **35**(12): p. 152.
99. Cuzick, J., et al., *Prognostic value of PTEN loss in men with conservatively managed localised prostate cancer.* Br J Cancer, 2013. **108**(12): p. 2582-9.
100. Bismar, T.A., et al., *Clinical utility of assessing PTEN and ERG protein expression in prostate cancer patients: a proposed method for risk stratification.* J Cancer Res Clin Oncol, 2018. **144**(11): p. 2117-2125.
101. Ahearn, T.U., et al., *A Prospective Investigation of PTEN Loss and ERG Expression in Lethal Prostate Cancer.* J Natl Cancer Inst, 2016. **108**(2).
102. Leapman, M.S., et al., *Comparing Prognostic Utility of a Single-marker Immunohistochemistry Approach with Commercial Gene Expression Profiling Following Radical Prostatectomy.* Eur Urol, 2018. **74**(5): p. 668-675.
103. Reid, A.H., et al., *Molecular characterisation of ERG, ETV1 and PTEN gene loci identifies patients at low and high risk of death from prostate cancer.* Br J Cancer, 2010. **102**(4): p. 678-84.
104. Lotan, T.L., et al., *PTEN loss is associated with upgrading of prostate cancer from biopsy to radical prostatectomy.* Mod Pathol, 2015. **28**(1): p. 128-137.

105. Tosoian, J.J., et al., *PTEN status assessment in the Johns Hopkins active surveillance cohort.* Prostate Cancer and Prostatic Diseases, 2019. **22**(1): p. 176-181.
106. Cuzick, J., et al., *Prognostic value of a cell cycle progression signature for prostate cancer death in a conservatively managed needle biopsy cohort.* Br J Cancer, 2012. **106**(6): p. 1095-9.
107. Klein, E.A., et al., *A 17-gene assay to predict prostate cancer aggressiveness in the context of Gleason grade heterogeneity, tumor multifocality, and biopsy undersampling.* Eur Urol, 2014. **66**(3): p. 550-60.
108. Erho, N., et al., *Discovery and Validation of a Prostate Cancer Genomic Classifier that Predicts Early Metastasis Following Radical Prostatectomy.* PLOS ONE, 2013. **8**(6): p. e66855.
109. Kim, H.L., et al., *Validation of the Decipher Test for predicting adverse pathology in candidates for prostate cancer active surveillance.* Prostate Cancer and Prostatic Diseases, 2019. **22**(3): p. 399-405.
110. Kornberg, Z., et al., *A 17-Gene Genomic Prostate Score as a Predictor of Adverse Pathology in Men on Active Surveillance.* J Urol, 2019. **202**(4): p. 702-709.
111. Cheng, H.H., *The resounding effect of DNA repair deficiency in prostate cancer.* Urol Oncol, 2018. **36**(8): p. 385-388.
112. Pritchard, C.C., et al., *Inherited DNA-Repair Gene Mutations in Men with Metastatic Prostate Cancer.* New England Journal of Medicine, 2016. **375**(5): p. 443-453.
113. Na, R., et al., *Germline Mutations in ATM and BRCA1/2 Distinguish Risk for Lethal and Indolent Prostate Cancer and are Associated with Early Age at Death.* Eur Urol, 2017. **71**(5): p. 740-747.
114. Schweizer, M.T., et al., *Genomic Characterization of Prostatic Ductal Adenocarcinoma Identifies a High Prevalence of DNA Repair Gene Mutations.* JCO Precision Oncology, 2019(3): p. 1-9.
115. Lotan, T.L., et al., *DNA damage repair alterations are frequent in prostatic adenocarcinomas with focal pleomorphic giant-cell features.* Histopathology, 2019. **74**(6): p. 836-843.
116. Velho, P.I., et al., *Molecular Characterization and Clinical Outcomes of Primary Gleason Pattern 5 Prostate Cancer After Radical Prostatectomy.* JCO Precis Oncol, 2019. **3**.
117. Risbridger, G.P., et al., *Patient-derived xenografts reveal that intraductal carcinoma of the prostate is a prominent pathology in BRCA2 mutation carriers with prostate cancer and correlates with poor prognosis.* Eur Urol, 2015. **67**(3): p. 496-503.
118. Khani, F., et al., *Intraductal carcinoma of the prostate in the absence of high-grade invasive carcinoma represents a molecularly distinct type of in situ carcinoma enriched with oncogenic driver mutations.* J Pathol, 2019. **249**(1): p. 79-89.
119. Pritchard, C.C., et al., *Complex MSH2 and MSH6 mutations in hypermutated microsatellite unstable advanced prostate cancer.* Nat Commun, 2014. **5**: p. 4988.

120. Nava Rodrigues, D., et al., *Immunogenomic analyses associate immunological alterations with mismatch repair defects in prostate cancer.* J Clin Invest, 2018. **128**(10): p. 4441-4453.
121. Abida, W., et al., *Analysis of the Prevalence of Microsatellite Instability in Prostate Cancer and Response to Immune Checkpoint Blockade.* JAMA Oncol, 2019. **5**(4): p. 471-478.
122. Guedes, L.B., et al., *MSH2 Loss in Primary Prostate Cancer.* Clin Cancer Res, 2017. **23**(22): p. 6863-6874.
123. Schweizer, M.T., et al., *Mismatch repair deficiency may be common in ductal adenocarcinoma of the prostate.* Oncotarget, 2016. **7**(50): p. 82504-82510.
124. Dominguez-Valentin, M., et al., *Frequent mismatch-repair defects link prostate cancer to Lynch syndrome.* BMC urology, 2016. **16**: p. 15-15.
125. Haraldsdottir, S., et al., *Prostate cancer incidence in males with Lynch syndrome.* Genet Med, 2014. **16**(7): p. 553-7.
126. Mohler, J.L. and E.S. Antonarakis, *NCCN Guidelines Updates: Management of Prostate Cancer.* J Natl Compr Canc Netw, 2019. **17**(5.5): p. 583-586.
127. Sartor, O. and J.S. de Bono, *Metastatic Prostate Cancer.* N Engl J Med, 2018. **378**(7): p. 645-657.
128. Nelson, P.S., *Targeting the androgen receptor in prostate cancer--a resilient foe.* N Engl J Med, 2014. **371**(11): p. 1067-9.
129. Gundem, G., et al., *The evolutionary history of lethal metastatic prostate cancer.* Nature, 2015. **520**(7547): p. 353-357.
130. Abida, W., et al., *Genomic correlates of clinical outcome in advanced prostate cancer.* Proceedings of the National Academy of Sciences, 2019. **116**(23): p. 11428-11436.
131. Sharp, A., et al., *Androgen receptor splice variant-7 expression emerges with castration resistance in prostate cancer.* J Clin Invest, 2019. **129**(1): p. 192-208.
132. Grasso, C.S., et al., *The mutational landscape of lethal castration-resistant prostate cancer.* Nature, 2012. **487**(7406): p. 239-243.
133. Scher, H.I., et al., *Association of AR-V7 on Circulating Tumor Cells as a Treatment-Specific Biomarker With Outcomes and Survival in Castration-Resistant Prostate Cancer.* JAMA Oncol, 2016. **2**(11): p. 1441-1449.
134. Armstrong, A.J., et al., *Prospective Multicenter Validation of Androgen Receptor Splice Variant 7 and Hormone Therapy Resistance in High-Risk Castration-Resistant Prostate Cancer: The PROPHECY Study.* J Clin Oncol, 2019. **37**(13): p. 1120-1129.
135. Antonarakis, E.S., et al., *AR-V7 and Resistance to Enzalutamide and Abiraterone in Prostate Cancer.* New England Journal of Medicine, 2014. **371**(11): p. 1028-1038.
136. Carreira, S., et al., *Tumor clone dynamics in lethal prostate cancer.* Sci Transl Med, 2014. **6**(254): p. 254ra125.
137. Scher, H.I., et al., *Assessment of the Validity of Nuclear-Localized Androgen Receptor Splice Variant 7 in Circulating Tumor Cells as a Predictive Biomarker for Castration-Resistant Prostate Cancer.* JAMA Oncol, 2018. **4**(9): p. 1179-1186.

138. Jayaram, A., D. Wetterskog, and G. Attard, *Plasma DNA and Metastatic Castration-Resistant Prostate Cancer: The Odyssey to a Clinical Biomarker Test.* Cancer Discovery, 2018. **8**(4): p. 392-394.
139. Annala, M., et al., *Circulating Tumor DNA Genomics Correlate with Resistance to Abiraterone and Enzalutamide in Prostate Cancer.* Cancer Discov, 2018. **8**(4): p. 444-457.
140. Hovelson, D.H., et al., *Rapid, ultra low coverage copy number profiling of cell-free DNA as a precision oncology screening strategy.* Oncotarget, 2017. **8**(52): p. 89848-89866.
141. Conteduca, V., et al., *Androgen receptor gene status in plasma DNA associates with worse outcome on enzalutamide or abiraterone for castration-resistant prostate cancer: a multi-institution correlative biomarker study.* Ann Oncol, 2017. **28**(7): p. 1508-1516.
142. Salvi, S., et al., *Circulating AR copy number and outcome to enzalutamide in docetaxel-treated metastatic castration-resistant prostate cancer.* Oncotarget, 2016. **7**(25): p. 37839-37845.
143. Romanel, A., et al., *Plasma AR and abiraterone-resistant prostate cancer.* Sci Transl Med, 2015. **7**(312): p. 312re10.
144. Salvi, S., et al., *Circulating cell-free AR and CYP17A1 copy number variations may associate with outcome of metastatic castration-resistant prostate cancer patients treated with abiraterone.* Br J Cancer, 2015. **112**(10): p. 1717-24.
145. Ablin, R.J., et al., *Precipitating antigens of the normal human prostate.* J Reprod Fertil, 1970. **22**(3): p. 573-4.
146. A. Rice, M. and T. Stoyanova, *Biomarkers for Diagnosis and Prognosis of Prostate Cancer*, in *Prostatectomy*. 2019.
147. McGrath, S., et al., *Prostate cancer biomarkers: Are we hitting the mark?* Prostate international, 2016. **4**(4): p. 130-135.
148. Miller, D.C., et al., *Incidence of initial local therapy among men with lower-risk prostate cancer in the United States.* J Natl Cancer Inst, 2006. **98**(16): p. 1134-41.
149. Moyer, V.A., *Screening for prostate cancer: U.S. Preventive Services Task Force recommendation statement.* Ann Intern Med, 2012. **157**(2): p. 120-34.
150. Emmett, L., et al., *Lutetium 177 PSMA radionuclide therapy for men with prostate cancer: a review of the current literature and discussion of practical aspects of therapy.* Journal of Medical Radiation Sciences, 2017. **64**(1): p. 52-60.
151. Mamoulakis, C., et al., *Chapter 48 - Prostate Cancer Biomarkers*, in *Biomarkers in Toxicology (Second Edition)*, R.C. Gupta, Editor. 2019, Academic Press. p. 869-881.
152. Netto, G.J. and J.I. Epstein, *Chapter 16 - Immunohistology of the Prostate, Bladder, Kidney, and Testis*, in *Diagnostic Immunohistochemistry (Third Edition)*, D.J. Dabbs, Editor. 2011, W.B. Saunders: Philadelphia. p. 593-661.
153. Chang, S.S., *Overview of prostate-specific membrane antigen.* Reviews in urology, 2004. **6 Suppl 10**(Suppl 10): p. S13-S18.
154. Shagera, Q.A., et al., *(68)Ga-PSMA PET/CT for response assessment and outcome prediction in metastatic prostate cancer patients treated with taxane-based chemotherapy.* J Nucl Med, 2021.

155. Goldstein, N.S., et al., *Cytokeratin 34 beta E-12 immunoreactivity in benign prostatic acini. Quantitation, pattern assessment, and electron microscopic study.* Am J Clin Pathol, 1999. **112**(1): p. 69-74.
156. Brawer, M.K., et al., *Keratin immunoreactivity in the benign and neoplastic human prostate.* Cancer Res, 1985. **45**(8): p. 3663-7.
157. Hedrick, L. and J.I. Epstein, *Use of keratin 903 as an adjunct in the diagnosis of prostate carcinoma.* Am J Surg Pathol, 1989. **13**(5): p. 389-96.
158. O'Malley, F.P., D.J. Grignon, and D.T. Shum, *Usefulness of immunoperoxidase staining with high-molecular-weight cytokeratin in the differential diagnosis of small-acinar lesions of the prostate gland.* Virchows Arch A Pathol Anat Histopathol, 1990. **417**(3): p. 191-6.
159. Shah, I.A., et al., *Cytokeratin immunohistochemistry as a diagnostic tool for distinguishing malignant from benign epithelial lesions of the prostate.* Mod Pathol, 1991. **4**(2): p. 220-4.
160. Wojno, K.J. and J.I. Epstein, *The utility of basal cell-specific anti-cytokeratin antibody (34 beta E12) in the diagnosis of prostate cancer. A review of 228 cases.* Am J Surg Pathol, 1995. **19**(3): p. 251-60.
161. Shah, R.B., et al., *Comparison of the basal cell-specific markers, 34betaE12 and p63, in the diagnosis of prostate cancer.* Am J Surg Pathol, 2002. **26**(9): p. 1161-8.
162. Weinstein, M.H., S. Signoretti, and M. Loda, *Diagnostic Utility of Immunohistochemical Staining for p63, a Sensitive Marker of Prostatic Basal Cells.* Modern Pathology, 2002. **15**(12): p. 1302-1308.
163. Parsons, J.K., et al., *p63 protein expression is rare in prostate adenocarcinoma: implications for cancer diagnosis and carcinogenesis.* Urology, 2001. **58**(4): p. 619-24.
164. Shah, R.B., et al., *Usefulness of basal cell cocktail (34betaE12 + p63) in the diagnosis of atypical prostate glandular proliferations.* Am J Clin Pathol, 2004. **122**(4): p. 517-23.
165. Zhou, M., et al., *Basal cell cocktail (34betaE12 + p63) improves the detection of prostate basal cells.* Am J Surg Pathol, 2003. **27**(3): p. 365-71.
166. Brimo, F. and J.I. Epstein, *Immunohistochemical pitfalls in prostate pathology.* Hum Pathol, 2012. **43**(3): p. 313-24.
167. Epstein, J.I., et al., *Best practices recommendations in the application of immunohistochemistry in the prostate: report from the International Society of Urologic Pathology consensus conference.* Am J Surg Pathol, 2014. **38**(8): p. e6-e19.
168. Ferdinandusse, S., et al., *Subcellular localization and physiological role of alpha-methylacyl-CoA racemase.* J Lipid Res, 2000. **41**(11): p. 1890-6.
169. Xu, J., et al., *Identification of differentially expressed genes in human prostate cancer using subtraction and microarray.* Cancer Res, 2000. **60**(6): p. 1677-82.
170. Jiang, Z., et al., *P504S: A New Molecular Marker for the Detection of Prostate Carcinoma.* The American Journal of Surgical Pathology, 2001. **25**(11).
171. Jiang, Z., et al., *P504S/alpha-methylacyl-CoA racemase: a useful marker for diagnosis of small foci of prostatic carcinoma on needle biopsy.* Am J Surg Pathol, 2002. **26**(9): p. 1169-74.

172. Jiang, Z., et al., *Alpha-methylacyl-CoA racemase: a multi-institutional study of a new prostate cancer marker.* Histopathology, 2004. **45**(3): p. 218-25.
173. Beach, R., et al., *P504S immunohistochemical detection in 405 prostatic specimens including 376 18-gauge needle biopsies.* Am J Surg Pathol, 2002. **26**(12): p. 1588-96.
174. Magi-Galluzzi, C., et al., *Alpha-methylacyl-CoA racemase: a variably sensitive immunohistochemical marker for the diagnosis of small prostate cancer foci on needle biopsy.* Am J Surg Pathol, 2003. **27**(8): p. 1128-33.
175. Zhou, M., Z. Jiang, and J.I. Epstein, *Expression and diagnostic utility of alpha-methylacyl-CoA-racemase (P504S) in foamy gland and pseudohyperplastic prostate cancer.* Am J Surg Pathol, 2003. **27**(6): p. 772-8.
176. Kunju, L.P., et al., *Diagnostic usefulness of monoclonal antibody P504S in the workup of atypical prostatic glandular proliferations.* Am J Clin Pathol, 2003. **120**(5): p. 737-45.
177. Adamo, P. and M.R. Ladomery, *The oncogene ERG: a key factor in prostate cancer.* Oncogene, 2016. **35**(4): p. 403-14.
178. Dwivedi, D.K., et al., *Multiparametric MR can identify high grade prostatic intraepithelial neoplasia (HGPIN) lesions and predict future detection of prostate cancer in men with a negative initial prostate biopsy.* Magn Reson Imaging, 2016. **34**(8): p. 1081-6.
179. Kurhanewicz, J., et al., *Combined magnetic resonance imaging and spectroscopic imaging approach to molecular imaging of prostate cancer.* Journal of magnetic resonance imaging : JMRI, 2002. **16**(4): p. 451-463.
180. Mondul, A.M., et al., *Metabolomic analysis of prostate cancer risk in a prospective cohort: The alpha-tocolpherol, beta-carotene cancer prevention (ATBC) study.* Int J Cancer, 2015. **137**(9): p. 2124-32.
181. Latonen, L., et al., *Integrative proteomics in prostate cancer uncovers robustness against genomic and transcriptomic aberrations during disease progression.* Nature Communications, 2018. **9**(1): p. 1176.
182. Shao, Y., et al., *Metabolomics and transcriptomics profiles reveal the dysregulation of the tricarboxylic acid cycle and related mechanisms in prostate cancer.* International Journal of Cancer, 2018. **143**(2): p. 396-407.
183. Srihari, S., et al., *Metabolic deregulation in prostate cancer.* Mol Omics, 2018. **14**(5): p. 320-329.
184. Costello, L.C. and R.B. Franklin, *The clinical relevance of the metabolism of prostate cancer; zinc and tumor suppression: connecting the dots.* Molecular cancer, 2006. **5**: p. 17-17.
185. Bader, D.A. and S.E. McGuire, *Tumour metabolism and its unique properties in prostate adenocarcinoma.* Nature Reviews Urology, 2020. **17**(4): p. 214-231.
186. Zadra, G., C. Photopoulos, and M. Loda, *The fat side of prostate cancer.* Biochim Biophys Acta, 2013. **1831**(10): p. 1518-32.
187. Huggins, C. and C.V. Hodges, *Studies on prostatic cancer: I. The effect of castration, of estrogen and of androgen injection on serum phosphatases in metastatic carcinoma of the prostate. 1941.* J Urol, 2002. **168**(1): p. 9-12.

188. Bader, D., J. Cerne, and S. McGuire, *Recent Developments in Androgen Deprivation Therapy for Locally Advanced Prostate Cancer.* Oncology & Hematology Review (US), 2014. **10**: p. 133.
189. Montgomery, R.B., et al., *Maintenance of intratumoral androgens in metastatic prostate cancer: a mechanism for castration-resistant tumor growth.* Cancer research, 2008. **68**(11): p. 4447-4454.
190. Nuhn, P., et al., *Update on Systemic Prostate Cancer Therapies: Management of Metastatic Castration-resistant Prostate Cancer in the Era of Precision Oncology.* Eur Urol, 2019. **75**(1): p. 88-99.
191. Visakorpi, T., et al., *In vivo amplification of the androgen receptor gene and progression of human prostate cancer.* Nat Genet, 1995. **9**(4): p. 401-6.
192. Taplin, M.E., et al., *Selection for androgen receptor mutations in prostate cancers treated with androgen antagonist.* Cancer Res, 1999. **59**(11): p. 2511-5.
193. Guo, Z., et al., *A novel androgen receptor splice variant is up-regulated during prostate cancer progression and promotes androgen depletion-resistant growth.* Cancer Res, 2009. **69**(6): p. 2305-13.
194. Stanbrough, M., et al., *Increased expression of genes converting adrenal androgens to testosterone in androgen-independent prostate cancer.* Cancer Res, 2006. **66**(5): p. 2815-25.
195. Dehm, S.M., et al., *Splicing of a novel androgen receptor exon generates a constitutively active androgen receptor that mediates prostate cancer therapy resistance.* Cancer Res, 2008. **68**(13): p. 5469-77.
196. Massie, C.E., et al., *The androgen receptor fuels prostate cancer by regulating central metabolism and biosynthesis.* Embo j, 2011. **30**(13): p. 2719-33.
197. Moon, J.S., et al., *Androgen stimulates glycolysis for de novo lipid synthesis by increasing the activities of hexokinase 2 and 6-phosphofructo-2-kinase/fructose-2,6-bisphosphatase 2 in prostate cancer cells.* Biochem J, 2011. **433**(1): p. 225-33.
198. Tsouko, E., et al., *Regulation of the pentose phosphate pathway by an androgen receptor-mTOR-mediated mechanism and its role in prostate cancer cell growth.* Oncogenesis, 2014. **3**(5): p. e103.
199. Bader, D.A., et al., *Mitochondrial pyruvate import is a metabolic vulnerability in androgen receptor-driven prostate cancer.* Nature Metabolism, 2019. **1**(1): p. 70-85.
200. Costello, L.C. and R.B. Franklin, *Testosterone regulates pyruvate dehydrogenase activity of prostate mitochondria.* Horm Metab Res, 1993. **25**(5): p. 268-70.
201. Liu, I.J., et al., *Fluorodeoxyglucose positron emission tomography studies in diagnosis and staging of clinically organ-confined prostate cancer.* Urology, 2001. **57**(1): p. 108-11.
202. Spratt, D.E., et al., *Utility of FDG-PET in clinical neuroendocrine prostate cancer.* Prostate, 2014. **74**(11): p. 1153-9.
203. Butler, W. and J. Huang, *Neuroendocrine cells of the prostate: Histology, biological functions, and molecular mechanisms.* Precis Clin Med, 2021. **4**(1): p. 25-34.

204. Massie, C.E., et al., *The androgen receptor fuels prostate cancer by regulating central metabolism and biosynthesis.* The EMBO Journal, 2011. **30**(13): p. 2719-2733.
205. White, M.A., et al., *GLUT12 promotes prostate cancer cell growth and is regulated by androgens and CaMKK2 signaling.* Endocrine-Related Cancer, 2018. **25**(4): p. 453-469.
206. Audet-Walsh, É., et al., *Androgen-Dependent Repression of ERRγ Reprograms Metabolism in Prostate Cancer.* Cancer Res, 2017. **77**(2): p. 378-389.
207. Audet-Walsh, É., et al., *Nuclear mTOR acts as a transcriptional integrator of the androgen signaling pathway in prostate cancer.* Genes Dev, 2017. **31**(12): p. 1228-1242.
208. Zacharias, N., et al., *Androgen Receptor Signaling in Castration-Resistant Prostate Cancer Alters Hyperpolarized Pyruvate to Lactate Conversion and Lactate Levels In Vivo.* Mol Imaging Biol, 2019. **21**(1): p. 86-94.
209. Poluri, R.T.K. and É. Audet-Walsh, *Genomic Deletion at 10q23 in Prostate Cancer: More Than PTEN Loss?* Frontiers in oncology, 2018. **8**: p. 246-246.
210. Khan, A.P., et al., *The role of sarcosine metabolism in prostate cancer progression.* Neoplasia, 2013. **15**(5): p. 491-501.
211. Ferro, M., et al., *Dysregulated metabolism: a relevant player in prostate cancer progression and clinical management.* Translational andrology and urology, 2019. **8**(Suppl 1): p. S109-S111.
212. Zhou, X., et al., *Effect of PTEN loss on metabolic reprogramming in prostate cancer cells.* Oncology letters, 2019. **17**(3): p. 2856-2866.
213. Liu, J., et al., *Aberrant FGFR Tyrosine Kinase Signaling Enhances the Warburg Effect by Reprogramming LDH Isoform Expression and Activity in Prostate Cancer.* Cancer Res, 2018. **78**(16): p. 4459-4470.
214. Bartrons, R., et al., *Fructose 2,6-Bisphosphate in Cancer Cell Metabolism.* Front Oncol, 2018. **8**: p. 331.
215. Bensaad, K., et al., *TIGAR, a p53-inducible regulator of glycolysis and apoptosis.* Cell, 2006. **126**(1): p. 107-20.
216. Gerin, I., et al., *Identification of TP53-induced glycolysis and apoptosis regulator (TIGAR) as the phosphoglycolate-independent 2,3-bisphosphoglycerate phosphatase.* Biochem J, 2014. **458**(3): p. 439-48.
217. Hers, H.G. and E. Van Schaftingen, *Fructose 2,6-bisphosphate 2 years after its discovery.* Biochem J, 1982. **206**(1): p. 1-12.
218. Van Schaftingen, E., *Fructose 2,6-bisphosphate.* Adv Enzymol Relat Areas Mol Biol, 1987. **59**: p. 315-95.
219. Hue, L. and M.H. Rider, *Role of fructose 2,6-bisphosphate in the control of glycolysis in mammalian tissues.* Biochem J, 1987. **245**(2): p. 313-24.
220. Rider, M. and R. Bartrons, *Fructose 2,6-bisphosphate: the last milestone of the 20th century in metabolic control?* Biochemical Journal, 2010.
221. Pilkis, S.J., et al., *6-Phosphofructo-2-kinase/fructose-2,6-bisphosphatase: a metabolic signaling enzyme.* Annu Rev Biochem, 1995. **64**: p. 799-835.
222. Sola-Penna, M., et al., *Regulation of mammalian muscle type 6-phosphofructo-1-kinase and its implication for the control of the metabolism.* IUBMB Life, 2010. **62**(11): p. 791-6.

223. Rider, M.H., et al., *6-phosphofructo-2-kinase/fructose-2,6-bisphosphatase: head-to-head with a bifunctional enzyme that controls glycolysis.* Biochem J, 2004. **381**(Pt 3): p. 561-79.
224. Okar, D.A., et al., *PFK-2/FBPase-2: maker and breaker of the essential biofactor fructose-2,6-bisphosphate.* Trends Biochem Sci, 2001. **26**(1): p. 30-5.
225. Goren, N., et al., *6-Phosphofructo-2-kinase/fructose-2,6-bisphosphatase expression in rat brain during development.* Brain Res Mol Brain Res, 2000. **75**(1): p. 138-42.
226. Sakakibara, R., et al., *Human placental fructose-6-phosphate,2-kinase/fructose-2,6-bisphosphatase: its isozymic form, expression and characterization.* Biosci Biotechnol Biochem, 1997. **61**(11): p. 1949-52.
227. Colomer, D., et al., *Control of phosphofructokinase by fructose 2,6-bisphosphate in B-lymphocytes and B-chronic lymphocytic leukemia cells.* Cancer Res, 1987. **47**(7): p. 1859-62.
228. Riera, L., et al., *Insulin induces PFKFB3 gene expression in HT29 human colon adenocarcinoma cells.* Biochim Biophys Acta, 2002. **1589**(2): p. 89-92.
229. Rousseau, G.G. and L. Hue, *Mammalian 6-phosphofructo-2-kinase/fructose-2,6-bisphosphatase: a bifunctional enzyme that controls glycolysis.* Prog Nucleic Acid Res Mol Biol, 1993. **45**: p. 99-127.
230. Yalcin, A., et al., *6-Phosphofructo-2-kinase (PFKFB3) promotes cell cycle progression and suppresses apoptosis via Cdk1-mediated phosphorylation of p27.* Cell Death Dis, 2014. **5**: p. e1337.
231. Staal, G.E., et al., *Subunit composition, regulatory properties, and phosphorylation of phosphofructokinase from human gliomas.* Cancer Res, 1987. **47**(19): p. 5047-51.
232. Chesney, J., et al., *Fructose-2,6-bisphosphate synthesis by 6-phosphofructo-2-kinase/fructose-2,6-bisphosphatase 4 (PFKFB4) is required for the glycolytic response to hypoxia and tumor growth.* Oncotarget, 2014. **5**(16): p. 6670-86.
233. Marsin, A.S., et al., *Phosphorylation and activation of heart PFK-2 by AMPK has a role in the stimulation of glycolysis during ischaemia.* Current Biology, 2000. **10**(20): p. 1247-1255.
234. Bobarykina, A.Y., et al., *Hypoxic regulation of PFKFB-3 and PFKFB-4 gene expression in gastric and pancreatic cancer cell lines and expression of PFKFB genes in gastric cancers.* Acta Biochim Pol, 2006. **53**(4): p. 789-99.
235. Ji, D., et al., *MACC1 expression correlates with PFKFB2 and survival in hepatocellular carcinoma.* Asian Pac J Cancer Prev, 2014. **15**(2): p. 999-1003.
236. Houles, T., et al., *RSK Regulates PFK-2 Activity to Promote Metabolic Rewiring in Melanoma.* Cancer Res, 2018. **78**(9): p. 2191-2204.
237. Zhao, S.J., et al., *SLIT2/ROBO1 axis contributes to the Warburg effect in osteosarcoma through activation of SRC/ERK/c-MYC/PFKFB2 pathway.* Cell Death Dis, 2018. **9**(3): p. 390.
238. Zhao, L., et al., *Long Noncoding RNA LINC00092 Acts in Cancer-Associated Fibroblasts to Drive Glycolysis and Progression of Ovarian Cancer.* Cancer Res, 2017. **77**(6): p. 1369-1382.

239. Novellasdemunt, L., et al., *Progestins activate 6-phosphofructo-2-kinase/fructose-2,6-bisphosphatase 3 (PFKFB3) in breast cancer cells.* Biochemical Journal, 2012. **442**(2): p. 345-356.
240. Ros, S., et al., *6-Phosphofructo-2-kinase/fructose-2,6-biphosphatase 4 is essential for p53-null cancer cells.* Oncogene, 2017. **36**(23): p. 3287-3299.
241. Ros, S., et al., *Functional metabolic screen identifies 6-phosphofructo-2-kinase/fructose-2,6-biphosphatase 4 as an important regulator of prostate cancer cell survival.* Cancer Discov, 2012. **2**(4): p. 328-43.
242. Jeon, Y.K., et al., *Sulforaphane induces apoptosis in human hepatic cancer cells through inhibition of 6-phosphofructo-2-kinase/fructose-2,6-biphosphatase4, mediated by hypoxia inducible factor-1-dependent pathway.* Biochim Biophys Acta, 2011. **1814**(10): p. 1340-8.
243. Talasniemi, J.P., et al., *Analytical investigation: assay of D-lactate in diabetic plasma and urine.* Clin Biochem, 2008. **41**(13): p. 1099-103.
244. Farhana, A. and S.L. Lappin, *Biochemistry, Lactate Dehydrogenase*, in *StatPearls*. 2021: Treasure Island (FL).
245. Phypers, B. and J.T. Pierce, *Lactate physiology in health and disease.* Continuing Education in Anaesthesia Critical Care & Pain, 2006. **6**(3): p. 128-132.
246. Gladden, L.B., *Lactate metabolism: a new paradigm for the third millennium.* J Physiol, 2004. **558**(Pt 1): p. 5-30.
247. Walenta, S., et al., *High lactate levels predict likelihood of metastases, tumor recurrence, and restricted patient survival in human cervical cancers.* Cancer Res, 2000. **60**(4): p. 916-21.
248. Faubert, B., et al., *Lactate Metabolism in Human Lung Tumors.* Cell, 2017. **171**(2): p. 358-371 e9.
249. van Hall, G., *Lactate kinetics in human tissues at rest and during exercise.* Acta Physiol (Oxf), 2010. **199**(4): p. 499-508.
250. Hui, S., et al., *Glucose feeds the TCA cycle via circulating lactate.* Nature, 2017.
251. Warburg O, W.F., Negelein E., *The metabolims of tumors in the body.* J Gen Physiol, 1927. **8**: p. 519–30.
252. Shim, H., et al., *c-Myc transactivation of LDH-A: implications for tumor metabolism and growth.* Proc Natl Acad Sci U S A, 1997. **94**(13): p. 6658-63.
253. Johnson, R.F. and N.D. Perkins, *Nuclear factor-kappaB, p53, and mitochondria: regulation of cellular metabolism and the Warburg effect.* Trends Biochem Sci, 2012. **37**(8): p. 317-24.
254. Lu, H., R.A. Forbes, and A. Verma, *Hypoxia-inducible factor 1 activation by aerobic glycolysis implicates the Warburg effect in carcinogenesis.* J Biol Chem, 2002. **277**(26): p. 23111-5.
255. Colegio, O.R., et al., *Functional polarization of tumour-associated macrophages by tumour-derived lactic acid.* Nature, 2014. **513**(7519): p. 559-63.
256. Bronte, V., *Tumor cells hijack macrophages via lactic acid.* Immunol Cell Biol, 2014. **92**(8): p. 647-649.
257. Chen, Y., Jr., et al., *Lactate metabolism is associated with mammalian mitochondria.* Nature Chemical Biology, 2016. **12**(11): p. 937-943.

258. Fan, T.W., et al., *Altered regulation of metabolic pathways in human lung cancer discerned by (13)C stable isotope-resolved metabolomics (SIRM).* Mol Cancer, 2009. **8**: p. 41.
259. Hensley, C.T., et al., *Metabolic Heterogeneity in Human Lung Tumors.* Cell, 2016. **164**(4): p. 681-94.
260. Pereira-Nunes, A., et al., *Targeting lactate production and efflux in prostate cancer.* Biochim Biophys Acta Mol Basis Dis, 2020. **1866**(11): p. 165894.
261. Li, F., et al., *Association between lactate dehydrogenase levels and oncologic outcomes in metastatic prostate cancer: A meta-analysis.* Cancer Med, 2020. **9**(19): p. 7341-7351.
262. Bok, R., et al., *The Role of Lactate Metabolism in Prostate Cancer Progression and Metastases Revealed by Dual-Agent Hyperpolarized (13)C MRSI.* Cancers (Basel), 2019. **11**(2).
263. Okorie, O.N. and P. Dellinger, *Lactate: biomarker and potential therapeutic target.* Crit Care Clin, 2011. **27**(2): p. 299-326.
264. van der Mijn, J.C., et al., *Lactic Acidosis in Prostate Cancer: Consider the Warburg Effect.* Case Reports in Oncology, 2017. **10**(3): p. 1085-1091.
265. Richard, J.P., *Mechanism for the formation of methylglyoxal from triosephosphates.* Biochem Soc Trans, 1993. **21**(2): p. 549-53.
266. PHILLIPS, S.A. and P.J. THORNALLEY, *The formation of methylglyoxal from triose phosphates.* European Journal of Biochemistry, 1993. **212**(1): p. 101-105.
267. Kalapos, M.P., *On the promine/retine theory of cell division: now and then.* Biochimica et Biophysica Acta (BBA) - General Subjects, 1999. **1426**(1): p. 1-16.
268. Thornalley, P.J., *Pharmacology of methylglyoxal: formation, modification of proteins and nucleic acids, and enzymatic detoxification--a role in pathogenesis and antiproliferative chemotherapy.* Gen Pharmacol, 1996. **27**(4): p. 565-73.
269. Kalapos, M.P., *Methylglyoxal in living organisms: chemistry, biochemistry, toxicology and biological implications.* Toxicol Lett, 1999. **110**(3): p. 145-75.
270. Vander Jagt, D.L. and L.A. Hunsaker, *Methylglyoxal metabolism and diabetic complications: roles of aldose reductase, glyoxalase-I, betaine aldehyde dehydrogenase and 2-oxoaldehyde dehydrogenase.* Chem Biol Interact, 2003. **143-144**: p. 341-51.
271. Bellier, J., et al., *Methylglyoxal, a potent inducer of AGEs, connects between diabetes and cancer.* Diabetes Res Clin Pract, 2019. **148**: p. 200-211.
272. Kalapos, M.P., *Methylglyoxal and glucose metabolism: a historical perspective and future avenues for research.* Drug Metabol Drug Interact, 2008. **23**(1-2): p. 69-91.
273. Thornalley, P.J., *Modification of the glyoxalase system in human red blood cells by glucose in vitro.* Biochemical Journal, 1988. **254**(3): p. 751-755.
274. Thornalley, P., *Advanced glycation and the development of diabetic complications. Unifying the involvement of glucose, methylglyoxal and oxidative stress*. Vol. 3. 1996. 149-166.
275. Wang, H., et al., *Fructose-induced peroxynitrite production is mediated by methylglyoxal in vascular smooth muscle cells.* Life Sciences, 2006. **79**(26): p. 2448-2454.

276. AHMED, N., et al., *Assay of advanced glycation endproducts (AGEs): surveying AGEs by chromatographic assay with derivatization by 6-aminoquinolyl-N-hydroxysuccinimidyl-carbamate and application to N∈-carboxymethyl-lysine- and N∈-(1-carboxyethyl)lysine-modified albumin.* Biochemical Journal, 2002. **364**(1): p. 1-14.
277. AHMED, N. and P.J. THORNALLEY, *Chromatographic assay of glycation adducts in human serum albumin glycated in vitro by derivatization with 6-aminoquinolyl-N-hydroxysuccinimidyl-carbamate and intrinsic fluorescence.* Biochemical Journal, 2002. **364**(1): p. 15-24.
278. Shipanova, I.N., M.A. Glomb, and R.H. Nagaraj, *Protein Modification by Methylglyoxal: Chemical Nature and Synthetic Mechanism of a Major Fluorescent Adduct.* Archives of Biochemistry and Biophysics, 1997. **344**(1): p. 29-36.
279. Oya, T., et al., *Methylglyoxal Modification of Protein: CHEMICAL AND IMMUNOCHEMICAL CHARACTERIZATION OF METHYLGLYOXAL-ARGININE ADDUCTS*.* Journal of Biological Chemistry, 1999. **274**(26): p. 18492-18502.
280. AHMED, M.U., et al., *Nε-(Carboxyethyl)lysine, a product of the chemical modification of proteins by methylglyoxal, increases with age in human lens proteins.* Biochemical Journal, 1997. **324**(2): p. 565-570.
281. Brinkmann, E., et al., *Characterization of an imidazolium compound formed by reaction of methylglyoxal and Nα-hippuryllysine.* Journal of the Chemical Society, Perkin Transactions 1, 1995(22): p. 2817-2818.
282. Lederer, M.O. and R.G. Klaiber, *Cross-linking of proteins by maillard processes: characterization and detection of lysine–arginine cross-links derived from glyoxal and methylglyoxal.* Bioorganic & Medicinal Chemistry, 1999. **7**(11): p. 2499-2507.
283. Rabbani, N. and P.J. Thornalley, *The Dicarbonyl Proteome.* Annals of the New York Academy of Sciences, 2008. **1126**(1): p. 124-127.
284. Bierhaus, A. and P.P. Nawroth, *Multiple levels of regulation determine the role of the receptor for AGE (RAGE) as common soil in inflammation, immune responses and diabetes mellitus and its complications.* Diabetologia, 2009. **52**(11): p. 2251-2263.
285. Sparvero, L.J., et al., *RAGE (Receptor for Advanced Glycation Endproducts), RAGE ligands, and their role in cancer and inflammation.* J Transl Med, 2009. **7**: p. 17.
286. Piperi, C., C. Adamopoulos, and A.G. Papavassiliou, *Potential of glycative stress targeting for cancer prevention.* Cancer Letters, 2017. **390**: p. 153-159.
287. Kwak, T., et al., *Targeting of RAGE-ligand signaling impairs breast cancer cell invasion and metastasis.* Oncogene, 2017. **36**(11): p. 1559-1572.
288. Thornalley, P.J. and N. Rabbani, *Glyoxalase in tumourigenesis and multidrug resistance.* Seminars in Cell & Developmental Biology, 2011. **22**(3): p. 318-325.
289. Murata-Kamiya, N., et al., *Methylglyoxal induces G:C to C:G and G:C to T:A transversions in the supF gene on a shuttle vector plasmid replicated in mammalian cells.* Mutation Research/Genetic Toxicology and Environmental Mutagenesis, 2000. **468**(2): p. 173-182.

290. Tu, C.-Y., et al., *Methylglyoxal induces DNA crosslinks in ECV304 cells via a reactive oxygen species-independent protein carbonylation pathway.* Toxicology in Vitro, 2013. **27**(4): p. 1211-1219.
291. Petrova, K.V., et al., *Characterization of the Deoxyguanosine–Lysine Cross-Link of Methylglyoxal.* Chemical Research in Toxicology, 2014. **27**(6): p. 1019-1029.
292. Mir, A.R., et al., *Methylglyoxal mediated conformational changes in histone H2A—generation of carboxyethylated advanced glycation end products.* International Journal of Biological Macromolecules, 2014. **69**: p. 260-266.
293. Jyoti, et al., *Neo-epitopes on methylglyoxal modified human serum albumin lead to aggressive autoimmune response in diabetes.* Int J Biol Macromol, 2016. **86**: p. 799-809.
294. Rabbani, N. and P.J. Thornalley, *The Critical Role of Methylglyoxal and Glyoxalase 1 in Diabetic Nephropathy.* Diabetes, 2014. **63**(1): p. 50-52.
295. Abate, G., et al., *Advanced Glycation End Products (Ages) in Food: Focusing on Mediterranean Pasta.* Journal of Nutrition and Food Sciences, 2015. **5**: p. 1-7.
296. Leone, A., et al., *The Dual-Role of Methylglyoxal in Tumor Progression – Novel Therapeutic Approaches.* Frontiers in Oncology, 2021. **11**(822).
297. Nokin, M.-J., et al., *Hormetic potential of methylglyoxal, a side-product of glycolysis, in switching tumours from growth to death.* Scientific Reports, 2017. **7**(1): p. 11722.
298. Thornalley, P.J., et al., *Imidazopurinones are markers of physiological genomic damage linked to DNA instability and glyoxalase 1-associated tumour multidrug resistance.* Nucleic Acids Research, 2010. **38**(16): p. 5432-5442.
299. Rosca, M.G., Monnier, V. M., Szweda, L. I. and Weiss, M. F. , *Alterations in renal mitochondrial respiration in response to the reactive oxoaldehyde methylglyoxal.* American Journal of Physiology-Renal Physiology, 2002. **283**(1): p. F52-F59.
300. Dobler, D., et al., *Increased Dicarbonyl Metabolism in Endothelial Cells in Hyperglycemia Induces Anoikis and Impairs Angiogenesis by RGD and GFOGER Motif Modification.* Diabetes, 2006. **55**(7): p. 1961-1969.
301. Pedchenko, V.K., et al., *Mechanism of Perturbation of Integrin-Mediated Cell-Matrix Interactions by Reactive Carbonyl Compounds and Its Implication for Pathogenesis of Diabetic Nephropathy.* Diabetes, 2005. **54**(10): p. 2952-2960.
302. Bair, W.B., 3rd, et al., *GLO1 overexpression in human malignant melanoma.* Melanoma Res, 2010. **20**(2): p. 85-96.
303. van Heijst, J.W.J., et al., *Argpyrimidine-modified Heat Shock Protein 27 in human non-small cell lung cancer: A possible mechanism for evasion of apoptosis.* Cancer Letters. **241**(2): p. 309-319.
304. Dafre, A.L., et al., *Methylglyoxal, the foe and friend of glyoxalase and Trx/TrxR systems in HT22 nerve cells.* Free Radic Biol Med, 2015. **89**: p. 8-19.
305. Antognelli, C., et al., *Role of glyoxalase I in the proliferation and apoptosis control of human LNCaP and PC3 prostate cancer cells.* Prostate, 2013. **73**(2): p. 121-32.
306. Galligan, J.J., et al., *Methylglyoxal-derived posttranslational arginine modifications are abundant histone marks.* Proceedings of the National Academy of Sciences, 2018. **115**(37): p. 9228-9233.

307. Galligan, J.J., et al., *Quantitative Analysis and Discovery of Lysine and Arginine Modifications.* Analytical Chemistry, 2017. **89**(2): p. 1299-1306.
308. Laurent, A., et al., *Controlling tumor growth by modulating endogenous production of reactive oxygen species.* Cancer Res, 2005. **65**(3): p. 948-56.
309. Al-Balas, Q.A., et al., *Recent Advances in Glyoxalase-I Inhibition.* Mini Rev Med Chem, 2019. **19**(4): p. 281-291.
310. Racker, E., *The mechanism of action of glyoxalase.* J Biol Chem, 1951. **190**(2): p. 685-96.
311. Thornalley, P.J., *Glyoxalase I – structure, function and a critical role in the enzymatic defence against glycation.* Biochemical Society Transactions, 2003. **31**(6): p. 1343-1348.
312. Kimura, A. and Y. Inoue, *Glyoxalase I in micro-organisms: Molecular characteristics, genetics and biochemical regulation.* Biochemical Society Transactions, 1993. **21**(2): p. 518-522.
313. Maiti, M.K., et al., *Molecular characterization of glyoxalase II from Arabidopsis thaliana.* Plant Mol Biol, 1997. **35**(4): p. 471-81.
314. Yadav, S.K., S.L. Singla-Pareek, and S.K. Sopory, *An overview on the role of methylglyoxal and glyoxalases in plants.* Drug Metabol Drug Interact, 2008. **23**(1-2): p. 51-68.
315. Thornalley, P.J., *The glyoxalase system: new developments towards functional characterization of a metabolic pathway fundamental to biological life.* Biochem J, 1990. **269**(1): p. 1-11.
316. Cameron, A.D., et al., *Crystal structure of human glyoxalase I--evidence for gene duplication and 3D domain swapping.* EMBO J, 1997. **16**(12): p. 3386-95.
317. Ridderström, M. and B. Mannervik, *Optimized heterologous expression of the human zinc enzyme glyoxalase I.* Biochemical Journal, 1996. **314**(Pt 2): p. 463-467.
318. Scott, G.F., et al., *Featured Article: Pyruvate preserves antiglycation defenses in porcine brain after cardiac arrest.* Exp Biol Med (Maywood), 2017. **242**(10): p. 1095-1103.
319. Ibi, M., et al., *Depletion of Intracellular Glutathione Increases Susceptibility to Nitric Oxide in Mesencephalic Dopaminergic Neurons.* Journal of Neurochemistry, 1999. **73**(4): p. 1696-1703.
320. Troyano, A., et al., *Effect of Glutathione Depletion on Antitumor Drug Toxicity (Apoptosis and Necrosis) in U-937 Human Promonocytic Cells: THE ROLE OF INTRACELLULAR OXIDATION.* Journal of Biological Chemistry, 2001. **276**(50): p. 47107-47115.
321. Rabbani, N., et al., *Multiple roles of glyoxalase 1-mediated suppression of methylglyoxal glycation in cancer biology-Involvement in tumour suppression, tumour growth, multidrug resistance and target for chemotherapy.* Semin Cancer Biol, 2017.
322. Thornalley, P.J., *Protecting the genome: defence against nucleotide glycation and emerging role of glyoxalase I overexpression in multidrug resistance in cancer chemotherapy.* Biochemical Society Transactions, 2003. **31**(6): p. 1372-1377.

323. Jang, S., et al., *Generation and characterization of mouse knockout for glyoxalase 1.* Biochem Biophys Res Commun, 2017.
324. Inoue, Y. and A. Kimura, *Identification of the structural gene for glyoxalase I from Saccharomyces cerevisiae.* J Biol Chem, 1996. **271**(42): p. 25958-65.
325. Hause, F., et al., *Accumulation of glycated proteins suggesting premature ageing in lamin B receptor deficient mice.* Biogerontology, 2017.
326. Xue, M., et al., *Transcriptional control of glyoxalase 1 by Nrf2 provides a stress-responsive defence against dicarbonyl glycation.* Biochem J, 2012. **443**(1): p. 213-22.
327. Ranganathan, S., et al., *Genomic sequence of human glyoxalase-I: analysis of promoter activity and its regulation.* Gene, 1999. **240**(1): p. 149-155.
328. Bellahcene, A., et al., *Methylglyoxal-derived stress: An emerging biological factor involved in the onset and progression of cancer.* Semin Cancer Biol, 2017.
329. Kurz, A., et al., *Alpha-synuclein deficiency leads to increased glyoxalase I expression and glycation stress.* Cell Mol Life Sci, 2011. **68**(4): p. 721-33.
330. Barati, M.T., Merchant, M. L., Kain, A. B., Jevans, A. W., McLeish, K. R. and Klein, J. B. , *Proteomic analysis defines altered cellular redox pathways and advanced glycation end-product metabolism in glomeruli of db/db diabetic mice.* American Journal of Physiology-Renal Physiology, 2007. **293**(4): p. F1157-F1165.
331. Lechner, M., et al., *A Proteomic View on the Role of Glucose in Peritoneal Dialysis.* Journal of Proteome Research, 2010. **9**(5): p. 2472-2479.
332. Chen, F., et al., *Role for glyoxalase I in Alzheimer's disease.* Proceedings of the National Academy of Sciences of the United States of America, 2004. **101**(20): p. 7687-7692.
333. Xue, M., et al., *Glyoxalase 1 copy number variation in patients with well differentiated gastro-entero-pancreatic neuroendocrine tumours (GEP-NET).* Oncotarget, 2017. **8**(44): p. 76961-76973.
334. Sakamoto, H., et al., *Glyoxalase I is involved in resistance of human leukemia cells to antitumor agent-induced apoptosis.* Blood, 2000. **95**(10): p. 3214-8.
335. Sakamoto, H., et al., *Selective activation of apoptosis program by S-p-bromobenzylglutathione cyclopentyl diester in glyoxalase I-overexpressing human lung cancer cells.* Clin Cancer Res, 2001. **7**(8): p. 2513-8.
336. Santarius, T., et al., *GLO1-A novel amplified gene in human cancer.* Genes Chromosomes Cancer, 2010. **49**(8): p. 711-25.
337. Hosoda, F., et al., *Integrated genomic and functional analyses reveal glyoxalase I as a novel metabolic oncogene in human gastric cancer.* Oncogene, 2015. **34**(9): p. 1196-206.
338. Antognelli, C., et al., *Alteration of glyoxalase genes expression in response to testosterone in LNCaP and PC3 human prostate cancer cells.* Cancer Biol Ther, 2007. **6**(12): p. 1880-8.
339. Rulli, A., et al., *A possible regulatory role of 17beta-estradiol and tamoxifen on glyoxalase I and glyoxalase II genes expression in MCF7 and BT20 human breast cancer cells.* Breast Cancer Res Treat, 2006. **96**(2): p. 187-96.

340. Fonseca-Sanchez, M.A., et al., *Breast cancer proteomics reveals a positive correlation between glyoxalase 1 expression and high tumor grade.* Int J Oncol, 2012. **41**(2): p. 670-80.
341. Burdelski, C., et al., *High-Level Glyoxalase 1 (GLO1) expression is linked to poor prognosis in prostate cancer.* The Prostate, 2017. **77**(15): p. 1528-1538.
342. Al-Balasa, A.Q., et al., *Novel Thiazole Carboxylic Acid Derivatives Possessing a "Zinc Binding Feature" as Potential Human Glyoxalase-I Inhibitors.* Letters in Drug Design & Discovery, 2017. **14**(11): p. 1324-1334.
343. Jin, T., et al., *Recent advances in the discovery and development of glyoxalase I inhibitors.* Bioorg Med Chem, 2020. **28**(4): p. 115243.
344. Wolff, D.G., *The formation of carbon monoxide during peroxidation of microsomal lipids.* Biochem Biophys Res Commun, 1976. **73**(4): p. 850-7.
345. Prabhakar, N.R., et al., *Carbon monoxide: a role in carotid body chemoreception.* Proceedings of the National Academy of Sciences of the United States of America, 1995. **92**(6): p. 1994-1997.
346. Higgins, C. *L-lactate and D-lactate-clinical significance of the difference October 2011*. 2016.
347. Santel, T., et al., *Curcumin inhibits glyoxalase 1: a possible link to its anti-inflammatory and anti-tumor activity.* PloS one, 2008. **3**(10): p. e3508-e3508.
348. Wang, Q., et al., *Characterization of monocarboxylate transport in human kidney HK-2 cells.* Mol Pharm, 2006. **3**(6): p. 675-85.
349. de Bari, L., L. Moro, and S. Passarella, *Prostate cancer cells metabolize d-lactate inside mitochondria via a D-lactate dehydrogenase which is more active and highly expressed than in normal cells.* FEBS Lett, 2013. **587**(5): p. 467-73.
350. Loeber, G., et al., *Human NAD(+)-dependent mitochondrial malic enzyme. cDNA cloning, primary structure, and expression in Escherichia coli.* J Biol Chem, 1991. **266**(5): p. 3016-21.
351. de Bari, L., et al., *D-Lactate transport and metabolism in rat liver mitochondria.* Biochem J, 2002. **365**(Pt 2): p. 391-403.
352. de Bari, L., et al., *Jerusalem artichoke mitochondria can export reducing equivalents in the form of malate as a result of D-lactate uptake and metabolism.* Biochem Biophys Res Commun, 2005. **335**(4): p. 1224-30.
353. Beier, U.H., et al., *Learning from cancer: Using D-lactate for therapeutic immunosuppression.* The Journal of Immunology, 2016. **196**(1 Supplement): p. 140.15-140.15.
354. Zhang, S., et al., *Glo1 genetic amplification as a potential therapeutic target in hepatocellular carcinoma.* Int J Clin Exp Pathol, 2014. **7**(5): p. 2079-90.
355. Kremer, C.L., et al., *Expression of mTOR signaling pathway markers in prostate cancer progression.* Prostate, 2006. **66**(11): p. 1203-12.
356. Petein, M., et al., *Morphonuclear relationship between prostatic intraepithelial neoplasia and cancers as assessed by digital cell image analysis.* Am J Clin Pathol, 1991. **96**(5): p. 628-34.
357. Kristiansen, G., *Markers of clinical utility in the differential diagnosis and prognosis of prostate cancer.* Mod Pathol, 2018. **31**(S1): p. S143-155.

358. Wu, C.L., et al., *Analysis of alpha-methylacyl-CoA racemase (P504S) expression in high-grade prostatic intraepithelial neoplasia.* Hum Pathol, 2004. **35**(8): p. 1008-13.
359. Zhou, M., et al., *Alpha-Methylacyl-CoA racemase: a novel tumor marker over-expressed in several human cancers and their precursor lesions.* Am J Surg Pathol, 2002. **26**(7): p. 926-31.
360. Scheifele, C., et al., *Glyoxalase 1 expression analysis by immunohistochemistry in breast cancer.* Pathol Res Pract, 2020. **216**(12): p. 153257.
361. Peng, H.T., et al., *Up-regulation of the tumor promoter Glyoxalase-1 indicates poor prognosis in breast cancer.* Int J Clin Exp Pathol, 2017. **10**(11): p. 10852-10862.
362. Baunacke, M., et al., *Exploring glyoxalase 1 expression in prostate cancer tissues: targeting the enzyme by ethyl pyruvate defangs some malignancy-associated properties.* Prostate, 2014. **74**(1): p. 48-60.
363. Cheng, W.L., et al., *Glyoxalase-I is a novel prognosis factor associated with gastric cancer progression.* PLoS One, 2012. **7**(3): p. e34352.
364. Wang, Y., et al., *Glyoxalase I (GLO1) is up-regulated in pancreatic cancerous tissues compared with related non-cancerous tissues.* Anticancer Res, 2012. **32**(8): p. 3219-22.
365. Antognelli, C., et al., *Overexpression of glyoxalase system enzymes in human kidney tumor.* Cancer J, 2006. **12**(3): p. 222-8.
366. Antognelli, C., et al., *Glyoxalase 1 sustains the metastatic phenotype of prostate cancer cells via EMT control.* J Cell Mol Med, 2018. **22**(5): p. 2865-2883.
367. van Leenders, G., et al., *The 2019 International Society of Urological Pathology (ISUP) Consensus Conference on Grading of Prostatic Carcinoma.* Am J Surg Pathol, 2020. **44**(8): p. e87-e99.
368. Cookson, M.S., et al., *Variation in the definition of biochemical recurrence in patients treated for localized prostate cancer: the American Urological Association Prostate Guidelines for Localized Prostate Cancer Update Panel report and recommendations for a standard in the reporting of surgical outcomes.* J Urol, 2007. **177**(2): p. 540-5.
369. Ng, V.W., et al., *Is triple immunostaining with 34betaE12, p63, and racemase in prostate cancer advantageous? A tissue microarray study.* Am J Clin Pathol, 2007. **127**(2): p. 248-53.
370. Rathod, S.G., D.G. Jaiswal, and R.S. Bindu, *Diagnostic utility of triple antibody (AMACR, HMWCK and P63) stain in prostate neoplasm.* J Family Med Prim Care, 2019. **8**(8): p. 2651-2655.
371. Wang, M., et al., *A basal cell defect promotes budding of prostatic intraepithelial neoplasia.* J Cell Sci, 2017. **130**(1): p. 104-110.
372. Jandova, J. and G.T. Wondrak, *Genomic GLO1 deletion modulates TXNIP expression, glucose metabolism, and redox homeostasis while accelerating human A375 malignant melanoma tumor growth.* Redox Biol, 2021. **39**: p. 101838.
373. Jandova, J., et al., *Genetic Target Modulation Employing CRISPR/Cas9 Identifies Glyoxalase 1 as a Novel Molecular Determinant of Invasion and*

*Metastasis in A375 Human Malignant Melanoma Cells In Vitro and In Vivo.* Cancers (Basel), 2020. **12**(6).
374. Davis, A.L., et al., *The Quinone Methide Aurin Is a Heat Shock Response Inducer That Causes Proteotoxic Stress and Noxa-dependent Apoptosis in Malignant Melanoma Cells*.* Journal of Biological Chemistry, 2015. **290**(3): p. 1623-1638.
375. Perer, J., et al., *The sunless tanning agent dihydroxyacetone induces stress response gene expression and signaling in cultured human keratinocytes and reconstructed epidermis.* Redox Biology, 2020. **36**: p. 101594.
376. Chiavarina, B., et al., *Methylglyoxal-Mediated Stress Correlates with High Metabolic Activity and Promotes Tumor Growth in Colorectal Cancer.* International Journal of Molecular Sciences, 2017. **18**(1): p. 213.
377. Sharma, N.S., et al., *Targeting tumor-intrinsic hexosamine biosynthesis sensitizes pancreatic cancer to anti-PD1 therapy.* J Clin Invest, 2020. **130**(1): p. 451-465.
378. Kouidhi, S., F. Ben Ayed, and A. Benammar Elgaaied, *Targeting Tumor Metabolism: A New Challenge to Improve Immunotherapy.* Front Immunol, 2018. **9**: p. 353.
379. Frieling, J.S., et al., *Prostate cancer-derived MMP-3 controls intrinsic cell growth and extrinsic angiogenesis.* Neoplasia, 2020. **22**(10): p. 511-521.
380. Hsieh, C.L., et al., *Reactive oxygen species-mediated switching expression of MMP-3 in stromal fibroblasts and cancer cells during prostate cancer progression.* Sci Rep, 2017. **7**(1): p. 9065.
381. Pang, X., et al., *Identification of SPP1 as an Extracellular Matrix Signature for Metastatic Castration-Resistant Prostate Cancer.* Frontiers in Oncology, 2019. **9**(924).
382. Pang, X., et al., *SPP1 Promotes Enzalutamide Resistance and Epithelial-Mesenchymal-Transition Activation in Castration-Resistant Prostate Cancer via PI3K/AKT and ERK1/2 Pathways.* Oxidative Medicine and Cellular Longevity, 2021. **2021**: p. 5806602.
383. https://www.proteinatlas.org/ENSG00000149968-MMP3/pathology/prostate+cancer. 2021.
384. Chen, Y., et al., *Research Progress of TXNIP as a Tumor Suppressor Gene Participating in the Metabolic Reprogramming and Oxidative Stress of Cancer Cells in Various Cancers.* Frontiers in Oncology, 2020. **10**(1861).
385. Xie, M., et al., *Thioredoxin interacting protein (TXNIP) acts as a tumor suppressor in human prostate cancer.* Cell Biology International, 2020. **44**(10): p. 2094-2106.
386. Al-Azayzih, A., F. Gao, and P.R. Somanath, *P21 activated kinase-1 mediates transforming growth factor β1-induced prostate cancer cell epithelial to mesenchymal transition.* Biochim Biophys Acta, 2015. **1853**(5): p. 1229-39.
387. Liu, H.-Q., et al., *Expression of MMP-3 and TIMP-3 in gastric cancer tissue and its clinical significance.* Oncology letters, 2011. **2**(6): p. 1319-1322.
388. Deraz, E.M., et al., *MMP-10/stromelysin-2 promotes invasion of head and neck cancer.* PLoS One, 2011. **6**(10): p. e25438.

389. Thalmann, G.N., et al., *Osteopontin: possible role in prostate cancer progression.* Clin Cancer Res, 1999. **5**(8): p. 2271-7.
390. Song, Z.Y., et al., *Identification of hub genes in prostate cancer using robust rank aggregation and weighted gene co-expression network analysis.* Aging (Albany NY), 2019. **11**(13): p. 4736-4756.
391. Gimba, E.R. and T.M. Tilli, *Human osteopontin splicing isoforms: known roles, potential clinical applications and activated signaling pathways.* Cancer Lett, 2013. **331**(1): p. 11-7.
392. McCandless, J., et al., *A human xenograft model for testing early events of epithelial neoplastic invasion.* Int J Oncol, 1997. **10**(2): p. 279-85.
393. Ellwood-Yen, K., et al., *Myc-driven murine prostate cancer shares molecular features with human prostate tumors.* Cancer Cell, 2003. **4**(3): p. 223-38.
394. Luna, L.G.A.F.I.o.P.A.F.I.o.P., *Manual of histologic staining methods of the Armed Forces Institute of Pathology*. 1968, New York: Blakiston Division, McGraw-Hill.
395. Beć, K.B., et al., *Principles and Applications of Vibrational Spectroscopic Imaging in Plant Science: A Review.* Frontiers in Plant Science, 2020. **11**(1226).
396. Rodriguez-Saona, L., H. Ayvaz, and R.L. Wehling, *Infrared and Raman Spectroscopy*, in *Food Analysis*, S.S. Nielsen, Editor. 2017, Springer International Publishing: Cham. p. 107-127.
397. Jackson, M., M.G. Sowa, and H.H. Mantsch, *Infrared spectroscopy: a new frontier in medicine.* Biophys Chem, 1997. **68**(1-3): p. 109-25.
398. Fernandez, D.C., et al., *Infrared spectroscopic imaging for histopathologic recognition.* Nature Biotechnology, 2005. **23**(4): p. 469-474.